Effects of coralline algal diffusion boundary layers on growth of newly settled sea urchins: implications for ocean acidification conditions

Erin Houlihan

A thesis submitted for the degree of Masters of Science (MSc) in Marine Science at the University of Otago, Dunedin, New Zealand

January 2019

Abstract

Macroalgae are able to modify their local environment via biological processes, thereby creating a diffusive boundary layer (DBL) where the chemical and physical environment differs from the overlying bulk seawater. In slow flow environments, the DBL has the potential to modulate effects of reduced seawater pH associated with ocean acidification (OA). OA poses a major threat to marine ecosystems and particularly to calcifying organisms. While implications for macroalgae and corals in the DBL have been studied, the effects on invertebrates settling and inhabiting the DBL are not well understood. This study examines the oxygen and pH conditions within coralline algal DBLs that change as a result of irradiance, flow and bulk seawater pH, in order to understand the effects of these variable conditions on growth of juvenile sea urchins in the DBL. Oxygen concentrations, used as a proxy for pH based on previous research, were measured above crustose coralline algal surfaces to determine DBL thickness and pH levels within the DBL. Newly settled juvenile sea urchins *Pseudechinus huttoni* were subsequently grown in these conditions for up to 11 days. Morphological measurements (test diameter and spine length) and scanning electron microscopy were used to examine growth and calcification of sea urchins.

Seawater pH levels above CCA varied as a result of irradiance, flow and bulk seawater pH. In static flow, CCA increased pH at its surface up to approximately 0.8 units above the overlying bulk seawater in the light, but only decreased pH up to nearly 0.09 units below bulk seawater in the dark. DBLs were thickest at zero or slow flow (1 cm s^{-1}) in the light. pH levels in the DBL varied from approximately pH_T 7.4 to 8.6, but there was no strong effect of these varying pH levels within the DBL on post-settlement growth of *P. huttoni* juveniles. Life in the diffusion boundary has allowed juveniles to adapt to grow and calcify in naturally fluctuating pH environments. This finding supports observations seen in other juvenile sea urchins, and is significant because it indicates that the early post-settlement stage may not be as sensitive to OA as the larval stage, where negative effects have been previously documented. Life in thick diffusion boundary layers above CCA in slow-flow fjord environments may have increased tolerance of juvenile *P. huttoni* to reduced bulk seawater pH, thereby conferring greater resilience to future ocean acidification conditions.

Acknowledgements

In sea urchins, settlement is a crucial life-history transition. Thank you to all the people who helped me “settle” and “metamorphose” here in New Zealand. Firstly, thank you to my supervisors. To Miles Lamare for showing me how to think outside the box. Your passion and energy for science are tangible. To Chris Cornwall for your patience and expertise. I have genuinely appreciated all your answers to my many questions. To Conrad Pilditch for hosting me in Hamilton and letting me use your annular flume for the year.

A huge thanks to Fulbright New Zealand for providing me with the opportunity and funding to spend a wonderful year in New Zealand. Thank you to my Fulbright cohort, and especially my Dunedin cohort. Cara, this year would not have been the same without you. Thanks for all the runs, ice creams, coffee and laughs. Every weekend (and sometimes every day) is a lot more fun (and a little scarier) with you around. Looking forward to all the future adventures. Oscar, while I may never agree with your savoury over sweet, you have shown me what dedication and compassion truly look like in a friend.

A big thank you to all the staff at PML, especially Reuben Pooley, Linda Groenewegen, Dave Wilson and Doug Mackie, for always extending a helping hand. Thank you to Kim Currie and Judith Murdoch from the chemistry department for offering carbonate chemistry advice and running my water samples. Thank you to Tim Jowett for all the statistics help. Thank you to my fellow marine science students, especially for the company and conversations in the Outlander rides. Special thank you to Erica and Nichola for all the help and to Celia for sharing our baby-raising experience. Thank you Nadjejda for answering all my sea urchin questions and waking up at weird hours with me to complete settlement experiments. Thank you Anna for letting me use your CCA settlement discs and for being a constant source of encouragement and wisdom.

Thank you to my “across-the-Bog” flatmates. You each taught me so many things and I would not have made it through this year without coming home every day to a wonderful lounge of familiar, friendly faces and yummy desserts. And of course, thank you to my family and friends back home, especially my mom who has always been a constant source of optimism, encouragement and compassion in everything I do.

Table of contents

List of tables

List of figures

List of appendices

Chapter 1: General introduction

1.1 Introduction to thesis

The diffusive boundary layer (DBL) is a micro-layer of seawater around marine organisms where, due to biological activity, the chemical and physical environment is altered from the mainstream seawater (Denny, 2000; Cornwall et al., 2013b). Through biological processes, such as photosynthesis and respiration, marine organisms such as macroalgae can alter the chemistry of their surrounding environment (Hurd et al., 2011; Cornwall et al., 2014; Cornwall et al., 2013b). While the importance of the DBL in controlling the availability and passage of nutrients and metabolites to and from algal surfaces is well known (Hurd, 2000; De Beer and Larkum, 2001), the characterisation and implications of the DBL, especially in the context of ocean acidification (OA, the reduction of seawater pH due to the uptake of elevated atmospheric CO_2 (Caldeira and Wickett, 2003)), are still being quantified. Reduced mainstream (or bulk) seawater pH due to OA poses a major threat to marine ecosystems and particularly to calcifying organisms (Hendriks et al., 2010; Kroeker et al., 2013; Dupont et al., 2010b; Dupont and Thorndyke, 2013; Byrne, 2011). This study explores how natural fluctuations in pH due to biological activity will interact with larger scale seawater pH changes associated with OA. In the field of OA, the DBL holds particular importance as a potential environmental buffer to corrosive reduced bulk seawater pH.

The boundary layer is rarely considered when modelling the effects of OA on marine species, such as sea urchins (Chan et al., 2016). Recent work has shown that the DBL may ameliorate some of the negative effects of OA on macroalgae, which are able to create a favourable microenvironment (Hurd et al., 2011; Cornwall et al., 2014; Cornwall et al., 2013b). However, the effects of a DBL on early life stages of marine organisms in future OA conditions remains unknown (Koehl and Hadfield, 2010; Espinel-Velasco et al., 2018). Early life history stages that settle and live on the benthos dominated by primary producers already experience strong and temporally variable gradients of pH, with the biggest fluctuations in the sub-millimetre microenvironments in the boundary layers on algal surfaces (Wahl et al., 2015b).

This study focuses on the post-metamorphic juvenile stage of sea urchin *Pseudechinus huttoni* Benham 1908 (Echinoidea, Temnopleuridae), a calcifying organism found in slow-flow environments such as fjords off the coast of New Zealand and the continental shelf (<60 m)

(Kirby et al., 2006). This species is known to settle on crustose coralline algae (CCA). The aims of this thesis are to quantify the pH conditions within crustose coralline algal diffusion boundary layers that change as a result of irradiance, flow and bulk seawater pH, in order to examine the effects of these variable conditions on growth of juvenile sea urchins in the DBL.

1.2 Boundary layers

Boundary layers exist around all marine organisms, creating a discrete layer of seawater with a different chemical and physical environment from the bulk seawater (Denny, 2000; Cornwall et al., 2013b). A boundary layer in the water column refers to the gradient region between the surface of a substrate, such as a marine organism, and the mainstream flow (Koehl, 2007; Vogel, 1994). The diffusion boundary layer (DBL) is of particular interest in ocean acidification studies because it can act as a buffer from mainstream seawater (Hurd et al., 2011). The DBL is defined as a region where the movement of dissolved substances, momentum and heat is predominantly through molecular diffusion (Vogel, 1994; Cornwall et al., 2013b). In marine algae, the DBL forms as a result of organisms taking up and releasing dissolved substances from the fluid adjacent to their thallus surface (Hurd, 2000). The DBL forms within the benthic boundary layer (BBL). The BBL is a layer of reduced seawater velocity at the seafloor (Hurd, 2000). The velocity boundary layer (VBL) is the velocity gradient within the BBL, present whenever a fluid flows over a solid (Hurd, 2000). The DBL is typically approximately 1/10 of the thickness of the VBL (Boudreau and Jorgensen, 2001). Additionally, within the VBL, there is also a concentration boundary layer (CBL). The CBL is a region where concentrations of dissolved substances are different than the mainstream seawater (Cornwall et al., 2013b). The CBL is used to distinguish the flux of mass from fluxes of momentum and heat that also travel via diffusion across the DBL (Hurd, 2015; Denny, 2000). For the purposes of this study, I focus on the DBL, but use the CBL, or the changes in concentration, to estimate DBL, since at small scales (e.g. <1 mm under turbulent flows) neither diffusion nor water velocity can be accurately measured (Nishihara and Ackerman, 2007). There are many factors that contribute to the boundary layer region thickness including biological processes, such as metabolic activity controlled by light, which change the measureable CBL but not the DBL, that interact with structural, chemical and physical processes (Hurd et al., 2011). I assume the CBL to be similar to the DBL within this study.

Metabolic processes (photosynthesis and respiration) controlled by light drive pH variability in the DBL above algae, while physical processes (seawater velocity) determine DBL

thickness (Figure 1.1; Hurd et al., 2011, Cornwall et al., 2014). Organism structure (size and morphology) and carbonate chemistry (pCO_2 conditions) also interact with the biological and physical processes to determine oxygen and pH conditions within the DBL (Hurd et al., 2011). Photosynthesis increases pH within the boundary layer, whereas calcification and respiration both reduce pH (Hurd et al., 2009; Cornwall et al., 2013b). During photosynthesis, there is a net uptake of CO_2, HCO_3^- and H^+. CO_2 is taken up faster than it can be resupplied from the atmosphere or deeper water. This causes an increase in pH in the light (daytime) because $pH = -\log[H^+]$ (see Cornwall et al. 2017 for further detail). Respiration and calcification, in opposition to photosynthesis, release CO_2 into the surrounding seawater, thus decreasing pH in the dark (Chan et al., 2016). In slow-flow environments, metabolic activity from organisms including coralline algae, seaweed and corals, drive large diurnal changes in seawater pH up to +/- 0.5 pH units (Hurd, 2015; Hurd et al., 2011; Noisette and Hurd, 2018; Chan et al., 2016).

While biology drives the direction of pH change, the local hydrodynamic conditions, including surface roughness, microtopography and ambient flow velocity, contribute to determining DBL thickness (Chan et al., 2016) . Rugosity has an effect on DBL thickness because small-scale (μm-mm) surface topographical features change DBL thickness; topographical features reduce the roughness Reynolds number or create a local depression, thereby increasing DBL thickness (Noisette and Hurd, 2018; Hurd and Pilditch, 2011; Wangpraseurt et al., 2012). This is relevant for crustose coralline algae, which can be both encrusting and erect in form. Additionally, DBLs are thinner in fast flow and thicker in slow flow (Chan et al., 2016). Generally, the DBL is micrometres to centimetres (~1 mm up to ~37 mm) thick in slow bulk seawater velocity (< 1cm s^{-1}) and is less than 0.1 mm in fast bulk seawater velocity (> 5 cm s^{-1}) (Cornwall et al., 2014; Hurd et al., 2011; Noisette and Hurd, 2018; Hendriks et al., 2017; Cornwall et al., 2013b; Chan et al., 2016). Slow flow conditions, that promote DBL thickness, enable metabolic processes to change local pH levels. Organisms that live in slow-flow environments above algal surfaces, such as juvenile sea urchins that have settled on coralline algae, likely experience large pH variability due to a thick diffusion boundary layer in their natural environment.

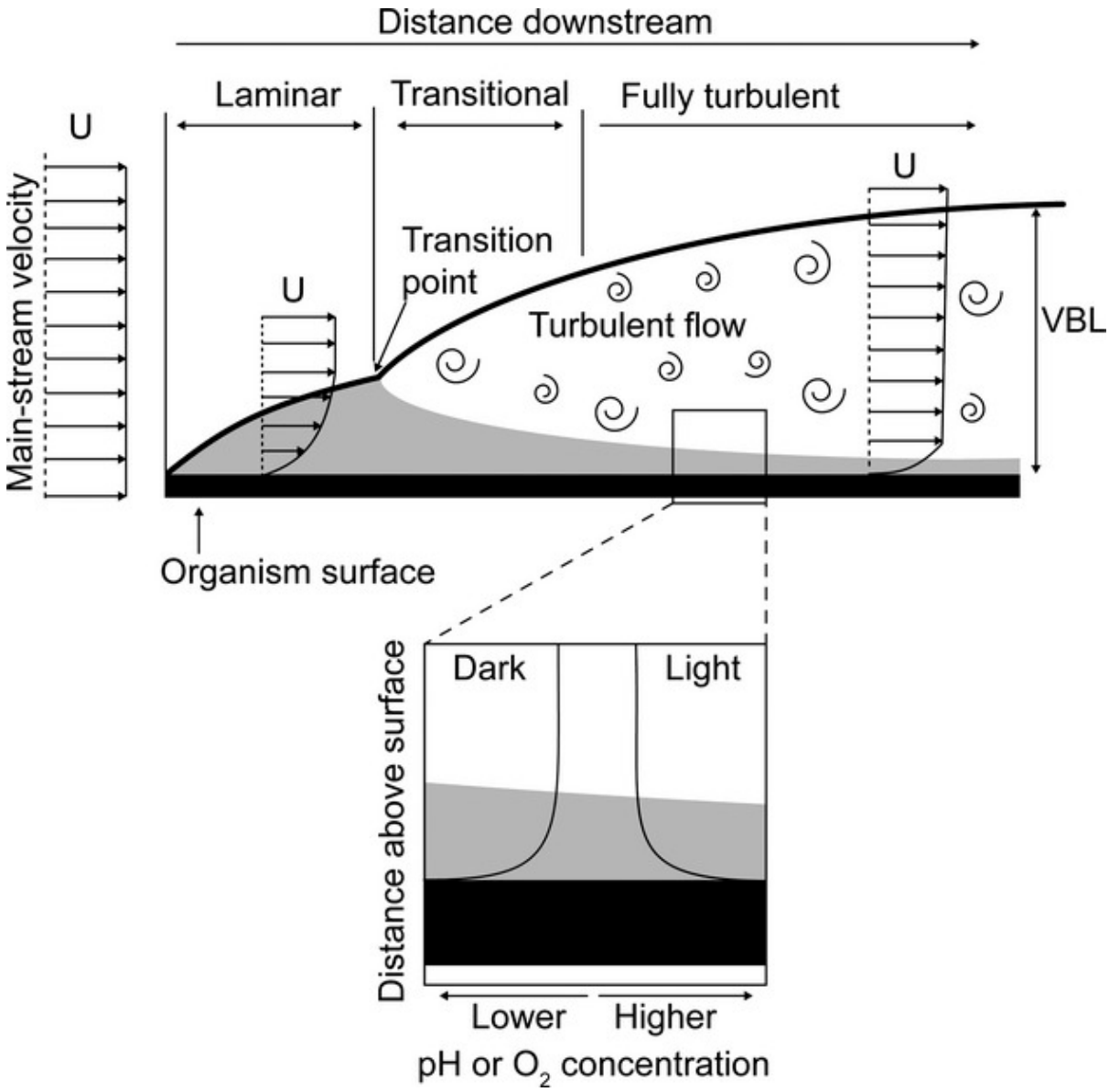

Figure 1.1 Conceptual diagram that illustrates the formation of a diffusion boundary layer (DBL) within a velocity boundary layer (VBL) as mainstream flow (indicated by arrows) encounters an organism surface. The DBL forms above the surface of the organism due to metabolic exchange at its surface. The maximum thickness of the DBL is set by the outer boundary of the laminar region of the VBL (shaded grey region). DBL thickness decreases with increasing turbulence and mainstream seawater velocity. The inset displays predicted gradients of pH and O_2 within the DBL at the surface of the organism in the light and dark; photosynthesis increases pH and O_2 in the light, while calcification and respiration decrease pH and O_2 in the dark. As taken from Hurd et al. (2011). Metabolically induced pH fluctuations by some coastal calcifiers exceed projected 22nd century ocean acidification: a mechanism for differential susceptibility? *Global Change Biology*, 17: page 3255 with permission.

1.3 Ocean acidification and seawater carbonate chemistry

Increasing concentrations of atmospheric carbon dioxide (CO_2) are lowering seawater pH and decreasing carbonate ion concentrations and saturation states, a phenomenon known as ocean acidification (OA) (Doney et al., 2009). These fundamental changes in seawater chemistry may be detrimental for marine biota. On a species level, reduced seawater pH can affect organism physiology, and on an ecosystem level, the decrease in pH can affect biodiversity and trophic interactions (Feely et al., 2009; Fabry et al., 2008; Caldeira and Wickett, 2003). In the past few decades, OA has become an increasingly crucial area of research (Dupont and Pörtner, 2013; Kroeker, 2010).

Since the beginning of the Industrial Revolution circa 1750, human activities, such as fossil fuel combustion and deforestation, have led to a dramatic increase in atmospheric CO_2. Atmospheric CO_2 has increased from pre-industrial levels of ~280 ppm to over 400 ppm in 2018 (IPCC, 2007; NOAA, 2018). By 2050, levels are predicted to reach over 500 ppm and exceed 800 ppm by 2100 (Friedlingstein et al., 2006; Feely et al., 2009). The ocean acts as a massive net sink for anthropogenic CO_2—approximately one third of the anthropogenic CO_2 produced in the past 200 years has been taken up by the oceans (Sabine et al., 2004). The conditions of the future ocean depend on the amount of carbon emitted in the coming decades, which varies according to different emissions scenarios. Global surface pH in the 21st century is estimated to decrease anywhere from 0.07 ± 0.001 units up to 0.33 ± 0.003 units relative to the years 1870-1879 (Gattuso et al., 2015).

Changes in seawater carbonate chemistry are governed by the following series of chemical reactions (Doney et al., 2009; Feely et al., 2009):

$$CO_2(atm) \leftrightarrow CO_2(aq)$$

$$CO_2(aq) + H_2O \leftrightarrow H_2CO_3 \leftrightarrow H^+ + HCO_3^- \leftrightarrow 2H^+ + CO_3^{2-}$$

The first reaction occurs as atmospheric CO_2 gas dissolves into seawater through air-sea gas exchange (Doney et al., 2009; Feely et al., 2009). The second set of reactions occurs when $CO_2(aq)$ reacts with water to form carbonic acid (H_2CO_3). Subsequently, carbonic acid (H_2CO_3) dissociates by losing hydrogen ions (H^+) to form bicarbonate ions (HCO_3^-) and carbonate (CO_3^{2-}) ions (Doney et al., 2009). In typical ocean surface conditions with pH_T 8.1, approximately 90% of the total dissolved inorganic carbon (DIC) occurs as bicarbonate ions (HCO_3^-), ~9% are carbonate ions (CO_3^{2-}) and the remaining 1% are dissolved CO_2 (Doney et

al., 2009). As CO_2 concentrations increase in seawater, aqueous CO_2, bicarbonate and hydrogen ion concentrations all increase.

Consequently, carbonate ion concentrations (CO_3^{2-}) decline because of the increasing H^+ concentrations. The decrease in CO_3^{2-} reduces the saturation state of calcium carbonate ($CaCO_3$), which is a biologically important mineral. The extent of $CaCO_3$ dissolution in the water column determines the ability of the ocean to absorb atmospheric CO_2 over long time scales (Doney et al., 2009; Feely et al., 2009). Additionally, many marine organisms actively secrete the mineral $CaCO_3$ in order to form their shell or skeleton such as planktonic coccolithophores, pteropods and invertebrate molluscs and corals (Doney et al., 2009; Feely et al., 2009). Thus, a third important reaction refers to the formation and dissolution of solid calcium carbonate minerals ($CaCO_3(s)$):

$$CaCO_3(s) \leftrightarrow CO_3^{2-} + Ca^{2+}$$

$CaCO_3$ formation and dissolution varies with saturation state (Ω), which is the ion product of calcium and carbonate ion concentrations:

$$\Omega = [Ca^{2+}][CO3^{2-}] / K'_{sp}$$

K'_{sp} depends on temperature, salinity, pressure and mineral phase (calcite or aragonite). Calcite and aragonite are the two main skeletal $CaCO_3$ polymorphs. Aragonite is a more soluble form of calcium carbonate than calcite, but a high magnesium calcite is even more soluble than aragonite (Doney et al., 2009; McNeil and Matear, 2008).

Increasing levels of atmospheric CO_2 drive changes in seawater carbonate chemistry, which threaten marine ecosystems. As atmospheric CO_2 increases, seawater CO_2 increases, and seawater pH and saturation state both decrease (Figure 1.2). However, pH is determined by the ratio of dissolved concentration of CO_2 to carbonate ions, while saturation state is largely controlled by absolute carbonate ion concentration. Consequently, changes in pH are often associated with changes in physiological processes (i.e. hypercapnia), while changes in saturation state are particularly important for shell development and growth (Waldbusser et al., 2015). It is important to understand both large-scale pH changes due to anthropogenic causes and pH fluctuations due to biological activity in order to examine their potential interactive effects.

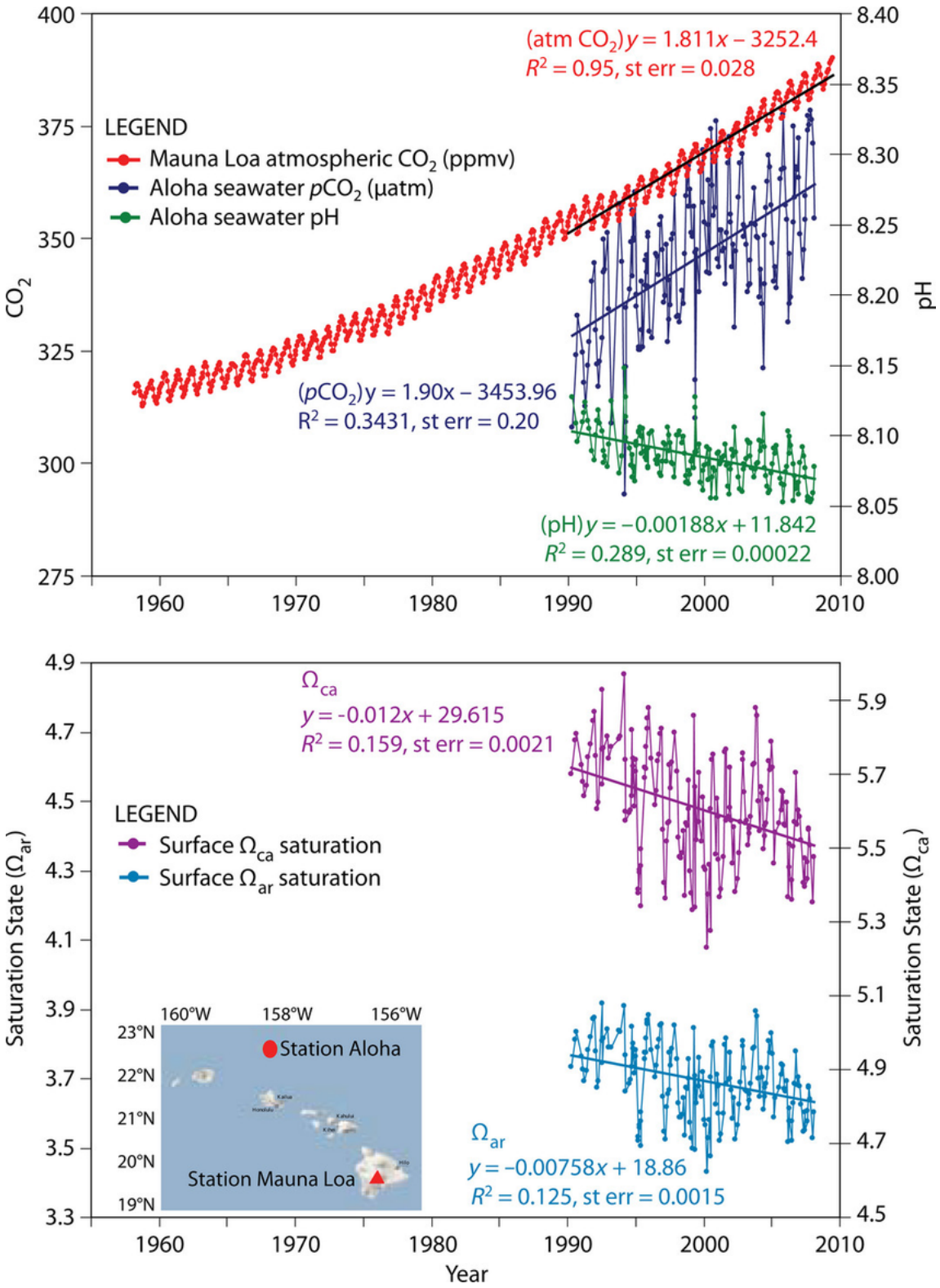

Figure 1.2 TOP: Time series of atmospheric CO_2 (red), oceanic pCO_2 (dark blue), and surface seawater pH (green) in the subtropical North Pacific Ocean. BOTTOM: Time series of oceanic calcite (purple) and aragonite (light blue) saturation state. Atmospheric CO_2 conditions were recorded from Station Mauna Loa and oceanic carbonate system conditions were recorded at Station Aloha (see insert map). As atmospheric CO_2 (red) increases, seawater pCO_2 (dark blue) increases and seawater pH (green) aragonite saturation state (light blue) and calcite saturation state (purple) decrease. As taken from Feely et al. (2009). Ocean acidification: Present conditions and future changes in a high-CO_2 world. *Oceanography* 22(4): page 38 with permission.

1.4 Effects of OA on marine ecosystems

Ocean acidification poses a major global threat to the ocean with widespread impacts on marine ecosystems (Kroeker et al., 2013; Doney et al., 2009; Orr et al., 2005; Feely et al., 2009). Marine organisms, from phytoplankton to fish, possess varying sensitivities to changes in seawater carbonate chemistry and their species-specific responses to OA could cause profound ecological shifts (Kroeker, 2010). This study focused on some of the key trends in biological impacts of ocean acidification, as reported by previous meta-analyses:

1. Calcification is the most sensitive process to OA. Heavily calcified organisms, such as coralline algae and echinoderms as used in this study, are more susceptible to OA and consequently, often the most negatively impacted (Kroeker, 2010; Kroeker et al., 2013).

2. Ocean acidification conditions and its accompanying carbonate chemistry changes often yield significant, negative effects on survival, growth, calcification and reproduction across a broad range of marine organisms, as seen in both CCA and echinoderms (Kroeker, 2010; Kroeker et al., 2013).

3. Biological responses to OA vary across taxonomic groups, life-history stages, and trophic levels (Harvey et al., 2013; Kroeker, 2010; Kroeker et al., 2013; Dupont et al., 2010a; Hendriks I.E., 2010). Early life history stages such as the larval and juvenile stages of echinoderms are thought to be particularly vulnerable (Kurihara, 2008).

4. Ocean acidification will not happen in isolation. Synergistic effects, such as the combined effects of ocean warming and acidification, have the potential to cause much stronger biological effects on marine organisms (Kroeker et al., 2013; Harvey et al., 2013). Additionally, natural pH fluctuations, such as those found in the diffusion boundary layer, can cause different biological effects than under stable pH conditions (Wahl et al., 2015b).

Consequently, this work examined the effects of natural pH fluctuations in the diffusion boundary layer above a heavily calcified photoautotroph (crustose coralline algae) on the early life stage of a marine calcifier (juvenile sea urchin *Pseudechinus huttoni*).

1.4.1 Effects of OA on calcification

Ocean acidification poses particularly major threats to calcifying organisms that produce shells, tests, or skeletons out of calcium carbonate (Hendriks I.E., 2010; Kroeker, 2010; Kroeker et al., 2013). The rate of calcification in organisms is linked to the seawater carbonate saturation state (Andersson et al., 2008; Marubini et al., 2003; Langdon et al., 2000). Thus, decreasing seawater saturation states due to OA may lead to net dissolution of carbonate structures as saturation states will be too low to support biogenic calcification (Hofmann et al., 2010). Under these conditions, marine calcifiers may experience unprecedented challenges and alteration to their function, structure and distribution with a lessened ability to compete for space and other important resources (Andersson et al., 2008).

Calcifying organisms in cold high latitude waters, such as the organisms used in this study, are even more at risk. Presently, saturation states are lowest in cold high-latitude regions and at depth (Doney et al., 2009; Feely et al., 2009), where colder water absorbs more CO_2 and is naturally lower in calcium carbonate concentration (McNeil and Matear, 2008). Assuming surface ocean CO_2 equilibrium with the atmosphere, the Southern Ocean (south of 60°S) is predicted to begin to experience aragonite undersaturation by the year 2050 (as shown in Figure 1.3), (McNeil and Matear, 2008). Consequently, organisms in these high-latitude environments will be the first to experience these seawater changes and are predicted to be especially vulnerable to seawater carbonate chemistry changes. There is already an overarching trend of decreasing magnesium (Mg) content in calcitic skeletons as a function of increasing latitude (Andersson et al., 2008). This is most likely due to the slower growth rate of these organisms in decreasing seawater carbonate saturation state and colder temperatures, a pattern also seen in sea urchins (Clark et al., 2009; McClintock et al., 2011; Andersson et al., 2008). Both focus organisms in this study, CCA and *P. huttoni* were selected as calcifying marine organisms that can be found in relatively high-latitude environments, and thus potentially extremely susceptible to OA.

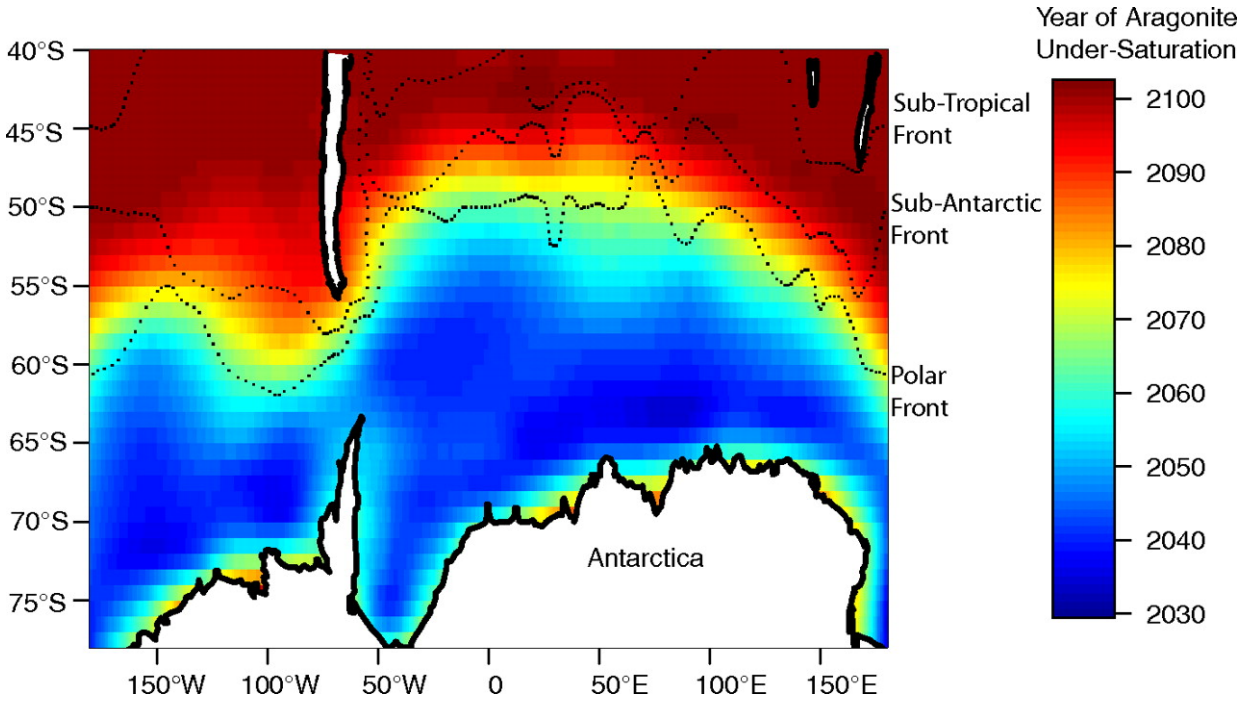

Figure 1.3 A contour plot of the year in which the onset of aragonite undersaturation in wintertime will occur under equilibrium conditions in the Southern Ocean. As taken from McNeil and Matear (2008). Southern Ocean Acidification: A tipping point at 450-ppm atmospheric CO_2, PNAS, 105: page 18863 with permission.

1.4.2 Effects of OA on crustose coralline algae

Crustose coralline algae (CCA) are key components of marine ecosystems, a widely distributed calcifying primary producer, and among the most abundant marine organisms that live on hard substratum in the photic zone (Steneck, 1986). CCA are the completely calcified or non-geniculate form of coralline algae (Nelson, 2009). They are found in rocky reefs in coastal ecosystems from the tropics to the poles (Nelson, 2009). There are many species of CCA, but New Zealand CCA are difficult to identify—the species can't be determined without detailed genetic analysis of reproductive material (Farr et al., 2009). Thus, for the purposes of this study, CCA refers to a mixed algal assemblage. Coralline algae are a crucial part of marine ecosystems and can induce larval settlement in a range of species through chemical settlement cues (Nelson, 2009). CCA provide refuge, grazing areas and settlement substrates for marine invertebrates such as molluscs (Roberts, 2001), corals (Morse et al., 1996) and sea urchins (Lamare and Barker, 2001). Coralline algae were selected for this study because they are a calcifying primary producer, abundant on the New Zealand coastlines, and a key settlement substrate for marine larvae such as sea urchins (Shears, 2007).

Calcifying algae are considered the most susceptible of all calcifiers to ocean acidification (Kroeker et al., 2013). CCA are thought to be additionally vulnerable to OA because they primarily precipitate high magnesium calcite in their cell walls (Kamenos et al., 2016) and high Mg calcite is one of the most soluble forms of biogenic $CaCO_3$ (Weiner and Dove, 2003). Thus, as pH decreases with OA, this form of calcium carbonate that CCA are composed of is increasingly susceptible to dissolution (Ries, 2006; Ries, 2011; Kamenos et al., 2016; Roleda et al., 2015; Cornwall et al., 2013a). Negative effects of OA on CCA include reductions in growth (Hofmann et al., 2012; Ragazzola et al., 2012), calcification (Gao and Zheng, 2010), distribution/abundance (Kuffner et al., 2008; Hall-Spencer et al., 2008; Porzio et al., 2011) and morphology (McCoy and Kamenos, 2015; Kamenos et al., 2016).

As key components of marine ecosystems, the direct impacts of OA on CCA will also have indirect impacts on ecological dynamics (McCoy and Pfister, 2014). Since CCA is a key settlement substrate and habitat for juvenile organisms, the ability of CCA to maintain settlement cues under OA is of key concern (reviewed by Espinel et al. 2018). Coralline algae exposure to low pH showed negative impacts on the algae, and reduced induction of settlement in larval corals *Acropora millepora* and *Acropora tenuis* (Webster et al., 2013), coral-eating crown of thorns sea stars (*Acanthaster* cf. *solaris*) (Uthicke et al., 2013) and the

larval sea urchin *Heliocidaris erythrogramma* (Huggett et al., 2018). However, exposure to low pH of four CCA genera from California didn't impact the ability of CCA to provide settlement cues to larval abalone *Haliotis rufescens* (O'Leary et al., 2017). While the exact outcomes remains unknown, CCA play a critical role in determining the fate of benthic coastal waters under ocean acidification conditions, in terms of both direct effects on their ability to grow and indirect effects on invertebrate population dynamics.

1.4.3 Effects of OA on sea urchins (echinoderms) and early life stages

Sea urchins are a Class (Echinoidea) of echinoderms, a significant and extensive presence in many marine ecosystems and a taxa predicted to be particularly vulnerable to OA (Dupont et al., 2010b). The *Pseudechinus* genus consists of 11 species of sea urchins, all restricted to the Southern hemisphere (McKnight, 1969; Kirby et al., 2006). The species used in this study, *Pseudechinus huttoni*, is endemic to New Zealand and can be found along New Zealand's continental shelf (<60m) and southern fjords (Kirby et al., 2006; McClary and Sewell, 2003).

Echinoderms are heavily calcified, benthic taxa typically with indirect lifecycles involving the transition from a pelagic to benthic environment during development (Dupont et al., 2010b). Echinopluteus larvae, which are generally planktotrophic, will develop from four to six to eight arms, with the ciliated arms used for swimming and suspension feeding. Sea urchin larvae also develop a juvenile rudiment as they reach competency to settle and metamorphose (Chino et al., 1994). During this stage, sea urchins transition from larvae to juveniles, which involves a switch from a pelagic to benthic environment (Dupont and Thorndyke, 2013). Larvae use a range of environmental signals to determine where to settle and metamorphose (Hadfield and Paul, 2001). During settlement, a pelagic echinopluteus larva descends to the seafloor and moves upon a substrate with or without attaching to it. Settlement is a reversible process, referring to all behaviours prior to loss of the swimming organs. Metamorphosis, on the other hand, is an irreversible process and includes the emergence of juvenile/adult-specific structures (Hadfield and Paul, 2001). For sea urchins, larval structures such as the arms and larval gut and mouth are reabsorbed and lost, while adult features such as spines, pedicellariae and tube feet increase. The early juvenile or post-settlement stage is considered to be especially sensitive to environmental stressors and a potential population bottleneck, determining population abundance and distribution as well as community structure (Wolfe et al. 2013, Gosselin and Qian 1997). Additionally, the complex lifecycle involving a shorter planktonic larval stage, followed by transition to a longer benthic adult stage makes early life

history stages particularly vulnerable to OA (Byrne, 2011; Byrne et al., 2017; Hofmann et al., 2010; Espinel-Velasco et al., 2018).

Sea urchins are generally thought to be more susceptible to the effects of OA because of their soluble, high-magnesium carbonate skeleton (McClintock et al., 2011), but some echinoderms have been found to be surprisingly robust to OA (Dupont et al., 2010b). The effects of OA have been documented in experimental studies across all life stages of echinoderms (Wolfe et al., 2013b; Byrne, 2011; Albright et al., 2012). Effects are varied and depend on the species and life-history stage (Byrne et al., 2009; Byrne et al., 2010b; Byrne et al., 2010c). General negative impacts on echinoderms include increased mortality, decreased fecundity, slower somatic and gonadal growth, and decreased growth rate (Dupont and Thorndyke, 2013; Siikavuopio et al., 2007; Dupont et al., 2010b; Stumpp et al., 2012; Havenhand et al., 2008). OA also leads to deleterious effects on development of larval echinoderms (see reviews by Dupont et al. 2010, Byrne 2011, Kroeker et al. 2013, Przeslawski et al. 2015, Byrne et al. 2017 and Espinel-Velasco et al. 2018). The study species in this work, *Pseudechinus huttoni*, displayed reduced survival, size and calcification in its larval stage at low pH; larval skeletons also degraded at low pH, although external morphology was unaffected (Clark et al., 2009).

While only a limited number of studies have focused on juvenile echinoids, the juvenile stage appears to be the most sensitive to OA, largely due to the high growth rates of this life history stage (Dupont and Thorndyke, 2013; Rodríguez et al., 2017; Byrne et al., 2010a; Albright et al., 2012; Wolfe et al., 2013b). Post-settlement development of invertebrates under OA conditions appears varied. Species such as corals show consistently reduced growth under low pH conditions (Albright et al., 2010; Albright and Langdon, 2011; Foster et al., 2015), but newly settled echinoderms display more diverse, sub-lethal and subtle responses. For example, OA showed no significant impacts on growth rate of the juvenile sea urchin *Loxechinus albus* in terms of diameter, vertical foraging speed or tenacity, but did significantly impact growth rate in terms of wet weight, metabolism and dissolution rate of empty urchin tests (Manríquez et al., 2017). Growth of a tropical sea urchin *Tripneustes gratilla* was slower at pH_{NBS} 7.6, but not 7.8 (Dworjanyn and Byrne, 2018). The survival and test growth of the juvenile sea urchin *Heliocidaris erythrogramma* were robust to low pH, and spine length decreased and morphology was altered under only the lowest pH levels (pH_T 7.4) (Wolfe et al., 2013b). Early benthic juveniles of the sea star *Parvulastra exigua* were tolerant of low pH, with negative effects seen only after four weeks at pH_T 7.24 (Nguyen and Byrne, 2014). Surprisingly, test diameter of the juvenile sea urchin *Paracentrotus lividus* was larger

when larvae and juveniles were reared at pH_{NBS} 7.7 compared to pH_{NBS} 8.1; however, the sea urchins in pH_{NBS} 7.7 also underwent metamorphosis eight days later which may account for some of these results (García et al., 2015). The lecithotrophic sea star *Crossaster papposus* developed faster in low pH with no visible effects on survival or skeletogenesis (Dupont et al., 2010b).

Some newly settled invertebrates appear sensitive to low pH, while others appear more resistant. Although low pH (at varying levels) appears to impair an organism's ability to calcify, thereby contributing to reduced growth rates, there are also other processes at play that may influence responses. For example, it remains unknown if post-settlement growth rates are altered due to physiological responses to low pH such as a change in metabolic rates or altered acid-base regulation (Espinel-Velasco et al., 2018).

One hypothesis to explain the surprising resilience of sea urchins to OA is that populations already exposed to variable pH levels in their natural environment are better suited to survive OA conditions because they are pre-adapted to living and growing in reduced pH (Dupont et al., 2010b). Due to their limited mobility, sea urchins may be more suited to survive OA conditions because they possess a strong plasticity and can thus acclimate to new environments overtime by modifying their morphology and physiology (Dupont et al., 2010b; Dupont and Thorndyke, 2013).

This study examines the crucial transition of a sea urchin from a pelagic environment with relatively constant pH levels to a benthic environment with natural fluctuating pH. The juvenile stage is necessary to maintain adult populations, and thus thought to be a potential population bottleneck in future OA conditions because of the high growth rates of this life history stage (Wolfe et al., 2013b). The early juvenile life stage of the calcifying sea urchin, *Pseudechinus huttoni* was selected as a study organism in this work because of its slow-flow fjord habitat with large natural pH fluctuations and documented negative effects of OA on the larval stage.

1.5 Implications of boundary layers for marine life under OA conditions

While boundary layers have long been studied as important processes for life in moving fluids, they have only recently been incorporated into studies of ocean acidification. Studying boundary layers is particularly important in order to understand the potential biological implications for OA because organisms with a thick DBL at their surface, or organisms living

within another organisms thick DBL, will experience a chemical and physical environment different than that of the mainstream seawater (Denny, 2000; Cornwall, 2013; Hurd et al., 2011). Physical processes such as seawater velocity control DBL thickness: slow flow conditions promote DBL thickness (Chan et al., 2016). Within the DBL, pH generally increases during the day and decreases at night due to metabolic processes (photosynthesis and respiration) controlled by light (Hurd et al., 2009; Cornwall et al., 2013b).

Three main hypotheses on the effects of a DBL on organisms under OA conditions have emerged. The DBL may (1) act as a temporary refuge from OA. Calcifiers may be exposed to corrosive low pH for shorter periods of time when pH is increased during the day (Wahl et al., 2018; Wahl et al., 2015b; Cornwall et al., 2014; Noisette and Hurd, 2018; Melzner et al., 2009). The DBL may also (2) act as a training ground for large daily pH fluctuations. Calcifiers who already live in these fluctuating pH environments may be pre-adapted and thus more tolerant to extreme pH levels. Fluctuating environments may have pre-selected for organisms with a higher phenotypic plasticity or more robust genotypes (Wahl et al., 2018; Wahl et al., 2015b; Noisette and Hurd, 2018; Melzner et al., 2009; Hurd et al., 2011; Boyd et al., 2016). Alternatively, the DBL may (3) already cause organisms in these fluctuating pH environments to be at extremely high levels of stress. Organisms in the DBL may not be able to cope with future changes in pH and will be pushed outside their tolerance threshold (Boyd et al., 2016; Hofmann et al., 2011). If this hypothesis is true, the effects of OA may therefore be underestimated by not incorporating these pre-existing, biologically driven fluctuations in pH.

These hypotheses have begun to be explored on the calcifiers that create the DBL, such as macroalgae (Hurd et al., 2011; Cornwall et al., 2013a; Cornwall et al., 2014; Cornwall et al., 2017; Cornwall et al., 2013b; Hendriks et al., 2017; Noisette and Hurd, 2018) and corals (Chan et al., 2016; Larkum et al., 2003), but effects on early life stages within the DBL are not well understood (Koehl and Hadfield, 2010). In support of the first hypothesis, slow flow conditions have been found to act as a refuge for some bioengineers that create a thick DBL, ameliorating some of the negative impacts of OA (Cornwall et al., 2014; Hurd, 2015; Noisette and Hurd, 2018). In low pH (pH_T 7.65), coralline algae grown in thick DBLs were able to maintain net growth and calcification, whereas algae in thin DBLs displayed net dissolution (Cornwall et al., 2014). The ability to modify local seawater pH, thereby creating boundary layers, may allow CCA the potential to ameliorate some of the negative effects of OA for both CCA and surrounding organisms. Additionally, as outlined by the second hypothesis,

macroalgae may be pre-adapted to living in environments with large pH fluctuations. The coastal environments in which CCA typically grow, already experience relatively large local fluctuations in seawater carbonate chemistry, which may impact their ability to respond to OA (Cornwall et al., 2013a). pH changes in coastal water occur due to both coastal acidification, driven by eutrophication and increased nutrient loading to estuaries, and biological activity (Wallace et al., 2014). The same metabolic processes that control seawater pH fluctuations on the µm to mm scale in the diffusion boundary layer also control seawater pH fluctuations on a larger (m to km) scale in coastal environments (Cornwall et al., 2013a).

Other organisms, besides macroalgae, that live in fluctuating pH environments have also demonstrated potential resilience to OA, in support of both the first and second hypotheses. The blue mussel, *Mytilus edulis* was able to shift the majority of calcification activity to the daytime, when photosynthesis of nearby macroalgae raised pH in the surrounding microenvironment (Wahl et al., 2018). This allowed the mussels to maintain calcification even under low pH conditions. Additionally, calcareous tubeworms, *Spirorbis spirorbis*, that live in boundary layers above algae, showed no significant difference in growth rates between ambient and elevated (1100ppm) pCO_2 conditions (Ni et al., 2018). The authors concluded that the tubeworms are resistant to the effects of acidification. It is possible that the tubeworms are either adapted to living at a variety of pH levels or boundary layers could have buffered the tubeworms during the experiment.

Boundary layers play a crucial role in determining the pH conditions that bioengineers and surrounding small (less than ~2 mm) marine organisms experience, thus boundary layers will also play a critical role in modulating the effects of reduced seawater pH associated with OA (Wahl et al., 2015b; Cornwall et al., 2014). However, algal boundary layers are rarely considered when studying the effects of reduced seawater pH on the settlement and early post-settlement growth of sea urchins (Chan et al., 2016). Newly settled juveniles are likely living in pH conditions different from the bulk seawater, which may account for some of the variability found in invertebrate responses to OA. Natural pH fluctuations may alter impacts of OA, but it remains unknown whether they amplify or mitigate the effects of reduced seawater pH (Wahl et al., 2018; Wahl et al., 2015b; Shaw et al., 2012). The direct effects of varying boundary layer seawater pH on larval settlement and early post-settlement growth, and subsequent implications for OA conditions, remain unknown (Espinel-Velasco et al., 2018). This study aimed to address this by manipulating the boundary layer through water flow and biological activity via irradiance, in different bulk seawater pH conditions, in order

to investigate the effects of pH levels in coralline algal diffusion boundary layers on the growth of newly settled sea urchins *Pseudechinus huttoni*.

1.6 Study aims

The aim of this study was to quantify the pH conditions within coralline algal diffusion boundary layers that change as a result of irradiance, flow and bulk seawater pH, in order to examine the effects of these variable conditions on growth of juvenile sea urchins *Pseudechinus huttoni* in the DBL. While previous studies have examined the diffusion boundary layers above various species of marine algae and other marine organisms, this is the first study to expose marine invertebrates to different DBL conditions in order to examine the direct impacts of boundary layers on growth of marine organisms. For this, two research questions were addressed:

1. **What is the variability of pH and oxygen fluctuations in coralline algal diffusion boundary layers?**

In order to address this question, oxygen concentrations were measured above CCA in experimentally manipulated irradiance, flow and bulk seawater pH conditions using an annular flume, making it is possible to demonstrate how different processes control the chemical conditions and thickness of the DBL. Additionally, oxygen concentrations were measured above CCA in different flow and irradiance treatments and irradiance and bulk seawater pH treatments---the same conditions that newly settled juvenile sea urchins were grown in to examine development. Oxygen was used as a proxy for pH based on previous research (Cornwall et al., 2014). It was predicted that in both ambient and reduced bulk seawater pH, crustose coralline algae will alter their chemical environment within the DBL as a result of flow and irradiance conditions (Figure 1.4). Oxygen/pH would increase in the light and decrease in the dark. The DBL will be thicker at zero or slow flow speeds.

2. **How does the variability of pH and oxygen in coralline algal diffusion boundary layers affect post-settlement growth of the sea urchin *Pseudechinus huttoni* and what are the potential implications for ocean acidification conditions?**

In order to address this question, test diameter and spine length measurements were used to examine the ability of newly settled sea urchins *Pseudechinus huttoni* to grow and calcify at different pH levels in coralline algal diffusion boundary layers. The pH levels in the DBL

were generated by experimental manipulations of irradiance, flow and bulk seawater pH. Scanning electron microscopy was also used to further characterize calcification and growth in experimental conditions. It was predicted that low pH within the DBL will reduce growth of the test and spines of newly settled *P. huttoni*, but that in OA conditions (reduced bulk seawater pH), daytime diffusion boundary layers above CCA will be able to increase local pH levels enough to allow normal growth and calcification of *P. huttoni* (Figure 1.5).

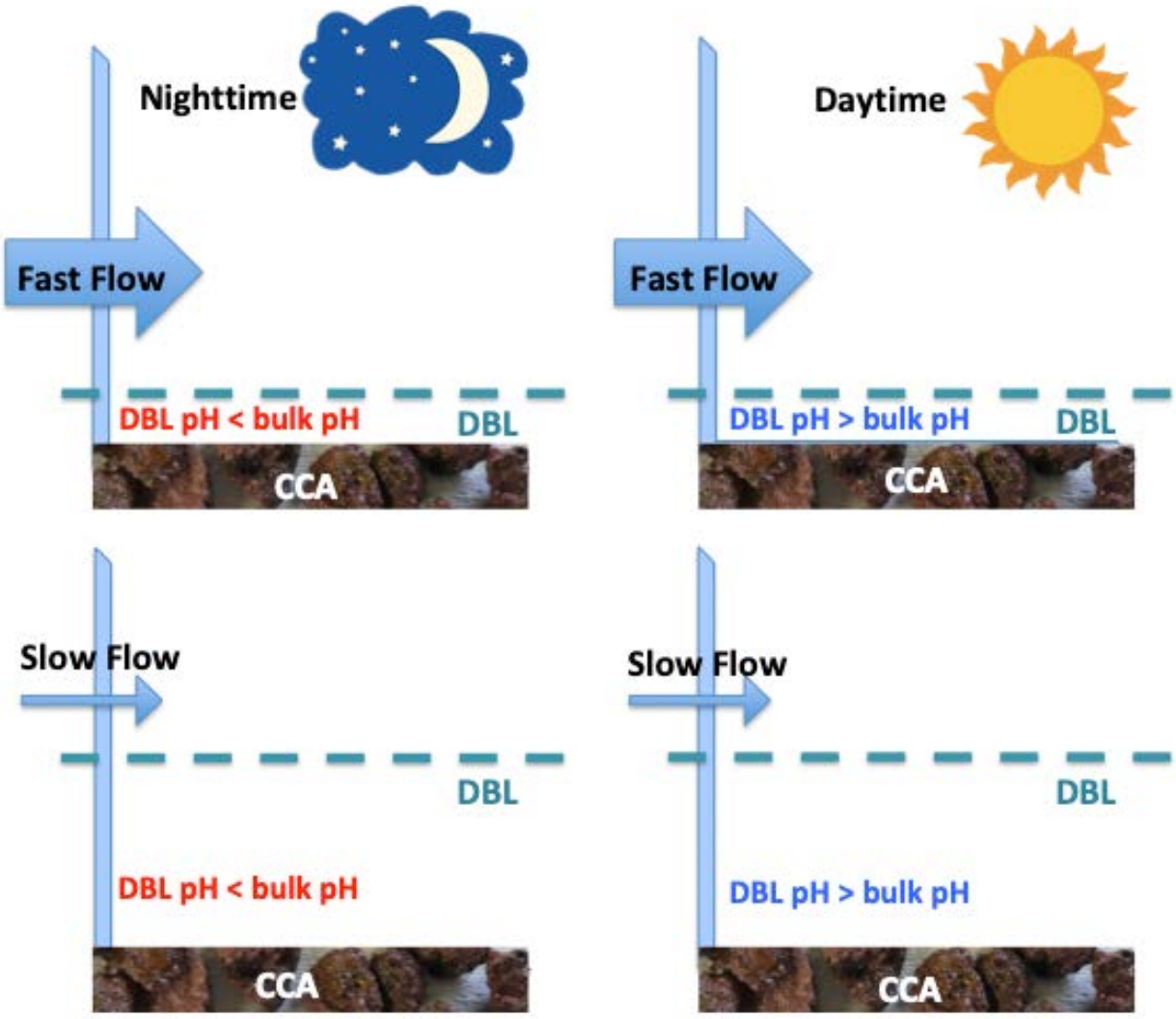

Figure 1.4 Schematic displaying predicted effects of flow and irradiance on diffusion boundary layer (DBL) thickness and pH levels within the DBL above crustose coralline algae (CCA). It is hypothesized that the DBL, as indicated by the blue dashed line, will be less thick in fast flow (top row) than slow flow (bottom row). pH within the DBL will be lower than bulk seawater pH in the dark at night (left column), and higher than bulk seawater pH in the light during the day (right column).

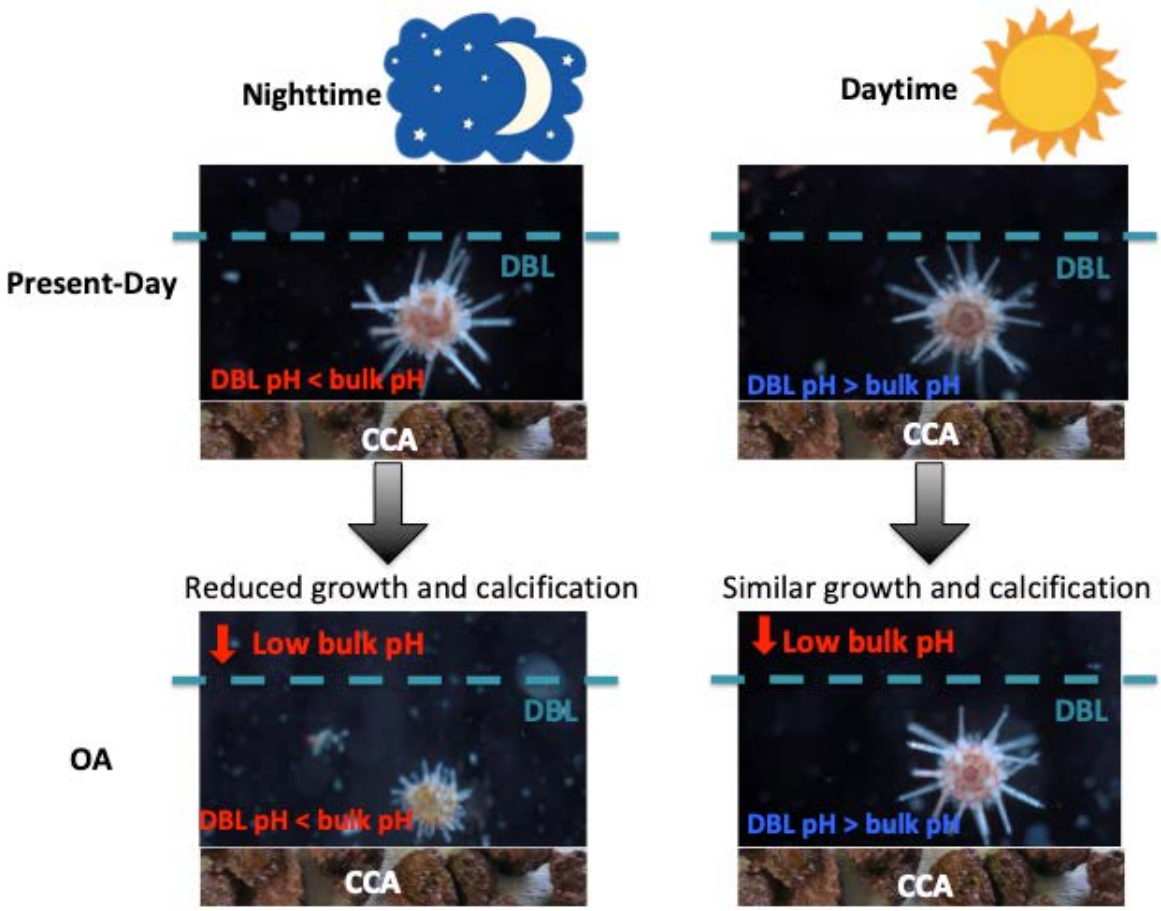

Figure 1.5 Schematic displaying predicted effects of coralline algal diffusion boundary layers on the growth of newly settled sea urchins *Pseudechinus huttoni*. It is hypothesized that in the dark, growth will be reduced in OA conditions (low bulk seawater pH), but in the light, growth will be similar in OA (low bulk seawater pH) and present-day (ambient bulk seawater pH) conditions due to increases of pH within the diffusion boundary layer (DBL, as represented by the blue dashed line).

Chapter 2: Coralline algal diffusion boundary layers

2.1 Introduction

As an abundant and widely distributed calcifying primary producer, crustose coralline algae (CCA) are key components of marine ecosystems because they are important bioengineers that can modify their surrounding environment, and provide habitat for marine invertebrates (Steneck, 1986; Shears, 2007; Hadfield and Paul, 2001). Corallines provide food, refuge and settlement substrates for many invertebrates including pāua (Roberts, 2001), corals (Morse et al., 1996) and sea urchins (Lamare and Barker, 2001). In the face of changing seawater chemistry, macroalgae such as CCA are of particular importance because they can alter the local seawater pH through biological processes such as photosynthesis, respiration and calcification, on both a millimetre scale in the diffusion boundary layer and a kilometre scale in coastal environments (Cornwall et al., 2013a). Within the DBL, photosynthesis increases pH while calcification and respiration both decrease pH (Hurd et al., 2009; Cornwall et al., 2013b). Physical processes such as seawater velocity control the magnitude of these pH changes (Cornwall et al., 2013b). The ability to modify local seawater pH, thereby creating boundary layers, may allow CCA the potential to modulate some of the effects of OA for both CCA and surrounding organisms. During the day, pH within the DBL above CCA is higher than bulk seawater pH, thus providing potential areas of refuge for calcifying organisms in future reduced bulk seawater pH.

This chapter explored the variability in pH and oxygen in coralline algal diffusion boundary layers, which are the conditions that small (~ less than 2 mm) calcifying marine organisms experience when they have settled on algal covered substrates. To demonstrate how different processes control the DBL, irradiance, flow and bulk seawater pH were experimentally manipulated in different experimental set-ups. For this, I firstly measured oxygen concentrations above CCA covered discs in known flow, irradiance and bulk seawater pH conditions using an annular flume. Secondly, I measured oxygen concentrations above CCA covered rocks in different flow, irradiance and bulk seawater pH conditions that juvenile sea urchins *Pseudechinus huttoni* were grown in during following experiments (see Chapter 3). While the conditions differed in the two set-ups due to experimental constraints, making direct comparison difficult, methodology was kept as similar as possible in order to extrapolate findings from one method to the other. Oxygen was used as a proxy for pH based on previous research (Cornwall et al., 2014; Noisette and Hurd, 2018; Chan et al., 2016; Cornwall, 2013).

2.2 Methods

2.2.1 Collection of settlement substrates

The substrates used in this work include rocks with CCA coverage (0.5-2 cm diameter and 4-7 cm diameter) and acrylic settlement discs with CCA coverage (5 cm diameter) (Figure 2.1). All rocks were collected at low tide on South Beach, a rocky shore adjacent to the Portobello Marine Laboratory (PML), Otago Harbour, New Zealand (45° 49' 40.74" S, 170° 38' 26.02" E) in July and August 2018. Rocks collected in the 4 to 7 cm diameter range were aimed o have an estimated 80% coverage of CCA on at least one side, while rocks collected in the 0.5 to 2 cm diameter range had an estimated 80% coverage overall. The settlement discs, 5 cm in diameter and made of PVC, were deployed and collected from a study site in Butterfly Bay, Karitane/Huriawa Peninsula, Otago (45°38´20.58´´S, 170°40´19.38´´E). This site is located 28 km north of Dunedin on the east coast of the South Island, New Zealand. Prior to deployment, one side of each disc was sanded to encourage the attachment of organisms, while the other side remained unmodified. Discs were deployed in August 2016 in the subtidal zone, at 10 m depth, close to permanent oceanographic moorings. The discs were attached to leaded rope and placed underneath the natural algal canopy, parallel to the shore. At 10 m depth at this site, the benthic communities are dominated by macroalgae, particularly *Ecklonia radiata* and small turfing rhodophytes. The surrounding boulders and rocky reefs are thickly covered in mixed CCA communities (Shears, 2007; Shears and Babcock, 2004a; Shears and Babcock, 2004b). In July 2018, the discs were collected and removed from the study site and transported back to PML. During collection and transport, discs were kept out of sunlight and were exposed to the air for as short a time as possible to prevent any damage to the organisms on the disc. At PML, the discs were immediately submerged in seawater in an insulated container to reduce temperature stress. The discs with the most CCA coverage were utilised in experiments and oxygen profiles were completed over the part of the disc with the most CCA coverage. Rocks and discs were then kept at PML in flow-through tanks (approximately 1 m x 1 m x 0.5 m) with UV treated seawater from the Otago Harbour. Typically during winter and spring, seawater from the Otago Harbour has salinity 33 ppt and temperature 7-11°C (Nelson, 2016). Rocks and discs were covered with mesh to limit excessive light until use in experiments. Additionally, prior to use in experiments, stainless steel washers were attached to the discs with silicone glue to force the disks to sink, and all rocks were visually examined for extraneous organisms and any organisms seen were removed using a scalpel.

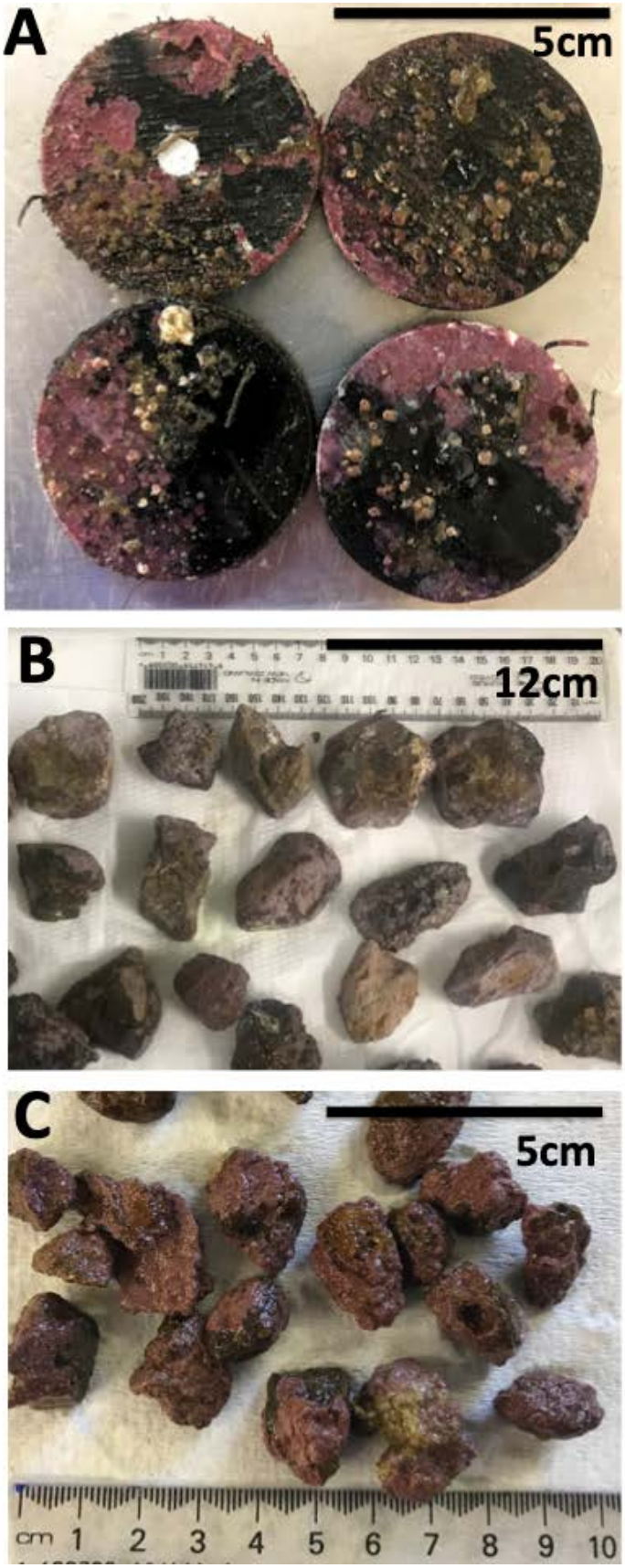

Figure 2.1 Examples of the three substrate types used during the experiments: (A) 5 cm diameter acrylic "settlement" discs covered with a mixed algal assemblage, (B) 4 to 7 cm diameter rocks covered with CCA and (C) 0.5 to 2 cm diameter rocks covered with CCA. Scale bars are (A) 5cm, (B) 12 cm and (C) 5 cm.

2.2.2 Experimental design

Oxygen profiling took place in three different experimental set-ups: (1) an annular flume, (2) 2.5 L glass jars, and (3) 3 L plastic aquaria (Table 2.1; Figure 2.2). The three different designs were used in order to test three experimental aims. In order to demonstrate how different processes control the chemical conditions and thickness of the DBL, the annular flume was used to examine the oxygen and pH variability in the DBL under quantifiable flow speeds, irradiance and bulk seawater pH. The 2.5 L glass jars were used to examine the effects of experimentally manipulated flow and irradiance on the DBL, and the subsequent effects on growth of newly settled sea urchins *Pseudechinus huttoni* (see Chapter 3). Lastly, in order to understand the implications for ocean acidification conditions, the 3 L aquaria were used to examine the effects of experimentally manipulated irradiance and bulk seawater pH on the DBL, and the subsequent effects on growth of newly settled *P. huttoni*. *P. huttoni* juveniles were grown in only the 2.5 L glass jars and 3 L aquaria due to necessary experimental replication. Oxygen was used as a proxy for pH based on previous research (Cornwall et al., 2014). Since factors, including surface topography, flow speed, and CCA coverage, varied in the different experimental set-ups, direct comparison is difficult, but as many factors as possible were kept similar in order to allow for extrapolation of results.

Table 2.1. Summary of experiments measuring oxygen concentrations in order to examine the effects of irradiance, flow and bulk seawater pH on the diffusion boundary layer (DBL) and post-settlement growth of *Pseudechinus huttoni* in the DBL.

Container	CCA Substrate	Treatment Levels	Sea Urchin Experiment # (Chapter 3)	Aim (Chapter 2 and 3)
annular flume	5 cm discs	2 flow (5.5 cm s^{-1} and 1 cm s^{-1}) x 2 irradiance (light and dark) x 2 bulk pH (7.4 and 8.1)	–	Characterize DBL in known flow, light and pH conditions
2.5 L glass jars	4 to 7 cm diameter rocks	2 flow (flow and no flow) x 3 irradiance (light, dark and 12h:12 h alternation)	Experiment # 1 Experiment # 2 Experiment # 3	Examine effects of irradiance and flow on DBL and post-settlement growth of *P. huttoni* in DBL
3 L aquaria	0.5 to 2 cm diameter rocks	2 irradiance (light and dark) x 3 bulk pH (7.4, 7.7 and 8.1)	Experiment # 4 Experiment # 5	Examine effects of irradiance and bulk seawater pH on DBL and post-settlement growth of *P. huttoni* in DBL

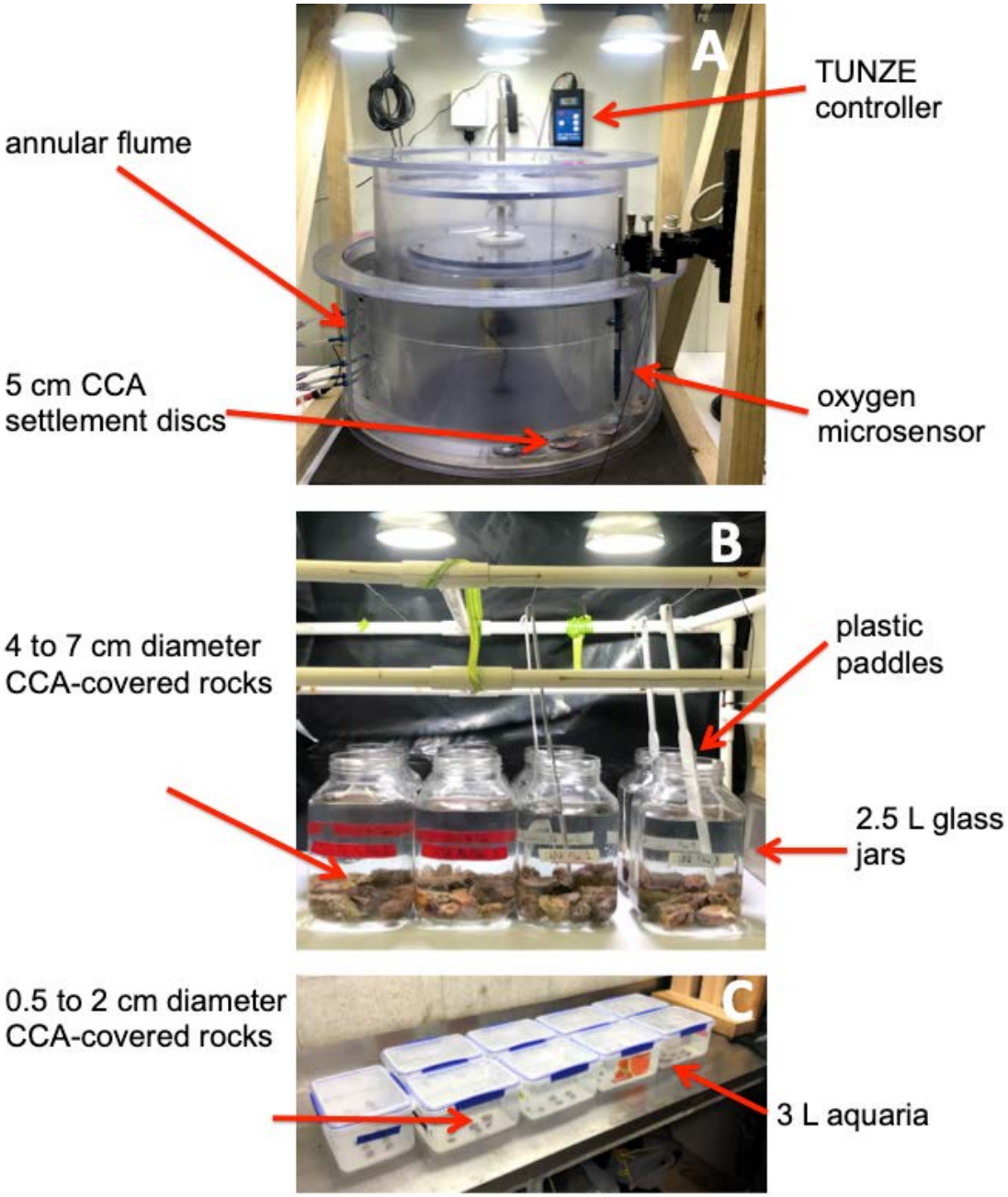

Figure 2.2 The experimental set-ups for oxygen profiling and rearing of *Pseudechinus huttoni* juveniles as discussed in Chapter 3. (A) The 40 L annular flume with 5 cm CCA discs on the bottom of the flume, an oxygen microsensor and a TUNZE pH controller in the background. (B) The 2.5 L glass jars with 4 to 7 cm diameter CCA covered rocks at the bottom. The four replicate glass jars on the left are in light and no flow; the jars on the right are in light and flow (generated by plastic paddles). (C) The 3 L aquaria with 0.5 to 2 cm diameter CCA covered rocks in the light.

The annular flume allowed for characterization of the DBL under quantifiable flow speeds. The flume is a 40 L annular (rotating-disc) flume. The flume has a 62 cm outer annulus, 42 cm inner annulus and channel width of 10 cm. The bed area is 0.17 m^2 and the maximum water depth is 30 cm with a maximum volume of 49 L (Widdows et al., 1998). Flow in the flume is generated by a computer-controlled rotating lid (Jones et al., 2011). Flow was measured using a Sontek micro-Accoustic Doppler Velocimeter (ADV) mounted on the system. Prior to filling the flume with 5 µm-filtered seawater at the beginning of every experiment day, four custom-built, quarter-circle acrylic inserts were placed on the bottom of the flume to create a smooth false bottom. One of these inserts had nine slots that were 1 cm thick and 5 cm diameter. Settlement discs (5 cm diameter) with partial coverage of a mixed assemblage of CCA were placed in these slots and the remaining slots were filled with dead or empty PVC discs (Figure 2.3).

Figure 2.3 A quarter-circle acrylic insert used to create a false bottom in the annular flume during oxygen profiling. The nine slots, 5 cm in diameter and 1 cm thick, were filled with 5 cm discs, either covered with a mixed algal assemblage or empty.

Four profiles were measured above the CCA discs in a total of eight treatments (two flow levels x two irradiance levels x two bulk levels). Flow speeds of 1 cm s^{-1} (slow) and 5.5 cm s^{-1} (fast) were achieved and controlled using the annular flume. Slow flow represents a "low flow" condition at which mass transfer can occur (Hurd, 2000). The 5.5 cm s^{-1} treatment represents a "fast flow" condition at which the DBL thickness is likely to be at its minimum (Cornwall, 2013; Hurd et al., 2011). Irradiance levels of 40 µmol m^{-2} s^{-1} (light) and <1 µmol m^{-2} s^{-1} (dark), thought to be representative of natural conditions, were achieved with overhead lighting (LED PAR38, 18W). Irradiance was measured using a flat underwater quantum sensor LI-250A (LI-COR, Lincoln, USA). Target bulk pH levels (pH_T) of 7.4 (low) and 8.1

(ambient) were measured spectrophotometrically using a Cresol purple dye (Dickson et al., 2007) and low levels were achieved and maintained using a TUNZE pH controller that adjusted pH by bubbling 100% CO_2 gas into the treatments as required (Cornwall et al., 2013b; Cornwall et al., 2014; Cornwall et al., 2013a). pH levels 7.4 represent ?, while pH levels 8.1 represent present day conditions.

The annular flume was filled with 5 µm-filtered seawater (temperature 11 ºC and salinity 33 ppt) from the flow through system of the laboratory at the beginning of every day of experiments. All flume profiles took place in a controlled-temperature room at 11ºC. When measuring oxygen profiles in ambient seawater, salinity and temperature were recorded at the beginning and end of each day of experiments, and pH was recorded at the end. Samples were taken for total alkalinity (A_T) and DIC once per day, at variable times. When measuring oxygen profiles in the low pH seawater, salinity, temperature and pH were recorded at the beginning and end of every day. After filling the flume with filtered seawater, 100% CO_2 gas was bubbled into the system using a TUNZE controller, calibrated with 4, 7 and 10 pH_{NBS} buffers to approximately pH_{NBS} 7.60. Water for total alkalinity (A_T) and DIC was taken twice a day—at the beginning and end of every day. pH_T was measured spectrophotometrically with a Cresol purple dye . Temperature and salinity were measured using an YSI Pro Plus 2030 meter (YSI, Yellow Springs, OH, USA). Samples for A_T and DIC were taken in 1L Schott bottles, immediately fixed with mercuric chloride, and later analysed at the University of Otago Chemistry Department.

In the 2.5 L glass jars, a minimum of four oxygen profiles were measured above 4 to 7 cm diameter CCA covered rocks in a total of four treatment combinations (two irradiance levels x two flow levels). Irradiance levels of 40 µmol photons m^{-2} s^{-1} (light) and <3 µmol photons m^{-2} s^{-1} (dark) were provided by overheard lights (LED PAR38, 18W). Irradiance was measured using a flat terrestrial LI-250A quantum sensor (LI-COR, Lincoln, USA). The two flow levels were “flow” and “no flow”. Flow was initiated using “urchin stirrers” or paddles that swing at a rate of 10 cycles per minute. Oxygen microprofiles were taken above CCA immediately next to the stirrer but not in the direct line of the urchin stirrer. “No flow” is characterized by zero flow (0 cm s^{-1}). In order to quantify flow, a dye experiment was completed to demonstrate the difference between the “flow” and “no flow” conditions. A 2.5 L glass jar, with rocks covering the bottom, was filled with freshwater. Saltwater mixed with a few drops of food colouring was slowly added to the bottom of the jar using a siphon and clamp system. The amount of time it took for the salty coloured water to be homogeneously

mixed was recorded with and without stirring. After one week, the jar with no flow was still not homogenously mixed, whereas the jar with "flow" took only 80 seconds to become homogenously mixed. This demonstrates that there are indeed two distinct flow conditions. "No flow" is dominated by a diffusion-dominated system and "flow" is a mixed system that breaks down boundary layers. However, flow speed in this experiment could not be specifically quantified.

In the 3 L aquaria, a minimum of four oxygen profiles was measured above 0.5 to 2 cm diameter CCA covered rocks in a total of six treatment combinations (two irradiance levels x three bulk pH levels). Irradiance levels of 10 μmol photons m^{-2} s^{-1} (light) and <1 μmol photons m^{-2} s^{-1} (dark) were provided by overheard lights (standard fluorescent tubes, 845). Irradiance was measured using a flat terrestrial LI-250A quantum sensor (LI-COR, Lincoln, USA). Target bulk pH levels (pH_T) of 8.1 (ambient), 7.7 (medium) and 7.4 (low) were achieved by using water from flow-through header tanks that were constantly maintained at each pH with a TUNZE controlled bubbling of 100% CO_2 gas into the system. In August 2018, water samples were taken to process for total alkalinity (A_T) and DIC. These water samples were taken in 1 L Schott bottles, immediately fixed with mercuric chloride, and later analysed at the University of Otago Chemistry Department. pH and temperature were recorded at the beginning and end of every profile. pH was measured spectrophotometrically using a Cresol purple dye and temperature was measured using a mercury thermometer.

2.2.3 DBL measurements

To quantify variation in the diffusion boundary layer (DBL), small-scale oxygen concentration changes were measured using an oxygen microsensor from the Unisense MicroRespiration System (Unisense, Aarhus, Denmark). These sensors are designed for high precision measurements of oxygen concentrations. The sensor was attached to a Unisense Microsensor Multimeter that was controlled by a Unisense automatic micromanipulator. Software programs SensorTrace Logger and SensorTrace Profiling were used to log data from the experiments (Figure 2.4). SensorTrace Logger was used to continuously log the equilibration period of the microsensor above the substrate. SensorTrace Profiling was used to log the microsensor profiles. At the beginning of every day of use, the oxygen probe was first pre-polarized with -0.80 V for at least 10 minutes and then calibrated in a fully aerated and anoxic solution in the SensorTrace Logger software. The aerated solution was prepared by vigorously bubbling air into seawater for at least 10 minutes. The signal (100% value) was recorded after water movement had stopped. The 0% value was recoded using an anoxic

solution. A 4 mL glass chamber was filled with a saturated sodium sulphate solution and then a glass lid with silicone tube was placed into the chamber to ensure no air bubbles were present. Using a syringe, the silicone tube was filled with seawater. The probe was then inserted into the silicone tube and the SensorTrace Logger program was used to track when all the oxygen in the tube was consumed and the reading stabilized (0% value). After calibration, the probe and substrate were set up for measurements.

The CCA substrate was placed in the respective container being used (annular flume, 2.5 L glass jar or 3 L aquaria) and the container was filled with 5 μm-filtered seawater. The microsensor was manually lowered with the micromanipulator until it was immediately above the surface of the substrate. This position is considered 0 μm. Due to fragility of the sensor, the tip could not actually touch the surface of the substrate every time. However, the use of an additional light source, a magnifying glass and small manual adjustments on the micromanipulator allowed the microsensor tip to get extremely close to the substrate surface. In this position, 40 min equilibration periods were allowed for the boundary layer of each treatment condition to build-up before vertical profiles began. Oxygen profiles were taken by using the micromanipulator to automatically raise the sensor and record oxygen concentrations (μmol L^{-1}) at each height. 60 seconds of measurements were taken at every height. The wait time between measurements was 0.1 s and the measurement period was 0.9 s, in which the Unisense program automatically averaged all the measurements over the 0.9 s measurement period. In the 2.5 L glass jars and 3 L aquaria, measurements were taken every 100 μm from 0 to 4 mm above the substrate and then every 1 mm from 4-10 mm. In the annular flume, measurements were taken every 100 μm from 0 to 2 mm above the substrate and subsequently every 1 mm from 2 to 10 mm. Of the 60 measurements at each height, the first and last 5 measurements at each height were discarded in case movement of the sensor affected readings. The remaining 50 measurements were averaged at each measurement height.

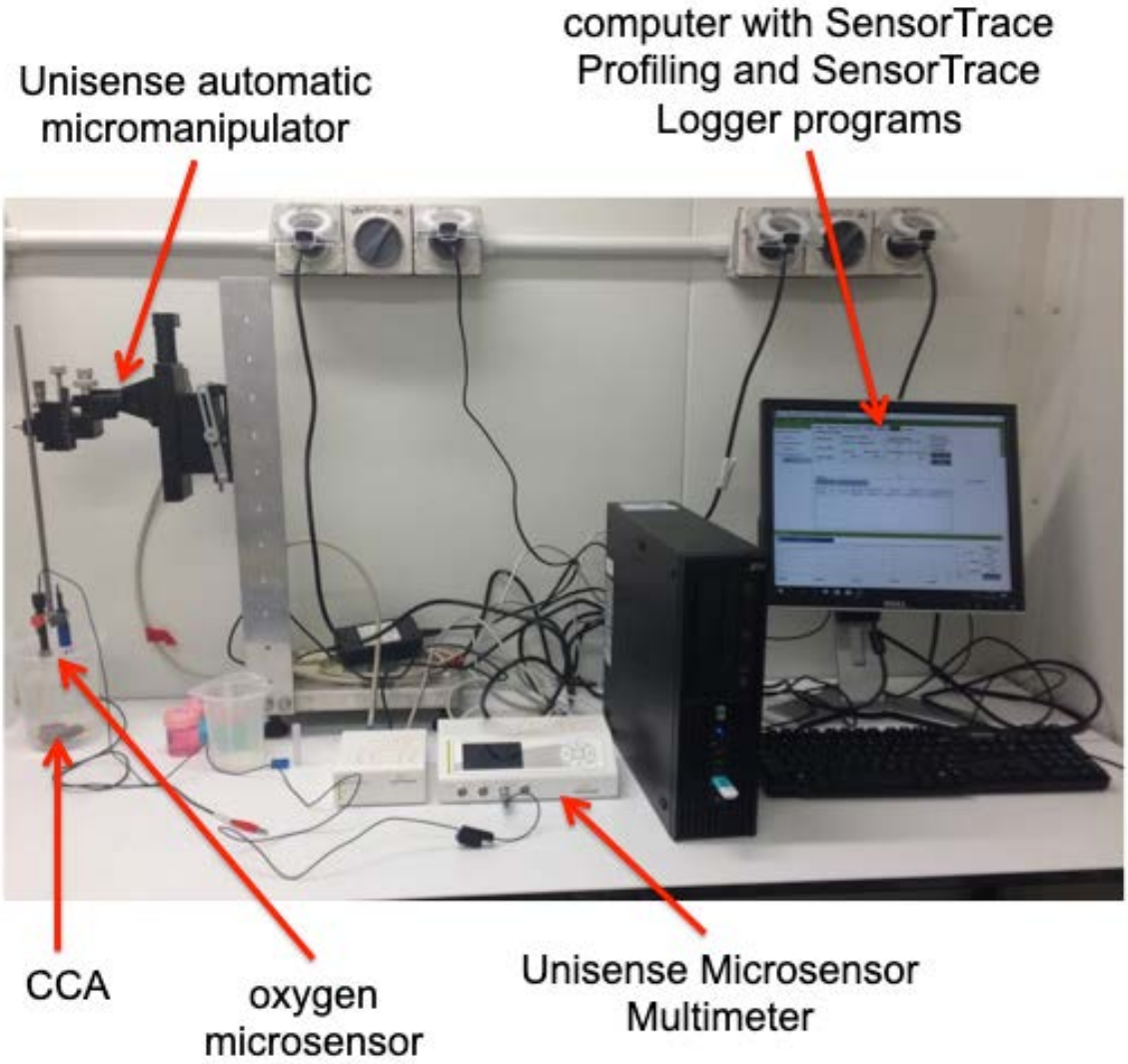

Figure 2.4 The equipment used to complete oxygen profiling. The computer with SensorTrace Profiling and SensorTrace Logger software were used to program the Unisense Microsensor Multimeter, which controlled the Unisense automatic mircromanipulator. The micromanipulator was used to raise and lower the oxygen microsensor above a CCA substrate.

2.2.4 DBL thickness

Diffusion boundary layer thickness was the distance above the surface of the CCA substrate at which the concentrations of O_2 (raw value) were <5% per 0.1 mm for four subsequent measurements. DBL thickness has previously been defined as the distance above the algae when changes were <10% (Cornwall, 2013; Cornwall et al., 2013b; Lichtenberg et al., 2017) and <1% (Hurd et al., 2011). 5% was used in these analyses because 1% was too small for a cut-off since bulk seawater concentrations didn't stay as constant due to the smaller volumes of seawater being used in the experiments, but 10% was too large to show adequate change, particularly in the dark conditions when raw oxygen values had smaller ranges. For two profiles in the light, the DBL was determined manually because of an unusual spike in oxygen concentration most likely due to movement in the electrode.

2.2.5 Oxygen profiles

In order to account for small variation among replicates in bulk seawater oxygen concentration, oxygen profiles were standardised by dividing the concentration at any given height by the bulk seawater concentration (the oxygen concentration 10 mm above the CCA substrate).

2.2.6 pH profiles

H^+ (pH) and O_2 concentrations have a strong relationship within the DBL (R^2=0.82) due to the uptake and release of CO_2 and O_2 during photosynthesis and respiration (Cornwall et al., 2014; Noisette and Hurd, 2018; Chan et al., 2016; Cornwall, 2013). The magnitude and direction of pH changes within the DBL have been found to be almost identical to changes in O_2 concentrations, with no statistical difference between DBL thickness measuring using changes in O_2 or H^+ (Cornwall et al., 2013b). Thus, O_2 can be used as a proxy for H^+ by estimating likely pH (Cornwall et al., 2014). Standardised O_2 concentrations were converted into H^+ concentrations using separate relationships for the light and dark treatments (as shown in Appendix 1) (Cornwall, 2013).

The H^+ and O_2 relationship in the dark (R^2=0.85) is defined by the formula:

$$y = 0.0621x^{-1.942}$$

where $y = H^+$ and $x = O_2$. The H^+ and O_2 relationship in the light (R^2=0.73) is defined:

$$y = 0.000004e^{-0.005x}$$

H^+ concentrations were converted into pH_T values using the equation $pH_T = -\log [H^+]$. pH values were standardised for each profile by dividing the concentration at any given height by the bulk seawater pH concentration to get pH deviation (pH units) in the DBL from the bulk (mainstream) pH. Next, estimated pH values were calculated by adding the pH deviation to the mean bulk seawater pH value for the respective treatment. All pH values in this experiment are reported on the total scale, unless specified otherwise.

2.2.7 pH_{DBL}

In order to estimate the pH conditions that juvenile *P. huttoni* were grown in during post-settlement growth experiments, pH was averaged from 0 to 0.5 mm above the CCA surface. 0

to 0.5 mm was chosen since newly settled sea urchins have an average test diameter of approximately 0.4 to 0.5 mm (see Chapter 3). Here within, pH_{DBL}, reported on the total scale, refers to the average pH from 0 to 0.5 mm above the CCA surface, or the average pH that newly settled *P. huttoni* on CCA substrates are experiencing.

2.2.8 Calcium carbonate saturation state

Average calcium carbonate saturation state (Ω_C) of the seawater from 0 to 0.5 mm above the surface of CCA, the area in which newly settled sea urchins are likely living in, was computed using the CO2SYS program, version 01.05 (Lewis and Wallace, 1998) from temperature, salinity, total alkalinity, and pH values. Temperature, salinity and total alkalinity values used were measurements (or means of measurements) made in the bulk seawater. pH values were pH_{DBL}, or the estimate of average pH from 0 to 0.5 mm above the CCA surface. Ω_C as calculated here, is an estimation only, made using calculated parameters and relying on the assumption that calcification is not occurring in the boundary layer (altering carbonate parameters such as total alkalinity) since some measurements were made in the bulk seawater only.

2.2.9 Statistical analysis

For surface O_2 concentration and DBL thickness, Levene's tests were used to test for homogeneity of variance (Appendix 2) and QQplots and Shapiro-Wilk tests were used to test for normality. DBL thickness data was square root transformed to meet the assumption of homoscedasticity, but was still non-normal, thus non-parametric Kruskal-Wallis tests were used to determine if there were any significant differences among individual treatments and among mainstream pH levels, flow levels and irradiance levels above the various substrates. A post-hoc Dunn test was used to show pairwise differences in all of the independent treatment conditions above the various substrates for DBL thickness (Appendix 3–5). Surface oxygen concentration failed to meet the assumptions of equal variances, thus a Welch's ANOVA, a one-way ANOVA with unequal variances, was used to test for significant differences. Surface oxygen concentration data was normal for all treatments in the 2.5 L glass jars and 3 L aquaria, and all but one treatment in the annular flume (light ambient fast), but since ANOVA's are considered relatively robust to normality and this was the only violation, the test is reported with appropriate conservative precaution when interpreting the results. A Games-Howell post-hoc test was used to compare combinations of treatments (Appendix 6–8). All statistical analyses were performed using RStudio, version 1.1.453 (RStudio Team, 2016).

2.3 Results

2.3.1 Seawater Parameters

Average carbonate chemistry parameters of the mainstream seawater in the annular flume, 3 L aquaria and 2.5 L glass jars are given in Table 2.2. There were two distinct pH treatments in the annular flume, referred to as bulk pH 8.1 and bulk pH 7.4 (reported on the total scale) (Table 2.2). Similar carbonate chemistry conditions were achieved in each experimental day of oxygen profiling. Experiments in 2.5 L glass jars took place in ambient bulk seawater, approximately pH_T 8.1. There were three distinct bulk pH treatments in the 3 L aquaria, referred to as bulk pH 8.1, bulk pH 7.7 and bulk pH 7.4 (reported on the total scale). Average bulk seawater pH measurements taken at the beginning and end of each oxygen profile in the 3 L aquaria demonstrate that pH levels stayed relatively constant throughout individual profiles, and that carbonate chemistry conditions remained similar throughout all profiling, as daily pH measurements appeared similar to pH measurements from the carbonate chemistry parameters taken only once (Table 2.2 and 2.3).

Table 2.2 Carbonate chemistry parameters (pH_T, total alkalinity, DIC, temperature, salinity, carbonate, saturation state for calcite, saturation state for aragonite and partial pressure of CO_2) in the annular flume (bulk pH 8.1 and bulk pH 7.4), 2.5 L jars (bulk pH 8.1) and 3 L aquaria (bulk pH 8.1, bulk pH 7.7 and bulk pH 7.4). Values represent mean ± SE and n= 5 for flume bulk pH 8.1 and n= 12 for flume bulk pH 7.4. Values represent one measurement for the 3 L aquaria and 2.5 L glass jars, thus no standard error is reported.

	Flume		**2.5 L jars**	**3 L aquaria**	
	Bulk pH 8.1	**Bulk pH 7.4**	**Bulk pH 8.1**	**Bulk pH 7.7**	**Bulk pH 7.4**
pH_T	8.09 ± 0.003	7.41 ± 0.02	8.09	7.68	7.48
A_T (µEq/kg)	2269 ± 3	2269 ± 2	2288	2286	2280
DIC (µmol/kg)	2072 ± 3	2300 ± 5	2085	2235	2289
Temperature (ºC)	10.7 ± 0.1	10.8 ± 0.1	10.5	10.5	10.5
Salinity	33.7 ± 0.2	33.1 ± 0.1	34.2	34.2	34.2
$[CO_3^{2-}]$ (µmol/kg)	143 ± 1.0	34.6 ± 1.4	146.8	63.1	40.7
Ω_{Ar}	2.2 ± 0.02	0.53 ± 0.02	2.23	0.96	0.62
Ω_{ca}	3.4 ± 0.03	0.84 ± 0.03	3.51	1.51	0.97
***p*CO_2 (µatm)**	356.2 ± 3.0	1933 ± 86	350.0	999.2	1620

Table 2.3 Mean seawater pH during oxygen profiling in the 3 L aquaria measured spectrophotometrically with Cresol purple dye. Measurements were recorded at the beginning and end of each oxygen profile. Values represent mean ± SE. n= 8.

	Bulk pH 8.1	**Bulk pH 7.7**	**Bulk pH 7.4**
	Mean ± SE	**Mean ± SE**	**Mean ± SE**
Light	8.10 ± 0.008	7.63 ± 0.003	7.48 ± 0.006
Dark	8.08 ± 0.008	7.72 ± 0.006	7.48 ± 0.006

2.3.2 Oxygen and pH profiles

The chemical environment immediately above the coralline algal surface differed from that of the bulk seawater. In all levels of bulk seawater pH, oxygen (and pH) increased in the light above CCA and decreased in the dark, with steeper gradients of change in fast flow (Figure 2.5–2.10). In seawater bulk pH 7.4 in the light, pH within the DBL reached nearly pH 8.1 (~ present-day ambient seawater) in 1 cm s^{-1} flow (Figure 2.6) and above pH 8.1 in static (no) flow (Figure 2.10). Irradiance had a significant effect on surface oxygen concentration in all three containers (Table 2.4); with surface oxygen (and estimated surface pH) reaching much higher values in the light than in the dark (Figure 2.5-2.10). Oxygen concentrations (and pH) in the dark had much smaller deviations from mainstream values than in the light. In slow flow treatments in the annular flume, pH varied up to ~0.6 units greater than the bulk seawater pH in the light, whereas pH only varied up to ~0.06 units less than the bulk seawater pH in the dark (Figure 2.6). In no flow treatments in 2.5 L glass jars, pH was up to ~0.6 units above the bulk seawater pH in the light, whereas pH was only ~0.09 units below the bulk seawater pH in the dark (Figure 2.8). At no flow in 3 L aquaria, pH varied up to ~0.8 units above the bulk seawater pH in the light, whereas pH only varied up to ~0.09 units below the bulk seawater pH in the dark (Figure 2.10).

Flow also impacted the shape of oxygen and pH profiles. Oxygen profiles at 1 cm s^{-1} or 0 cm s^{-1} were much more gradual, with a wider range of O_2 (and pH) values than in fast flow (5.5 cm s^{-1}) or flow treatments (Figure 2.5–2.8). In the annular flume, in the light at bulk pH 7.4, in slow flow treatments, mean pH values varied by ~0.6 units, whereas in fast flow treatments, mean pH values varied by only up to nearly ~0.2 units (Figure 2.6). Under light at ambient pH in 2.5 L jars, mean pH values varied by ~0.6 units without flow, but only by ~0.006 units under flow (Figure 2.8). Flow significantly altered surface oxygen concentration (Table 2.4); surface oxygen concentrations in flow were lower in the light and higher in the dark, in comparison to their no flow counterparts. In fast flow, CCA were still able to raise oxygen concentrations immediately above them, but to a lesser extent than in slow flow; O_2

concentrations (and esimated pH) reached mainstream values much quicker in fast flow. Bulk seawater pH did not have a signiifcant effect on standardised surface oxygen concentrations (Table 2.4). The shape of oxygen and pH profiles, and subsequent deviations from bulk concentrations, were similar in all bulk seawater pH treatments. However, bulk seawater pH does influence the estimated pH values reached as the mainstream value differs even though pH deviations are similar.

Figures 2.5–2.10 display the mean profile for each treatment based on four or five replicates and thus, outlier profiles, or pieces of profiles, can influence the shape of the mean profile displayed. For example, in panel B of Figure 2.7, occasional spikes in oxygen at different heights above the substrate, as shown by the larger error bars, which prevented the mean oxygen concentrations from reaching bulk seawater concentrations by 4 mm above the substrate as displayed in the figure. In the water column in light treatments particularly, there were occasional, random, brief spikes in oxygen concentration more than 2 or 3 mm above the substrate. However, these spikes are attributed to movement of the electrode rather than metabolic processes since it was not a complex algal canopy and they occurred in only a few profiles at different heights. Additionally, sometimes oxygen concentrations reached mainstream values more slowly, although still clearly out of the boundary layer. For example, in panel A of Figure 2.5, oxygen concentrations were >5% different than bulk seawater at the CCA surface, and then stabilized within the water column above 0.1 mm reached within 5% of the bulk seawater concentrations, but didn’t quite reach within 1% of the bulk seawater until higher in the water column.

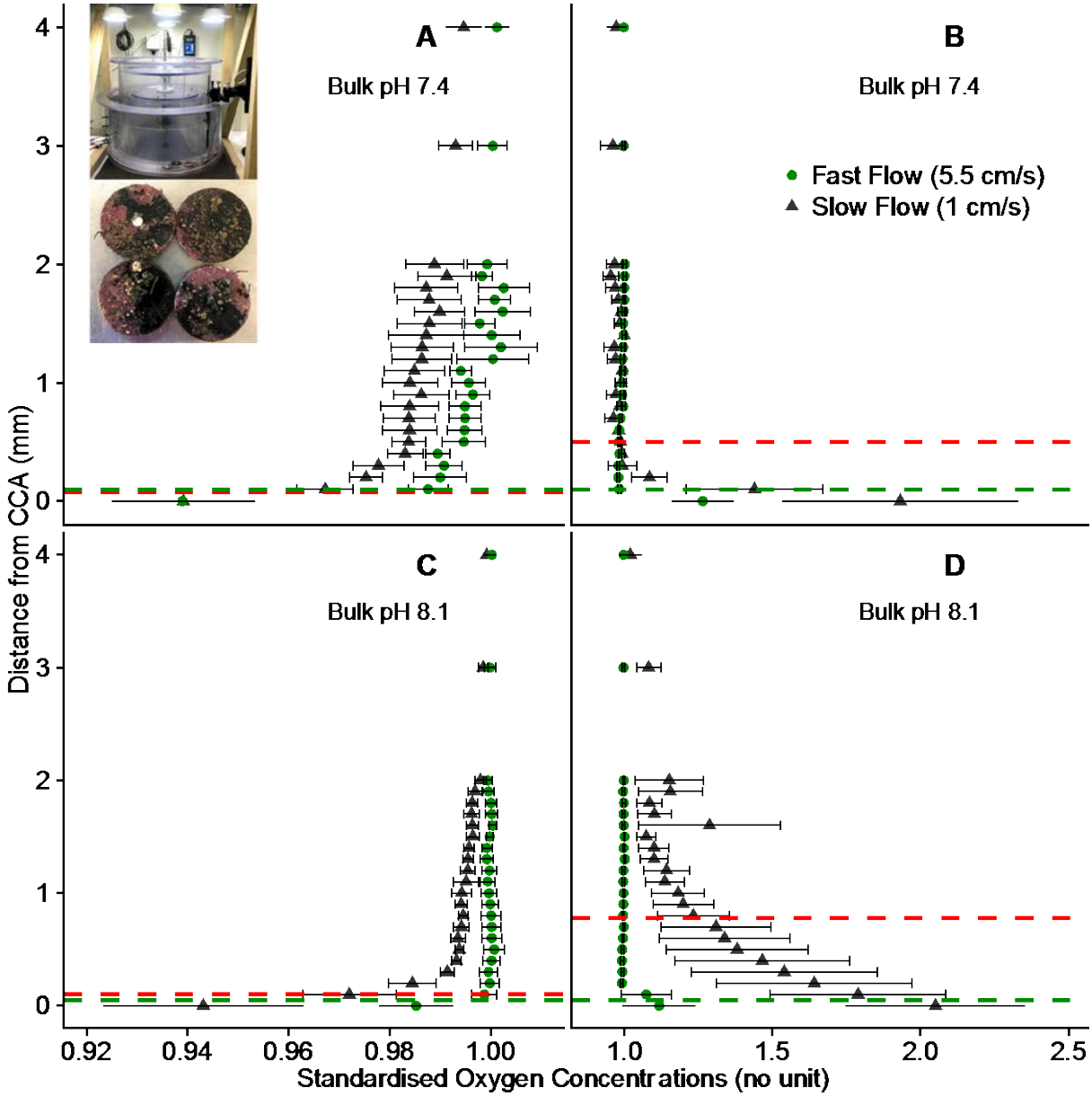

Figure 2.5 O_2 standardised profiles measured above CCA in the annular flume, in bulk pH 7.4 in the (A) dark and (B) light, and in bulk pH 8.1 in the (C) dark and (D) light. Circles (green) represent O_2 concentrations measured at fast flow (5.5 cm s^{-1}), while triangles represent O_2 concentrations measured at slow flow (1 cm s^{-1}). The red line indicates the mean DBL thickness in slow flow conditions and the green line indicates the mean DBL thickness in fast flow conditions. Values are mean ± SE, n=4 or 5.

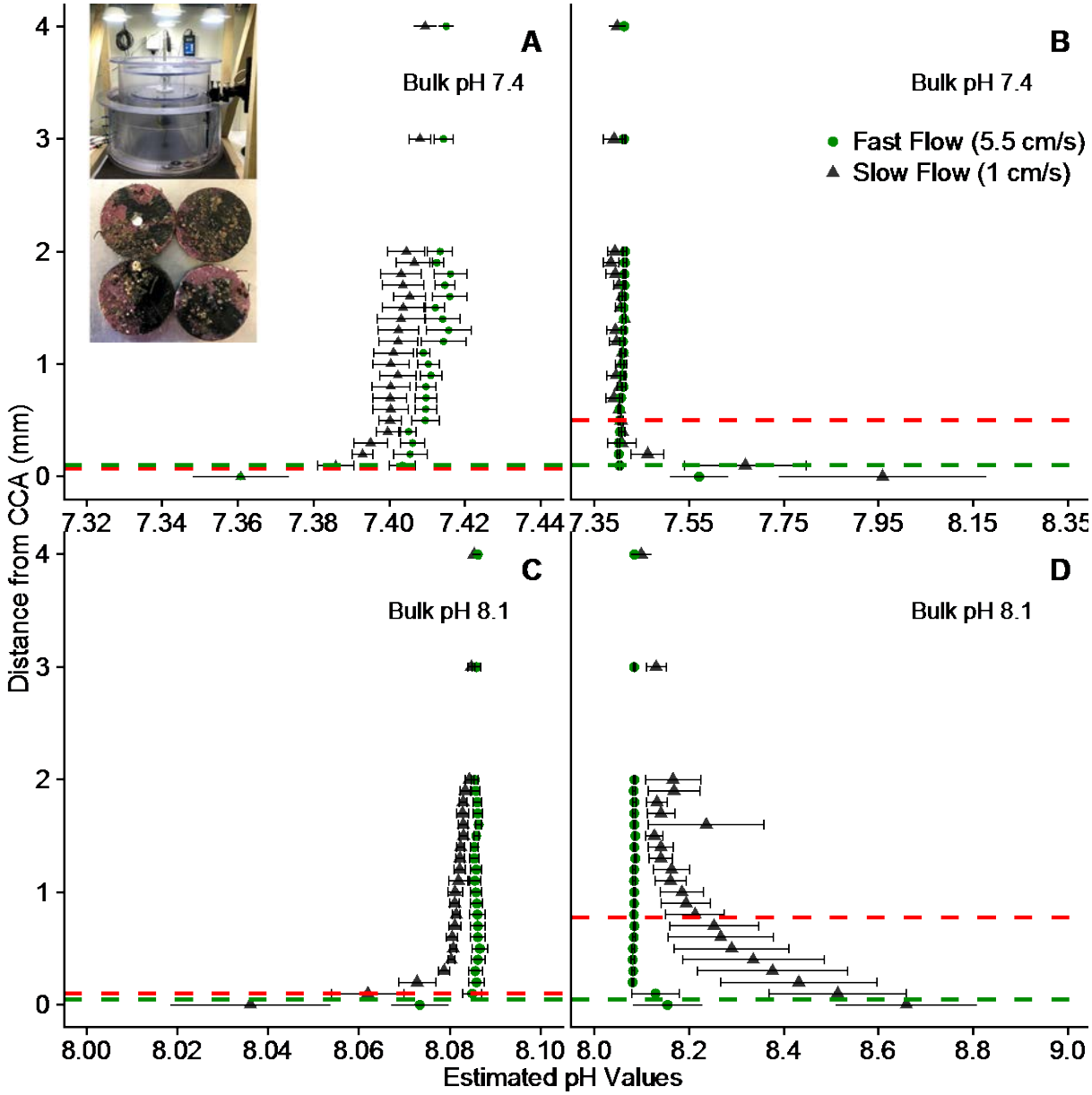

Figure 2.6 Calculated pH_T profiles above CCA in the annular flume in bulk pH 7.4 in the (A) dark and (B) light, and in bulk pH 8.1 in the (C) dark and (D) light. Circles (green) represent O_2 concentrations measured at fast flow (5.5 cm s^{-1}), while triangles represent O_2 concentrations measured at slow flow (1 cm s^{-1}). The red line indicates the mean DBL thickness in slow flow conditions and the green line indicates the mean DBL thickness in fast flow conditions. Values are mean ± SE, n=4. pH values were estimated using oxygen as a proxy.

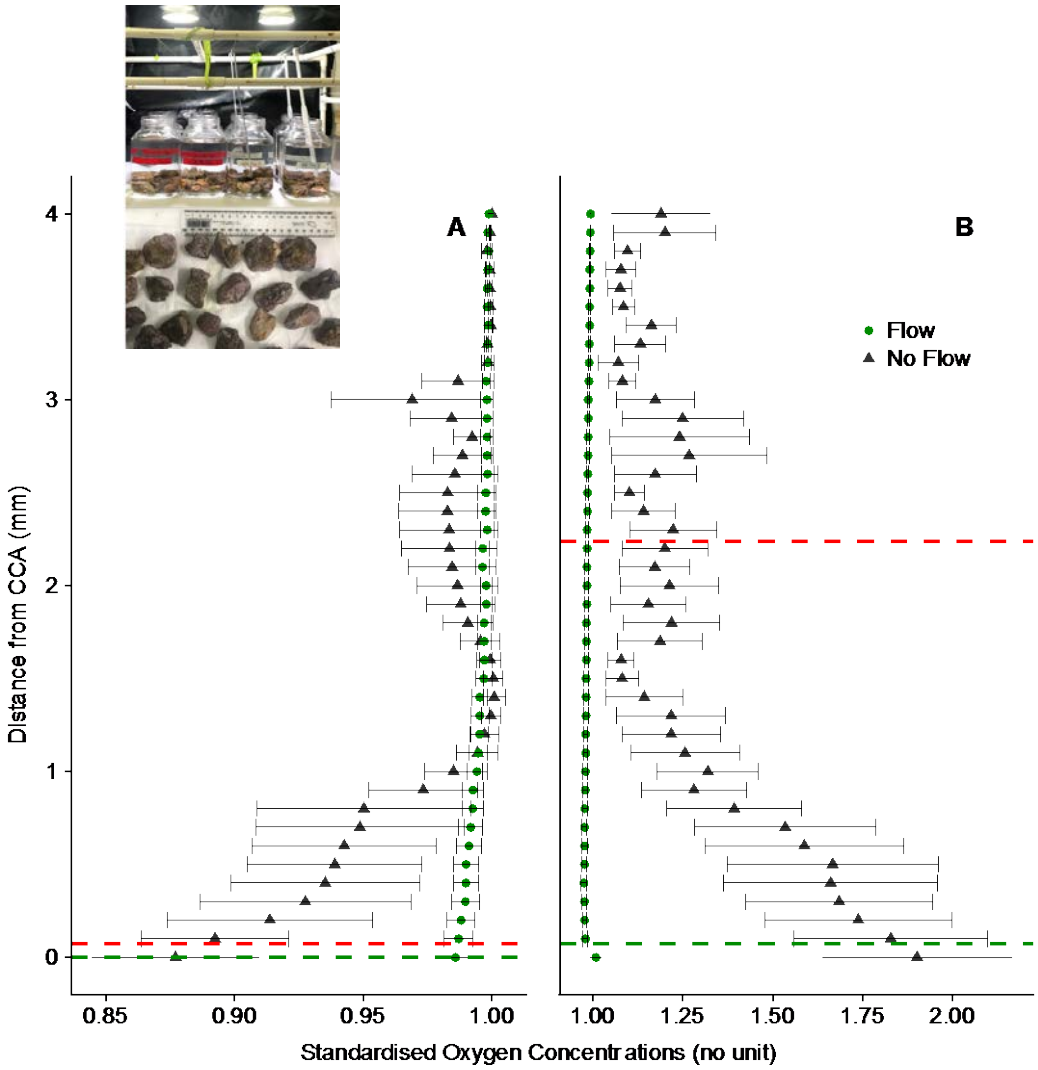

Figure 2.7 O_2 standardised profiles measured above CCA in 2.5 L glass jars, in the (A) dark and (B) light. Circles (green) represent O_2 concentrations measured at flow, while triangles symbols represent O_2 concentrations measured at no flow. The red line indicates the mean DBL thickness in no flow conditions and the green line indicates the mean DBL thickness in flow conditions. Values are mean ± SE, n=4 or 5.

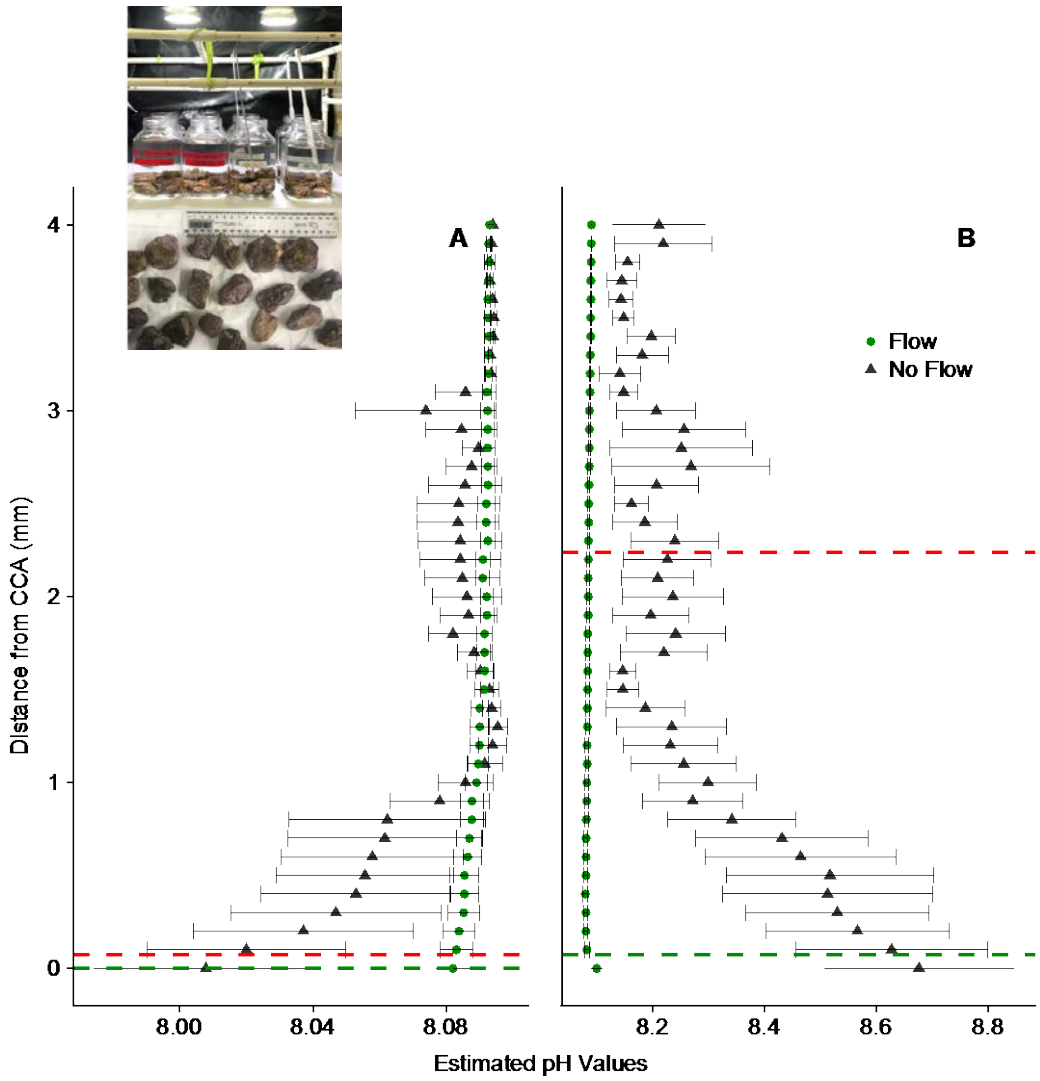

Figure 2.8 Calculated pH_T profiles above CCA in 2.5 L glass jars, in the (A) dark and (B) light. Circles (green) represent pH values in flow, while triangles symbols represent pH values in no flow. The red line indicates the mean DBL thickness in no flow conditions and the green line indicates the mean DBL thickness in flow conditions. Values are mean ± SE, n=4 or 5. pH values were estimated using oxygen as a proxy.

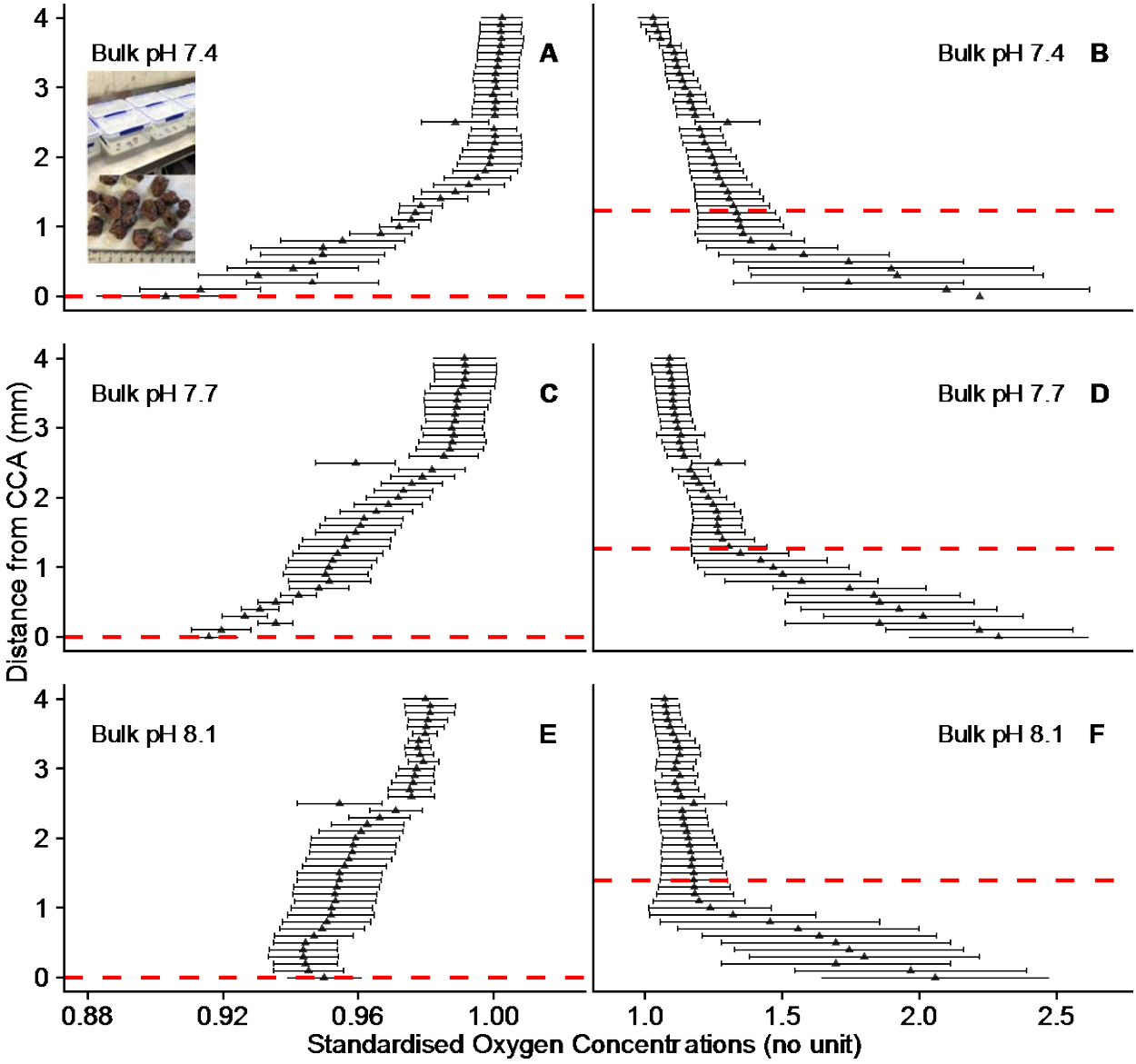

Figure 2.9 O_2 standardised profiles measured above CCA in 3 L aquaria at three pH levels. O_2 standardised profiles were measured in bulk pH 7.4 in the (A) dark and (B) light, bulk pH 7.7 in the (C) dark and (D) light, and in bulk pH 8.1 in the (E) dark and (F) light. The red line indicates the mean DBL thickness. Values are mean ± SE, n=4.

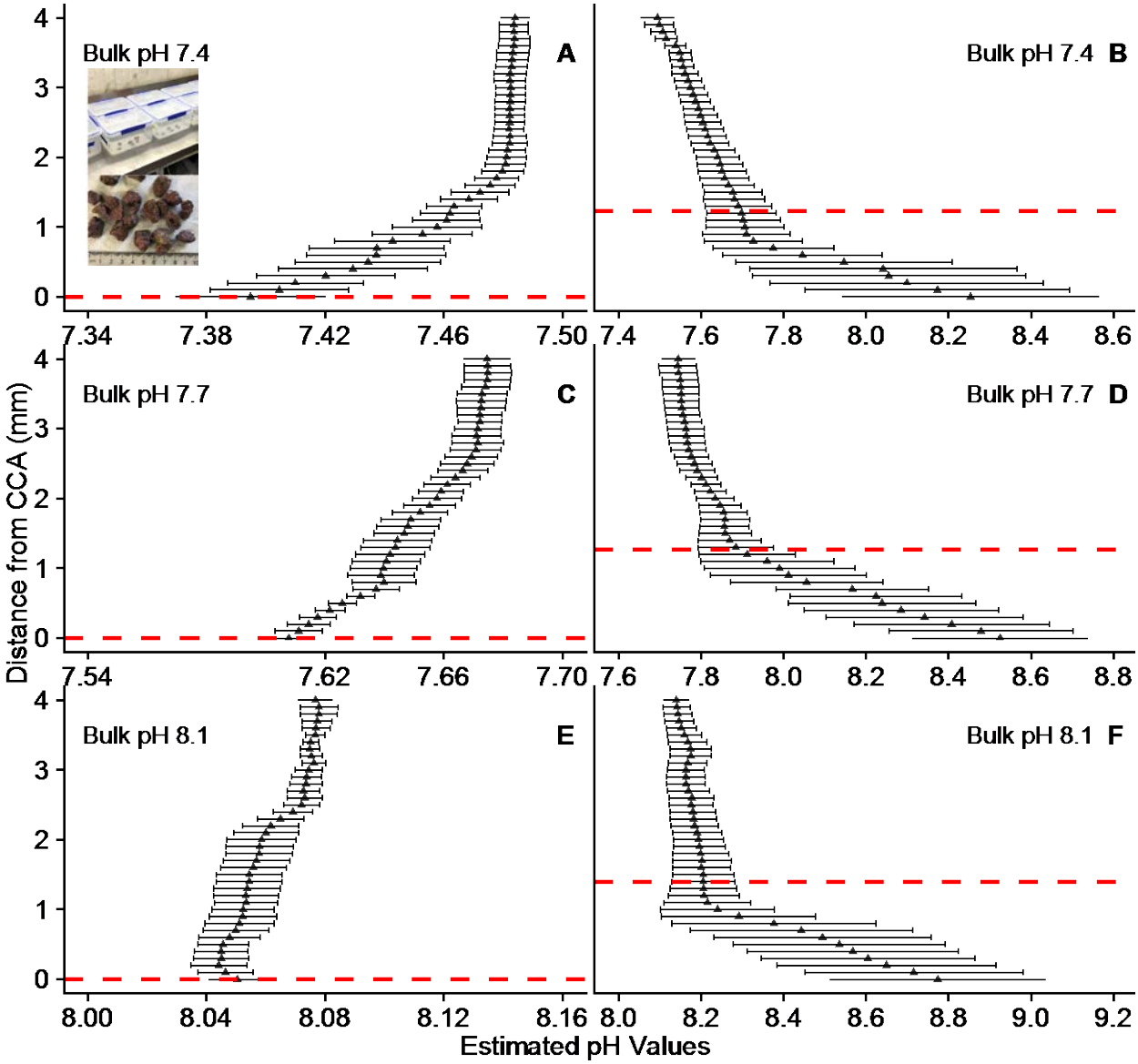

Figure 2.10 Calculated average pH values above CCA in 3 L aquaria at three pH levels. O_2 standardised profiles were measured in bulk pH 7.4 in the (A) dark and (B) light, bulk pH 7.7 in the (C) dark and (D) light, and in bulk pH 8.1 in the (E) dark and (F) light. The red line indicates the mean DBL thickness. Values are mean ± SE, n=4. pH values were estimated using oxygen as a proxy.

Table 2.4 Welch's ANOVA, with unequal variances, examining the effects of treatment, bulk pH, flow and irradiance on standardised surface O_2 concentration in the annular flume, 2.5 L glass jars and 3 L aquaria. *p* values less than 0.05 are in bold

		Standardised Surface O_2			
Experiment Design	**Factor**	**F**	**num df**	**Denom df**	***p*-value**
Annular Flume	Treatment	4.54	7	9.87	**0.016**
	Bulk pH	<0.001	1	30.0	0.978
	Flow	4.54	1	17.3	**0.048**
	Irradiance	16.3	1	15.1	**0.001**
2.5 L Glass Jars	Treatment	11.4	3	5.96	**0.007**
	Flow	6.18	1	8.02	**0.038**
	Irradiance	9.38	1	8.15	**0.015**
3 L Aquaria	Treatment	5.61	5	7.83	**0.017**
	Bulk pH	0.027	2	13.9	0.973
	Irradiance	31.7	1	11.1	**<0.001**

2.3.3 DBL thickness

DBLs were thickest in light conditions under no (zero) or slow flow (Figure 2.11 and 2.12; Table 2.5). In Figures 2.11 and 2.12, DBL thickness is displayed as negative in the dark to represent the pH decrease below bulk seawater in contrast to the increase above bulk pH in light conditions. However, DBL thickness is not actually negative. The thickest mean DBL measured was 2.24 mm ± 0.50 (Mean ± SE), measured under light, at no flow and bulk pH 8.1 in 2.5 L glass jars (Figure 2.12). DBLs were significantly different (thicker) in the light than in the dark (Table 2.6). In 3 L aquaria, all DBL thicknesses in the dark were 0 mm (Table 2.5). DBLs were also significantly thicker under no or slow flow than in flow (Table 2.6). In 2.5 L glass jars, post-hoc comparisons indicated that the DBL in light no flow was significantly different (thicker) than all other treatments (Appendix 4). In the annular flume, the DBL in the light bulk pH 8.1 slow flow was significantly different (thicker) than all other treatments, except the other light slow flow at bulk pH 7.4, which was also significantly different (thicker) than most other treatments (Appendix 3). In the light at bulk pH 8.1, in the annular flume, mean DBL thickness was 0.78 mm ± 0.28 (Mean ± SE) in slow flow, but only 0.05 mm ± 0.05 (Mean ± SE) in fast flow (Figure 2.11). Bulk seawater pH did not have a significant effect on DBL thickness (Table 2.6). Under bulk pH 7.4, 7.7 and 8.1, all mean DBLs ranged between 1.2 and 1.4 mm (Figure 2.12).

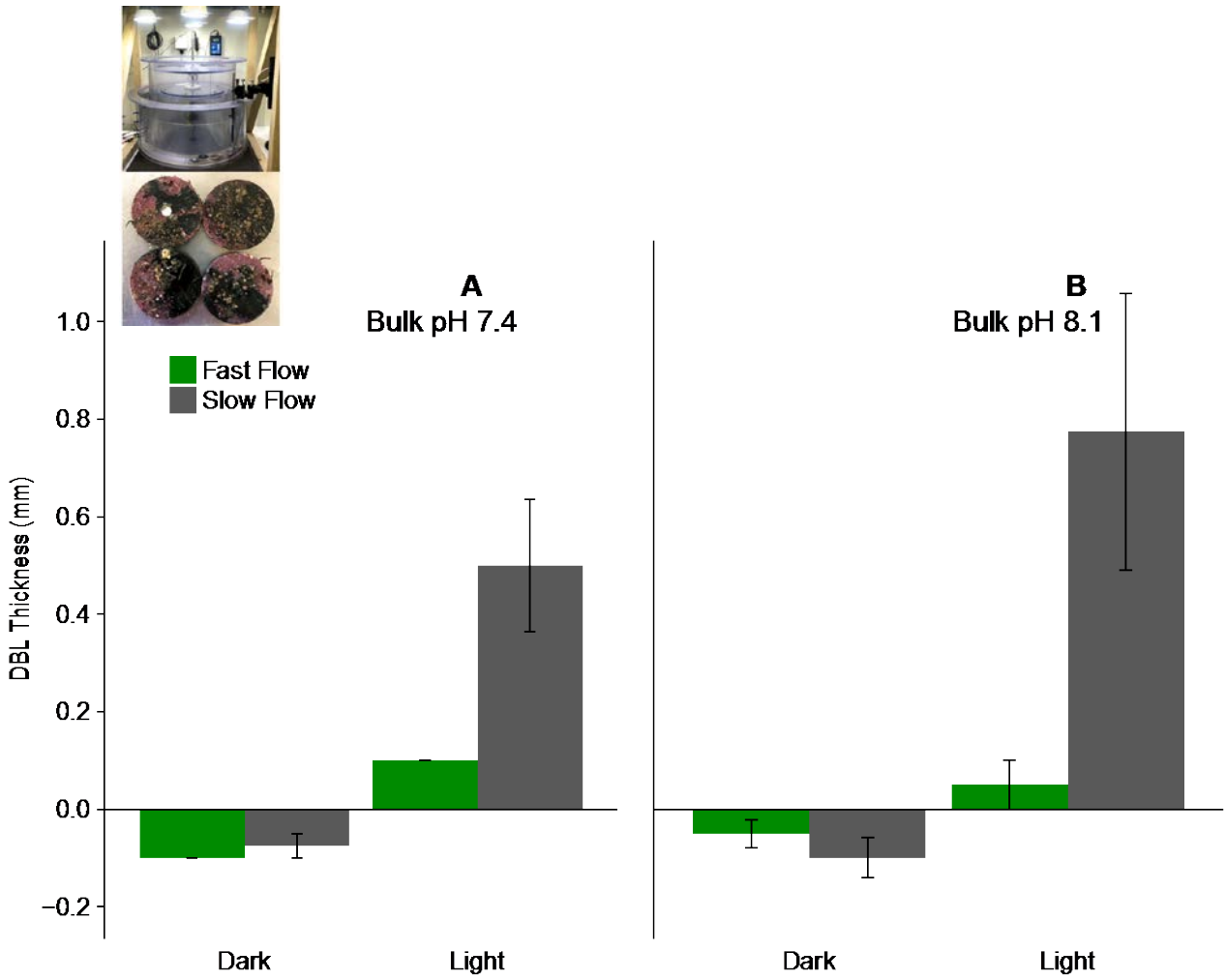

Figure 2.11 Diffusive boundary layer (DBL) thickness (mm) above settlement discs in the annular flume at (A) bulk pH 7.4 and (B) bulk pH 8.1 in fast flow (green bars) and slow flow (grey bars). DBL thickness in the dark are displayed as negative to represent the decrease in pH below mainstream seawater in comparison to the light conditions are positive to represent the increase above mainstream seawater, although the DBL thickness itself is not actually negative. Values are mean ± SE, n=4.

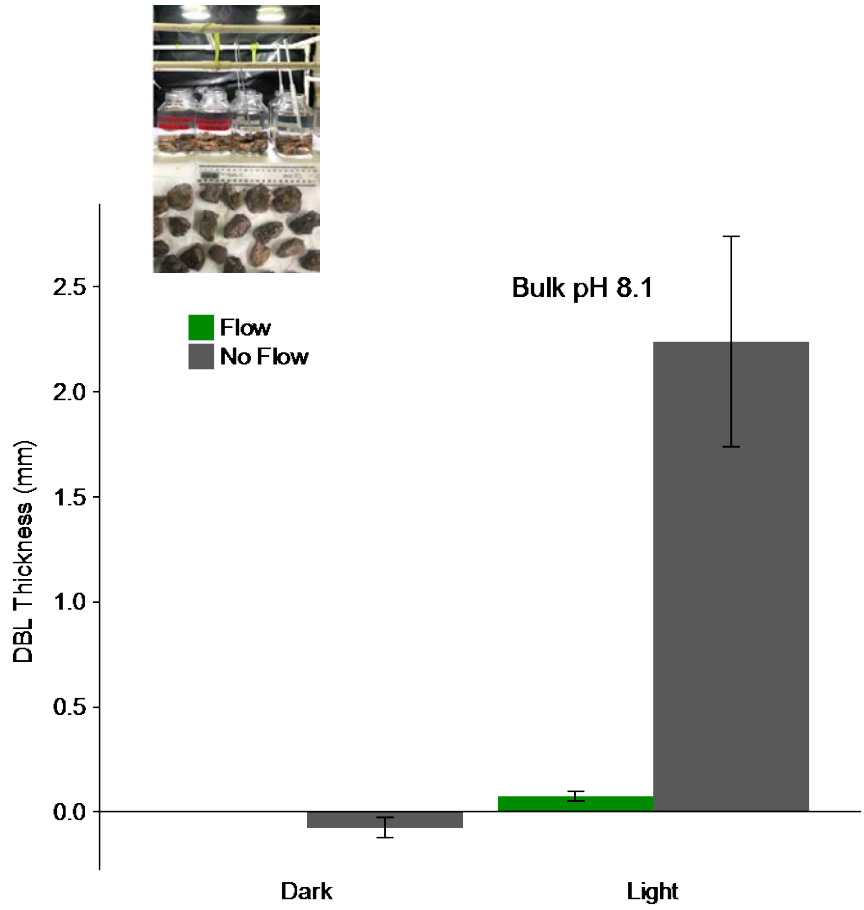

Figure 2.12 Diffusive boundary layer (DBL) thickness (mm) in 2.5 L glass jars, at bulk pH 8.1 in fast flow (green bars) and no flow (grey bars). Dark conditions are displayed as negative to represent the decrease in pH in comparison to the increase in pH under the light conditions. Values are mean ± SE, n=4 or 5.

Table 2.5 Diffusive boundary layer (DBL) thickness (mm) above crustose coralline algae in 3 L aquaria at (A) bulk pH 7.4, (B) bulk pH 7.7 and (C) bulk pH 8.1. All measurements were completed at no flow. Values are mean ± SE, n=4.

Irradiance	Bulk pH (pH_T)	DBL Thickness (mm)
Dark	pH 7.4	0 ± 0
	pH 7.7	0 ± 0
	pH 8.1	0 ± 0
Light	pH 7.4	1.2 ± 0.40
	pH 7.7	1.3 ± 0.40
	pH 8.1	1.4 ± 0.53

Table 2.6 Non-parametric Kruskal-Wallis examining the effects of treatments, bulk pH, flow and irradiance on DBL thickness in the annular flume, 2.5 L glass jars and 3 L aquaria. *p* values less than 0.05 are in bold.

Experiment Design		DBL Thickness		
	Factor	Df	Chi-squared	*p* value
Annular Flume*	Treatment	7	26.0	**<0.001**
	Bulk pH	1	0.538	0.464
	Flow	1	7.67	**0.006**
	Irradiance	1	10.6	**0.001**
2.5 L Glass Jars*	Treatment	3	12.5	**0.006**
	Flow	1	5.56	**0.018**
	Irradiance	1	7.08	**0.008**
3 L Aquaria*	Treatment	5	9.78	0.082
	Bulk pH	2	2.45	0.294
	Irradiance	1	4.10	**0.043**

*Data square root transformed to meet assumptions of homoscedasticity.

2.3.4 Calcium carbonate saturation state

Estimated average calcium carbonate saturation states (Ω_C) of the seawater from 0 to 0.5 mm above the surface of CCA were highest in light conditions at ambient pH (bulk pH 8.1) (Figure 2.13–2.15). At bulk pH 8.1, the seawater immediately above CCA is supersaturated in all irradiance and flow treatments. Calcium carbonate saturation states were generally lower in the dark than in the light. Ω_C was similar in all dark treatments, regardless of flow whereas in the light, Ω_C was higher in no flow or slow flow treatments. Reduced bulk seawater pH decreased calcium carbonate saturation state, in both the light and the dark (Figure 2.13 and 2.15). At bulk pH 7.4 and 7.7, the calcium carbonate saturation state of the seawater immediately above CCA was lower, and potentially undersaturated in the dark and in the light under fast flow (Figure 2.13 and 2.15).

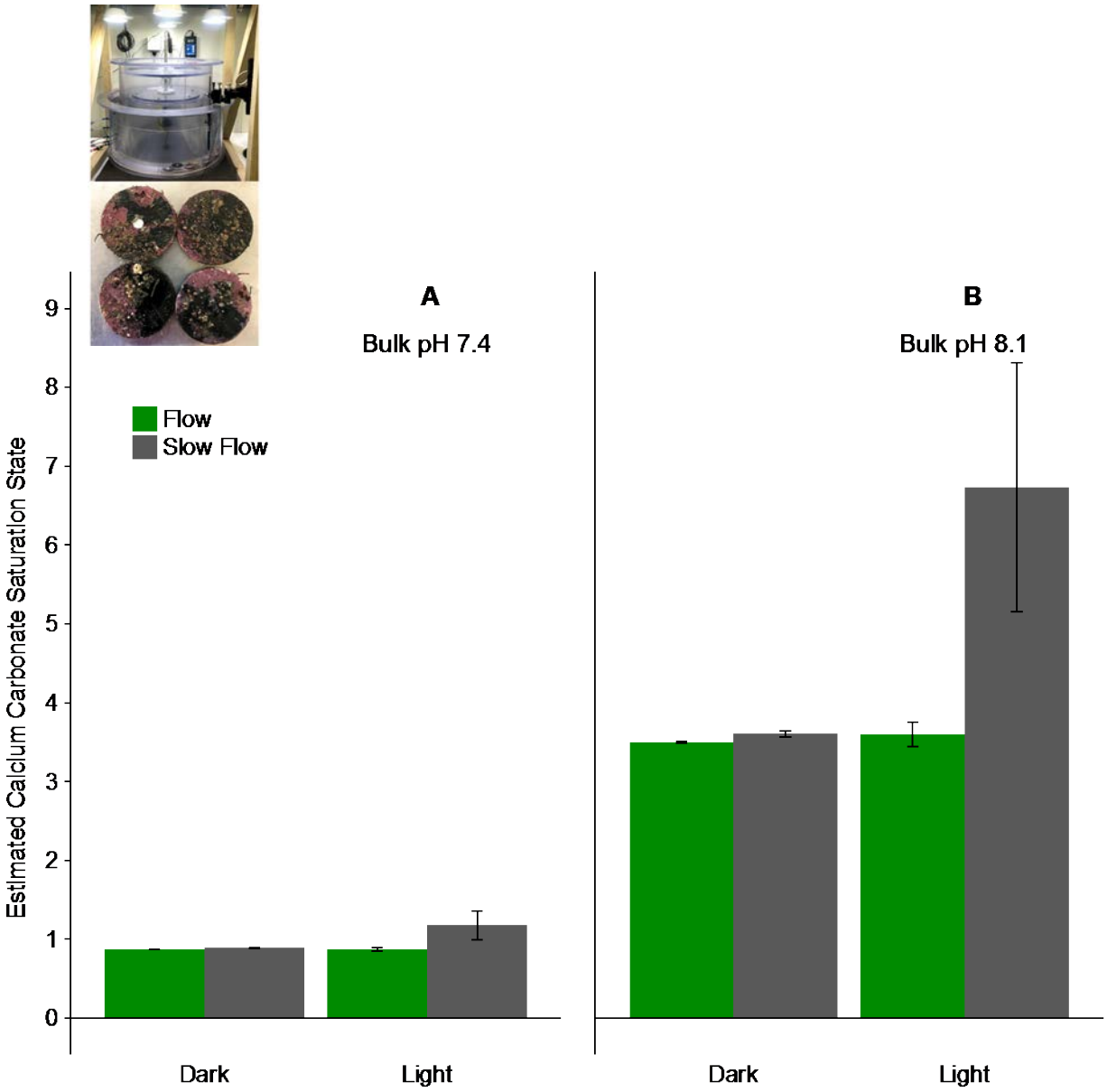

Figure 2.13 Estimated calcium carbonate saturation state of seawater from 0 to 0.5 mm above CCA substrate in the annular flume at (A) bulk pH 7.4 and (B) bulk pH 8.1 in fast flow (green bars) and slow flow (grey bars). Values are mean ± SE, n=4. Ω_C is an estimation only, which relies on the assumption that calcification is not occurring during measurements.

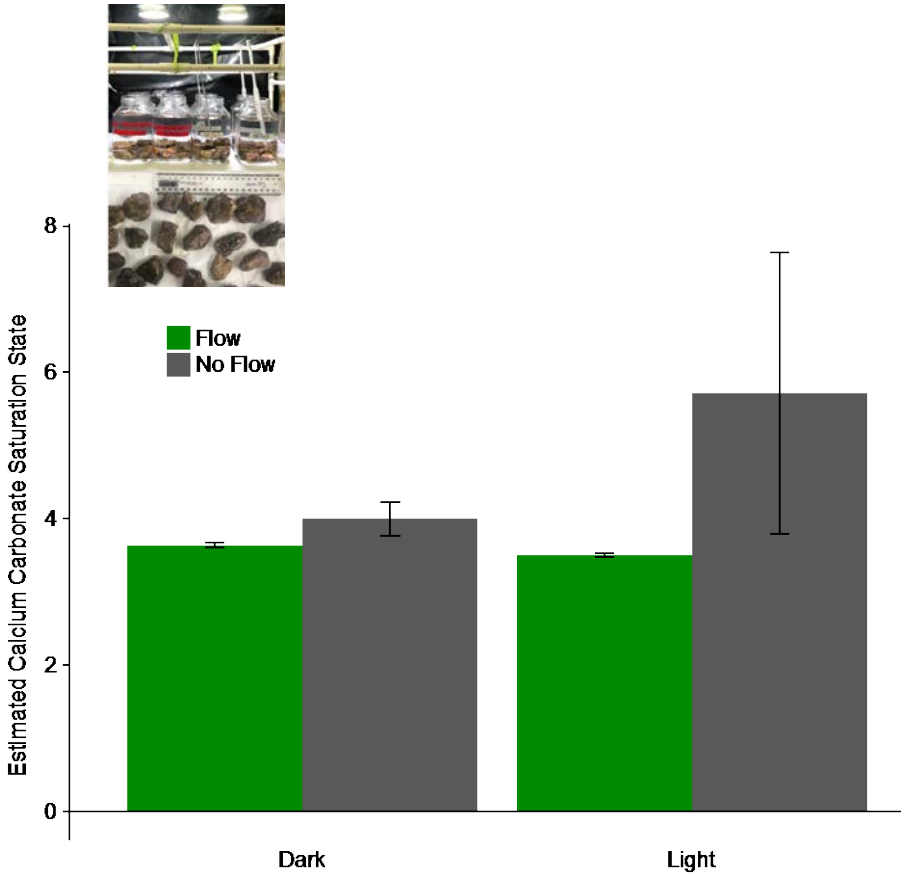

Figure 2.14 Average computed calcium carbonate saturation state of seawater from 0 to 0.5 mm above CCA substrate in 2.5 L glass jars at bulk pH 8.1 in flow (green bars) and no flow (grey bars). Values are mean ± SE, n=4 or 5. Ω_C is an estimation only, which relies on the assumption that calcification is not occurring during measurements.

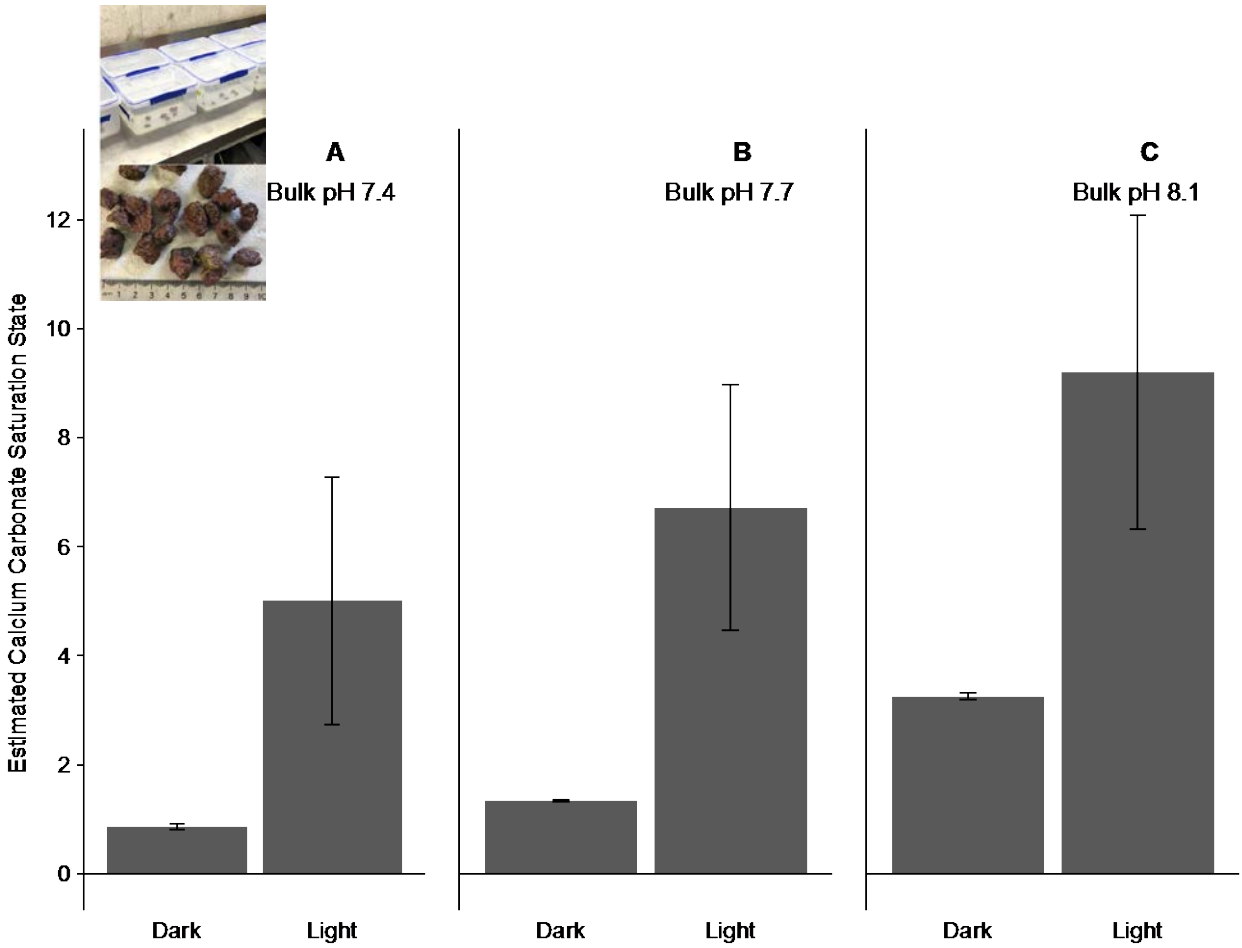

Figure 2.15 Average computed calcium carbonate saturation state of seawater from 0 to 0.5 mm above CCA substrate in 3 L aquaria at (A) bulk pH 7.4, (B) bulk pH 7.7 and (C) bulk pH 8.1. All measurements were completed in no flow. Values are mean ± SE, n=4. Ω_C is an estimation only, which relies on the assumption that calcification is not occurring during measurements.

2.4 Discussion

Macroalgae are able to modify the chemical environment at and immediately above their surface in the DBL (Hurd, 2015; Hurd et al., 2011; Cornwall, 2013; Cornwall et al., 2013a; Cornwall et al., 2014; Cornwall et al., 2013b; Noisette and Hurd, 2018; Wahl et al., 2018; Chan et al., 2016). The oxygen and pH levels occurring within the DBL manipulated via irradiance flow and bulk seawater pH in this study, demonstrate that organisms within the DBL will experience chemical conditions that are different to that of the bulk seawater as a result of algal metabolism. In the light, CCA caused the surface oxygen and calculated pH concentrations to increase substantially, up to approximately 0.8 pH units above the bulk seawater pH in some treatments. This increase was much greater at zero or slow flow. In the dark, coralline algae caused the surface oxygen and calculated pH concentrations to decrease, but to a smaller extent than the increase in the light (a decrease of only approximately 0.09 units).

As originally hypothesized, DBL thickness and oxygen/pH profiles varied with both flow and irradiance, but not bulk seawater pH (Cornwall, 2013; Cornwall et al., 2014; Cornwall et al., 2013b; Chan et al., 2016). Flow speed determined the size of the DBL. The DBL was thicker and pH/oxygen deviations larger at zero or slow flow. Thicker DBLs and larger oxygen/pH deviations from the bulk seawater also occurred in the light compared to the dark (Cornwall et al., 2013b). Irradiance, driven by the metabolic processes of photosynthesis and respiration, determined the direction of the oxygen/pH changes. Photosynthesis causes pH within the DBL to increase due to the uptake of CO_2 (or HCO_3^- and H^+), while respiration (and calcification when occurring) causes pH within the DBL to decrease due to the release of CO_2 (Raven and Hurd, 2012; De Beer and Larkum, 2001; Hurd et al., 2011). Slow bulk seawater velocity in light conditions favoured the thickest DBL and the largest pH/oxygen deviations. In this experiment, DBL thicknesses reached up to 2 mm in no flow, and up to nearly 1 mm in 1 cm s^{-1} flow, but ranged between 0 and 0.5 mm in 5.5 cm s^{-1} flow. DBL thickness typically ranges from 0.1 to 10.2 mm (Table 2.7), depending on the organisms' surface morphology and the seawater velocity (Hurd, 2015; Raven and Hurd, 2012). Studies measuring DBL thickness use a range of seawater velocities, from 0 to 10 cm s^{-1}, which represent speeds at which the DBL reaches maximal and minimal values (Noisette and Hurd, 2018; Chan et al., 2016; Hansen et al., 2011). Speeds of 0 cm s^{-1} are relatively unrealistic by allowing a near infinite build-up of a boundary layer, thus accounting for some of the variability seen at zero flow. However, examining very slow velocities is still important as flows can be extremely

slow (<1 cm s^{-1}) within macroalgal turf communities, including communities where CCA are found (Pöhn et al., 2001; Hurd, 2000).

Table 2.7 Summary of studies in which DBL thickness has been measured above algal, coral, or sea urchin surfaces, in the light, using pH or oxygen microsensors. Bulk pH was assumed to be ambient unless otherwise stated. The mean DBL thickness is reported, and in some cases, thickness was estimated from reported figures. This figure is representative, not all studies examining the DBL above algal or coral are included. Modified from Raven & Hurd (2012). Ecophysiology of photosynthesis in macroalgae. *Photosynthesis Research* 113(105): page 116 with permission.

Substrate Species	Bulk pH	Minimum flow speed (cm s^{-1})	Maximum flow speed (cm s^{-1})	DBL Thickness (mm) at minimum flow speed	DBL Thickness (mm) at maximum flow speed	Reference
Lithothamnion sp.	8.1	0	1 to 3	2.5	0.1 to 0.2	Kaspar (1992)
Halimeda discoidea	8.1	0	-	0.5	-	De Beer and Larkum (2001)
Feldmannia caespitula	8.1	0	-	1.3	-	Pöhn et al. (2001)
Fucus serratus	8.1	0	4.6	1.0-1.5	0.4	Irwin and Davenport (2002)
Epilithic coral reef algal community	8.1	0	8	2	0.18-0.59	Larkum et al. (2003)
*Fucus vesiculosus (*glabrous blade)	8.1	-	1.5	-	0.5	Spilling et al. (2010)
*Fucus vesiculosus (*pilose cryptostomata)	8.1	-	1.5	-	0.8	
Sporolithium durum apex (calcifying seaweed)	8.11	0	10	8.8	0.2	Hurd et al. (2011)
	7.5	0	10	5	3	
Sporolithium durum crenulation (calcifying seaweed)	8.11	0	10	10.2	0.4	
	7.5	0	10	13	0.05	
Evechinus chloroticus (sea urchin)	7.79	1.5	10	4.5	0	
Macrocystis pyrifera (within corrugation of wave - exposed blades)	8.1	0.8	4.5	0.8	0.67	Hurd and Pilditch (2011)
Macrocystis pyrifera (apex corrugation of wave - exposed blades)	8.1	0.8	4.5	0.4	0	
Macrocystis pyrifera (within undulation of wave - sheltered blades)	8.1	0.8	4.5	0.73	not detectable	

Macrocystis pyrifera (apex undulation of wave - sheltered blades)	8.1	0.8	4.5	0.07	not detectable	

Algal turf	8.1	-	8.9	-	0.4	Wangpraseurt et al. (2012)
Crustose coralline algae	8.1	-	8.9	-	0.4	Wangpraseurt et al. (2012)
	7.65	0	10	66	0	
Carpophyllum canopy with *Corallina* understory	8.1	2	8	22.5	2	Cornwall et al. (2015)
Corallina understory	8.1	2	8	8	1	
Favites (coral)	8.1	0	5	2	0.25	Chan et al. (2017)
Favites (coral)	7.8	0	5	0.8	0.45	
Pocillopora damicornisi (coral)	8.1	0	5	1.5	0.08	
Fucus vesiculosus (hyaline hairs on the thallus)	8.1	1.65	4.88	1.2	0.6	Lichtenberg et al. (2017)
Fucus vesiculosus	8.1	0.028	-	0.8	-	Hendriks et al. (2017)
Ascophyllum nodosum	8.1	0.028	-	0.5	-	
Ulva lactuca	8.1	0.028	-	1.6	-	
Zostera marina	8.1	0.028	-	0.6	-	
Saccharina longicruris	8.1	0.028	-	1.2	-	
Agarum clathratum	8.1	0.028	-	1.3	-	
Acropora aspera (coral)	8.1	3	-	9	-	Schoepf et al. (2018)
Acropora aspera (bleached coral)	8.1	3	-	0.5	-	
Ecklonia radiata (bare kelp blade)	8.09	<0.5	8	0.45	0.1	Noisette and Hurd (2018)
	7.71	<0.5	8	0.55	0.09	
Ecklonia radiata colonized by *M. membranacea* (kelp blade with bryozoans)	8.09	<0.5	8	0.65	0.3	
	7.71	<0.5	8	0.94	0.25	
Crustose coralline algal assemblage	8.1	1	5.5	0.78	0.05	This study
	7.4	1	5.5	0.5	0.1	

In addition to irradiance and flow speed, there are a number of other abiotic and biotic factors that influence DBL thickness, including substrate extent, substrate assemblage, substrate species, location on substrate measured, experimental volume of seawater and type of flow, among others. The thickest DBLs in this experiment were found in zero (no) flow and light, above the largest CCA covered substrate and the smallest volume of water, supporting the idea that DBL thickness depends on many of these factors. In the field, DBL thickness can be highly variable because of the complexity and the number of co-varying factors occurring naturally. For example, concentration boundary layer (CBL) thickness has been found to be ~3 times higher (a maximum CBL of 66 mm) than previously measured above similar species due to the existence of a seaweed canopy, allowing a compound CBL to form (Cornwall et al., 2013b). In this case, the high density of the algal (*A. corymbosa*) assemblage, the metabolism of the macroalgae within and the thickness of the canopy, all contributed to the extremely thick concentration boundary layer (Cornwall et al., 2013b). Additionally, substrate assemblage can have an effect on boundary layer thickness by changing the surface topographical features and other biotic factors. For example, the presence of bryozoans led to lower oxygen concentrations in the DBL and more complex pH fluctuations on the surface of *Ecklonia radiata* kelp blades (Noisette and Hurd, 2018). There are many factors that contribute to the chemical and physical parameters of the DBL microenvironment.

While the present work focused on pH changes observed on the millimetre scale due to diurnal fluctuations, natural fluctuations of the carbonate system also occur at larger spatial scales and also on temporal scales (Wahl et al., 2015b). In order to understand changes in the carbonate chemistry system due to climate change, environmental temporal and spatial fluctuations must be taken into account in order to discern natural pH changes from pH changes due to anthropogenic causes (Wahl et al., 2015b). Carbonate chemistry can vary temporally, on both an interannual scale due to periodic climactic events such as the North Atlantic Oscillation and the El Niño-La Niña succession, and on a seasonal scale due to changes in biological activity, light, temperature, salinity, rain and wind intensity (Delille et al., 2009; Saderne et al., 2013; Manzello, 2010; Wahl et al., 2015a; Frankignoulle and Distèche, 1984; Shaw et al., 2012). Fluctuations can also occur on a much greater physical scale than the millimetre scale this work focused on. Coral reef habitats are capable of inducing pH fluctuations over multiple kilometres (Anthony et al., 2011). Seawater pH can fluctuate by 1 pH unit or more in seagrass meadows (Semesi et al., 2009). Kelp forests are capable of changing pCO_2 by 160 µatm in winter and 340 µatm in summer during a day-night cycle (Delille et al., 2009). On both large and small physical scales, the magnitude of the pH

deviation from the bulk seawater is determined by the degree of exchange between the area of seawater influenced by the metabolism of the organisms and the bulk seawater (Cornwall et al., 2013a; Cornwall et al., 2013b). Larger shifts in pH occur in more stagnant water, such as rockpool habitats or tide pools in comparison to more open reefs; diurnal variation of pCO_2 can exceed 1000uatm/day in tide pools (Truchot and Duhamel-Jouve, 1980; Morris and Taylor, 1983; Nguyen and Byrne, 2014; Cornwall et al., 2013b; Björk et al., 2004). The hydrodynamic mechanisms (flow) that control pH deviations within the DBL are similar to the hydrodynamic mechanisms that control pH deviations on larger physical scales. While this study emphasizes the need to focus on the pH fluctuations at very small scales, which have the largest amplitudes by far in biogenic pH fluctuation, the implications are extensive, as pH fluctuations are found across all scales (Spilling et al., 2010; Wahl et al., 2015b; Hurd and Pilditch, 2011).

While the existence of boundary layers at the surface of organisms, particularly seaweed, is well-studied, its application to ocean acidification is more recent (Hurd et al., 2011). The application of boundary layers to OA is multifaceted because of the complexity with which CCA fares under reduced bulk seawater pH, but also crucial because of the unknown potential of whether boundary layers will provide a buffer from OA or cause additional stress. Coralline algae are extremely vulnerable to OA. As pH decreases with OA, the high magnesium content of the corallines $CaCO_3$ skeleton is increasingly susceptible to dissolution (Ries, 2006; Ries, 2011; Cornwall et al., 2017; Kamenos et al., 2016). In OA conditions, CCA has displayed reduced growth (Hofmann et al., 2012; Ragazzola et al., 2012), calcification (Gao and Zheng, 2010), epithelial integrity (Burdett et al., 2012) and distribution/abundance (Kuffner et al., 2008; Hall-Spencer et al., 2008; Porzio et al., 2011). In reduced bulk seawater pH, CCA are still able to maintain the pH of their calcifying fluid, but this ability is notably limited (Cornwall et al., 2017; Kamenos et al., 2013; Kamenos et al., 2016; Martin et al., 2013).

Although CCA can be buffered from low pH by local daytime increases in pH within their own DBL (Cornwall et al. 2014), low pH conditions can still be quite harmful (Cornwall et al., 2013a). The upregulation of the pH of the calcifying fluid doesn't fully buffer coralline algae from the effects of OA. The slope of the relationship between seawater pH and the pH of the calcifying fluid is thought to determine the sensitivity of the calcification rate to decreased seawater pH (Cornwall et al., 2017). Net calcification of coralline algae generally declines as seawater pH decreases, with extent of the decrease being species-specific

(Cornwall et al., 2017). For example, for three different coralline algal species examined, the change in pH of the calcifying fluid per unit external seawater pH was not 1 for all the species (Cornwall et al., 2017).

In a 40-day lab experiment, coralline macroalgae showed reduced growth rates in bulk seawater pH_T 7.65, compared to pH_T 8.05. Moreover, diel pH fluctuations led to additional reduced growth in bulk seawater pH_T 7.65 (Cornwall et al., 2013a). The effect of reduced seawater pH on the DBL and its respective carbonate chemistry and metabolic processes remains unclear. In this study, on a short term (minutes to hours) scale, DBL thickness and surface oxygen concentration were not significantly impacted by bulk seawater pH, but there may be other variables to consider as there are a number of physiological processes in CCA that control the regulation of carbonate chemistry at the site of calcification (Cornwall et al., 2017). Although bulk seawater pH didn't have a significant effect on DBL thickness or surface oxygen concentration in this study, there was an observable trend of decreasing DBL thickness with decreasing bulk sewater pH; in 3 L aquaria, the thickest DBL was found at bulk seawater pH 8.1, followed by bulk pH 7.7, and the thinnest DBL at bulk pH 7.4. The extent to which changes in pH in the bulk seawater affect DBL thickness and the ability of macroalgae to modify their local environment is an area of ongoing research.

It is also likely that other variables besides pH play crucial rules in determining the effects of OA on CCA and coralline algal diffusion boundary layers. This study only measured oxygen directly due to the lack of available pH microsensors. While the relationship between pH and oxygen is relatively well established within the DBL (Cornwall et al., 2014; Noisette and Hurd, 2018; Chan et al., 2016; Cornwall, 2013), the pH values in this experiment had to be estimated. pH values were calculated from raw oxygen values based on relationships between pH and oxygen defined in similar previous experiments (Cornwall, 2013), but it is possible that the same pH-oxygen relationship doesn't apply as well in reduced bulk seawater pH. This may be because the physiological processes within the DBL and at the site of calcification differ under ambient and reduced bulk seawater pH conditions. Additionally, parameters like total alkalinity cannot yet be measured within the DBL. Thus, calcium carbonate saturation state, which is calculated from DIC and total alkalinity data, was also indirectly calculated. In present-day conditions, when pH varies due to diel fluctuations, pH levels may decrease substantially, but calcite saturation states might not become undersaturated (Figure 2.14). However, in OA conditions, the additive effects of diel fluctuations and reduced seawater pH may cause saturation states to cross a critical threshold, revealing previously unseen effects.

Future research could examine and account for multiple carbonate chemistry parameters in the DBL in order to better determine the calcification environment for marine organisms in the DBL in OA conditions.

The ability of macroalgae such as CCA to modify their local chemical environment is an important factor contributing to the extremely variable and fluctuating pH conditions within the DBL. Measuring the oxygen and pH fluctuations above algal substrates in different conditions that control DBL thickness, such as flow, irradiance and bulk seawater pH provides insight into the variable conditions organisms actually experience over a 24-hour period. The DBL significantly changes the conditions that CCA and potential organisms living within the DBL endure. This finding has pronounced importance in the field of OA, as previous research has shown that DBLs ameliorate some of the negative effects of OA on macroalgae by buffering them from the corrosive effect of reduced seawater pH (Cornwall et al., 2014). However, the effects of the DBL remain unknown for other marine organisms living with the DBL, such as newly settled sea urchins. There is very limited research on understanding the effects of ocean acidification on species interactions and ecosystem functioning (O'Leary et al., 2017; Kroeker et al., 2012). The next chapter of this thesis (Chapter 3) aims to fill that gap in order to understand how pH variability within coralline algal diffusion boundary layers will affect growth of newly settled sea urchin, *P. huttoni* in present-day and ocean acidification conditions.

Chapter 3: Growth of newly settled sea urchins in coralline algal diffusion boundary layers

3.1 Introduction

Marine organisms, such as sea urchins, whose planktonic larvae swim and settle in microhabitats dominated by primary producers, experience relatively large and rapid spatial and temporal changes in seawater pH due to the boundary layer above algal surfaces (Wahl et al., 2015b; Cornwall et al., 2014). However, the direct effects of varying boundary layer seawater pH on larval settlement and early post-settlement growth remain unknown (Espinel-Velasco et al., 2018). Studying boundary layers is therefore, particularly important in order to understand the potential biological implications for OA because organisms living within a thick diffusion boundary layer (DBL) will experience a chemical and physical environment different to that of the overlying bulk seawater (Denny, 2000; Cornwall, 2013; Hurd et al., 2011).

Decreasing surface seawater pH, also known as ocean acidification, poses a major threat to marine ecosystems and particularly to calcifying organisms such as echinoderms (Hendriks et al., 2010; Kroeker et al., 2013; Dupont et al., 2010b; Dupont and Thorndyke, 2013; Byrne, 2011). Echinoderms, such as sea urchins, are thought to be additionally vulnerable to OA because of their indirect lifecycle—the transition from a planktonic larval stage to a benthic adult stage (Byrne, 2011; Byrne et al., 2017; Hofmann et al., 2010; Espinel-Velasco et al., 2018). The early juvenile or post-settlement stage is considered to be especially sensitive to environmental stressors and a potential population bottleneck (Wolfe et al. 2013, Gosselin and Qian 1997).

Ocean acidification has deleterious effects on development of invertebrates in their larval stage (see reviews by Dupont et al. 2010, Byrne 2011, Kroeker et al. 2013, Przeslawski et al. 2015, Byrne et al. 2017 and Espinel-Velasco et al. 2018). However, the effects on the development of echinoderms in the post-settlement period are varied. Test diameter of the juvenile sea urchin *Paracentrotus lividus* was larger when larvae and juveniles were reared at pH_{NBS} 7.7 compared to pH_{NBS} 8.1; the sea urchins in pH_{NBS} 7.7 also underwent metamorphosis 8 days later (García et al., 2015). The lecithotrophic sea star *Crossaster papposus* developed faster in low pH with no visible effects on survival or skeletogenesis (Dupont et al., 2010b). More neutral or limited effects were found in other species, such as the

juvenile sea urchin *Heliocidaris erythrogramma*, where survival and test growth were robust to low pH, while spine length decreased and morphology altered under only the lowest pH levels (pH_T 7.4) (Wolfe et al., 2013b). Early benthic juveniles of the sea star *Parvulastra exigua* were tolerant of low pH, with negative effects seen only after four weeks at pH_T 7.24 (Nguyen and Byrne, 2014). *Arbacia lixula* juveniles were smaller when larvae were grown in pH_T 7.7 in comparison to pH_T 8.1, but temperature elicited larger effects than acidification (Wangensteen et al., 2013). Reduced seawater pH appears to disrupt growth of sea urchins, particularly at early life stages, but these effects are complex, varied and depend on both the pH levels and species examined.

Diffusion boundary layers (DBL), which control the difference in pH between overlying bulk seawater and the substrate that the organisms are living on, are rarely considered when studying the effect of reduced seawater pH on the settlement and early post-settlement growth of sea urchins (Chan et al., 2016). Newly settled juveniles might be living in pH conditions that are different from the bulk seawater, which may account for some of the variability found on post-settlement development of invertebrate responses to OA conditions. Examining whether pH fluctuations within the DBL will augment or alleviate the impacts of reduced bulk seawater pH due to OA is crucial (Wahl et al., 2018; Wahl et al., 2015b; Shaw et al., 2012).

This chapter aimed to examine the effects, and implications under future ocean acidification pH levels, of coralline algal diffusion boundary layers on growth of newly settled sea urchins in the DBL. To examine the effects of the DBL, which is controlled by seawater velocity and biological activity controlled by light, I firstly measured test diameter and spine length of newly settled sea urchins *Pseudechinus huttoni* under experimentally manipulated irradiance and flow conditions. Secondly, to examine the effects and implications of the DBL under future OA pH conditions, I measured test diameter and spine length of juvenile *P. huttoni* under experimentally manipulated bulk seawater pH and irradiance conditions. I also used scanning electron microscopy to further characterize calcification and growth in experimental conditions at reduced bulk seawater pH.

3.2 Methods

3.2.1 Collection of settlement substrates

CCA covered rocks (0.5-2 cm diameter and 4-7 cm diameter) were collected in July and August 2018. Details of collection sites are provided in Chapter 2.

3.2.2 Collection and spawning of *P. huttoni*

Adult *Pseudechinus huttoni* were collected from Hall Arm in Doubtful Sound, Fiordland National Park, New Zealand on June 7, 2018 by SCUBA divers. After collection, adults were transported to a flow through aquarium tank at the Portobello Marine Lab. On June 11, 2018, adults were spawned following standard techniques of injection with 0.5 mol l^{-1} KCL (Figure 3.1).

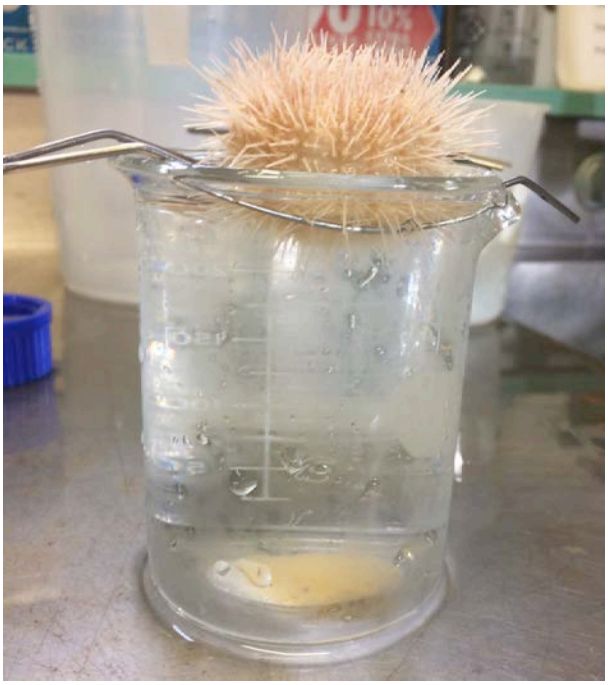

Figure 3.1 Spawning of adult *Pseudechinus huttoni* into a 250 mL beaker during their natural spawning regime in the austral winter month of June in 2018. The animal is held inverted on a steel gradle, meaning the gonopores (the site of gamete release) are submerged. Eggs can be seen accumulating on the bottom of the beaker.

3.2.3 Rearing of *P. huttoni*

Larvae were reared at 10-13°C in replicate 2.5 L glass jars at densities ranging from 3 to 20 larvae per mL. Larvae were initially kept at higher densities, and as they developed, were progressively thinned to lower densities. Jars were cleaned periodically, as needed, per visual inspection. Cultures were stirred continuously with large plastic paddles, at a rate of 10 swings per minute, to keep larvae and food suspended in the water column. Larvae were fed a combination of *Rhodomonas lens* and *Dunaliella primolecta* daily at 8000 cells ml^{-1}. Water was changed every third day, with larvae photographed weekly to monitor development (Figure 3.2). The first evidence of metamorphosis was observed at 53 days post-fertilisation, with most larvae showing signs of competency (e.g. well-developed rudiments) from 60-75 days post-fertilisation. Larvae were checked for competency to settle based on trial settlement experiments, where approximately ten larvae were placed in each well of a 6-well dish and

checked every hour for % settlement and metamorphosis. Once over 50% had settled within a few hours, larvae were deemed competent to settle and were thus used in settlement experiments.

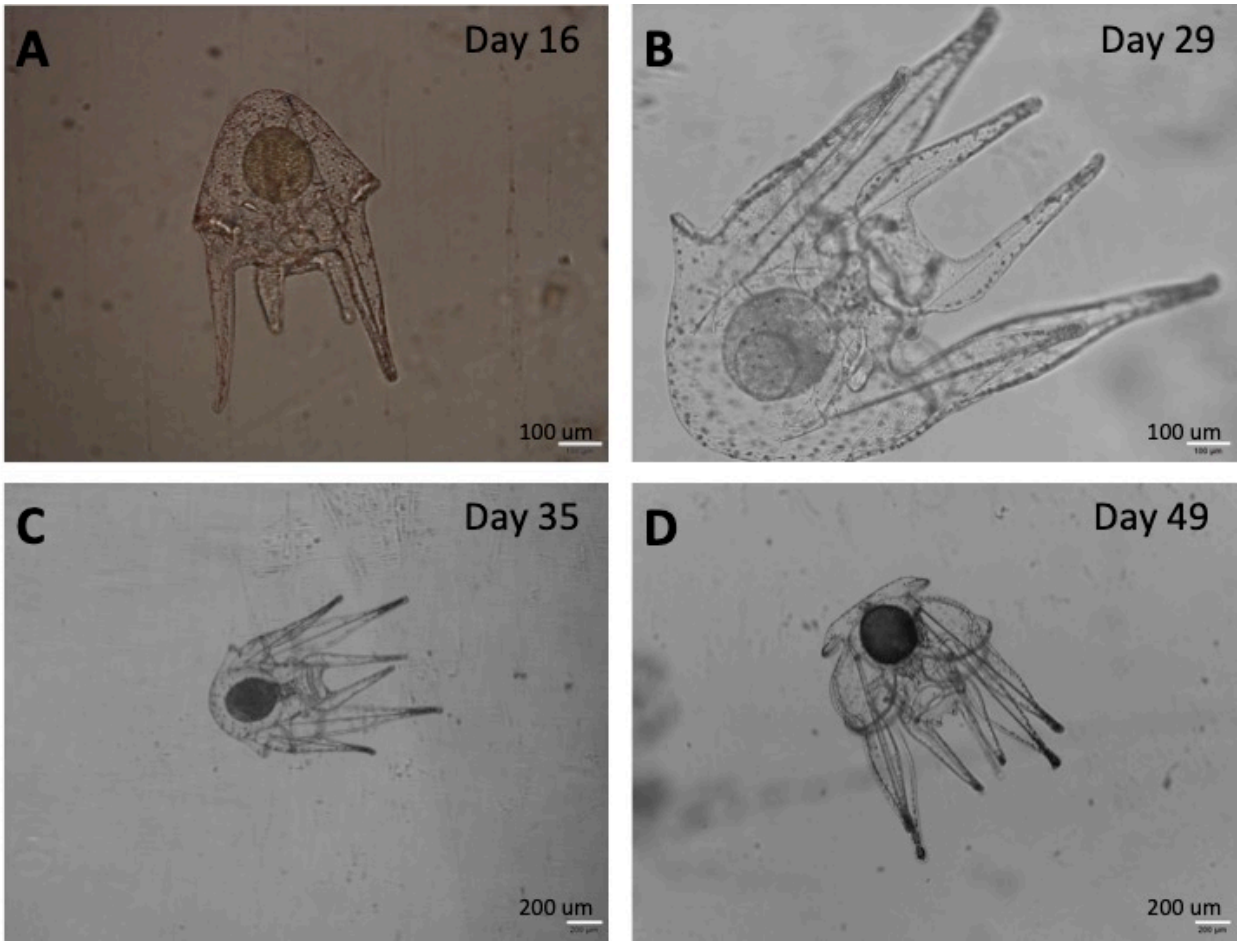

Figure 3.2 Images showing the larval development of the sea urchin *Pseudechinus huttoni* (A) 16, (B) 29, (C) 35 and (D) 49 days post-spawning. Scale bars ~100 µm on the top row and ~200 µm on the bottom row.

3.2.4 Boundary layer measurements

In order to determine the chemical conditions in the DBL that juvenile sea urchins grew, oxygen concentrations were measured with microsensors above CCA surfaces in a range of flow, irradiance and bulk seawater pH conditions. Details of measurements are given in Chapter 2. Oxygen concentration (µmol L^{-1}) was used as a proxy for seawater pH based on previous research (Cornwall et al., 2014). pH_{DBL}, as described in Chapter 2, represents the average pH from 0 to 0.5 mm above the CCA surface. This is an estimation of the pH levels that juvenile sea urchins experienced in this study. A thickness of 0 to 0.5 mm above the surface was chosen since the newly settled sea urchins have test diameters of approximately 0.4 to 0.5 mm. For juveniles in the 12-hour light/12-hour dark alternation treatment, the pH_{DBL} of the light and dark conditions were averaged.

3.2.5 Summary of experimental design

P. huttoni juveniles were grown in experimental conditions in order to determine the effect of coralline algal diffusion boundary layers on early post-settlement growth and the subsequent implications for ocean acidification pH conditions (Table 3.1; Figure 3.3). The set up with the 2.5 L glass jars was used to examine the effects of irradiance and flow on growth of newly settled *P. huttoni* in the DBL (Experiments #1-3), and the 3 L aquaria were used to examine the effects of irradiance and bulk seawater pH on growth in the DBL in order to understand the implications for OA (Experiments #4 and 5).

Table 3.1. Summary of experiments completed to examine the effects of irradiance, flow and bulk seawater pH on post-settlement growth of *Pseudechinus huttoni*. Three experiments manipulated irradiance and flow in order to examine growth in the DBL in ambient pH bulk seawater. Two experiments manipulated irradiance and bulk seawater pH in order to examine growth in the DBL under OA conditions.

Bulk Seawater pH	Container	Treatment Levels	Duration of Experiment (days post-settlement)	Reference
Ambient pH 8.1	2.5 L Glass Jars	2 irradiance (dark or light) x 2 flow (no flow or flow)	4 and 9	Experiment # 1
			11	Experiment # 2
			6	Experiment # 3
Ambient (pH 8.1), predicted near future (pH 7.7) and extreme (pH 7.4)	3 L Aquaria	2 irradiance (dark or light) x 3 bulk pH (7.4, 7.7 or 8.1)	~4	Experiment # 4
			4	Experiment # 5

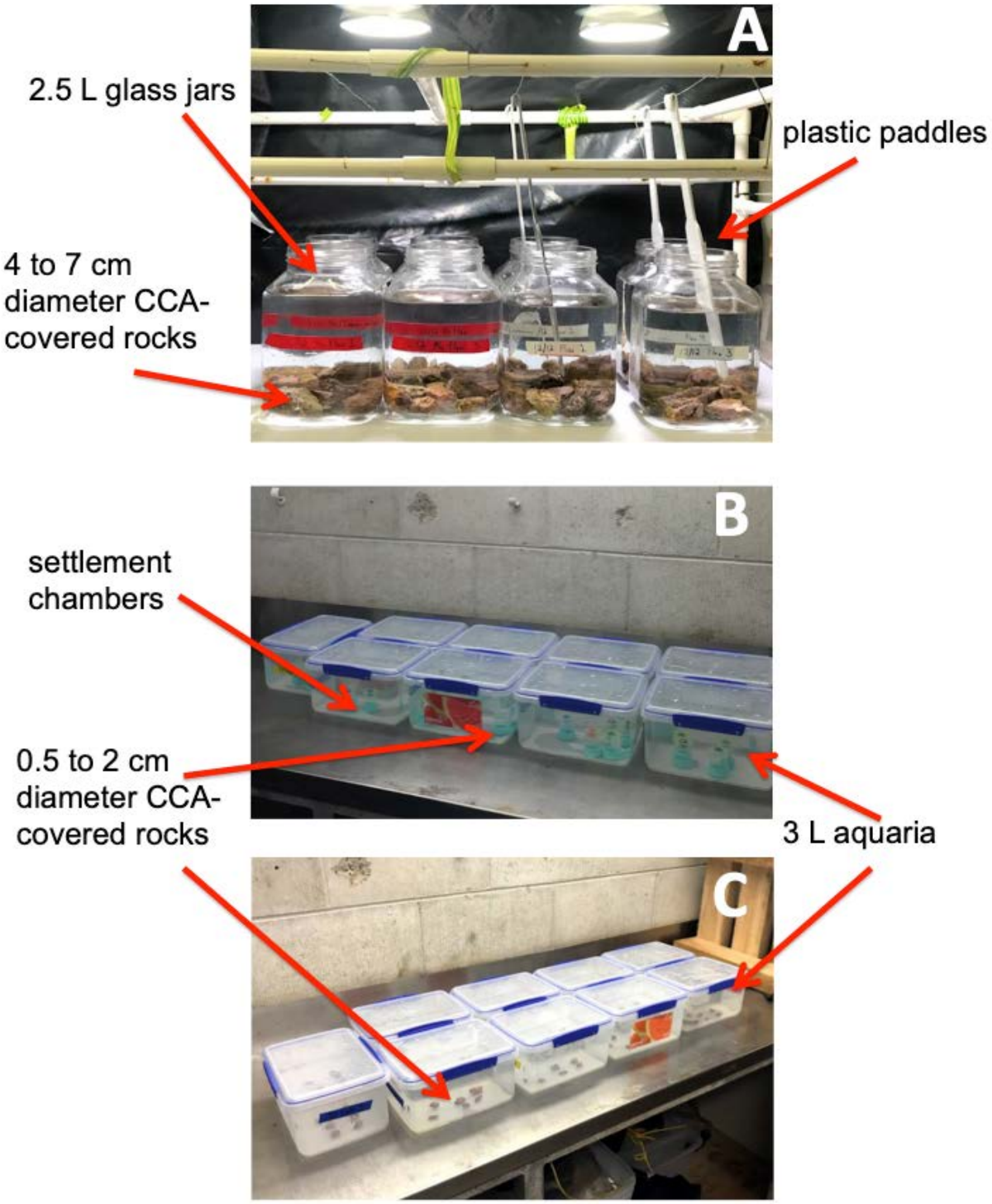

Figure 3.3 The experimental set-ups for examining post-settlement growth of *Pseudechinus huttoni*. (A) The 2.5 L glass jars with 4 to 7 cm diameter CCA covered rocks at the bottom. The four replicate glass jars on the left are in light and no flow; the jars on the right are in light and flow (generated by plastic paddles). (B) The 3 L aquaria with 0.5 to 2 cm diameter CCA covered rocks in settlement chambers (falcon tubes) where *P. huttoni* larvae were pipetted into and allowed to settle. (C) The 3 L aquaria with 0.5 to 2 cm diameter CCA covered rocks where *P. huttoni* larvae were previously settled upon.

3.2.6 Effects of irradiance and flow

Three experiments were completed examining the effects of irradiance and flow on post-settlement growth of *P. huttoni*. There were a total of six treatments (2 flow x 3 irradiance) with four replicate 2.5 L glass jars per treatment. The two flow levels were "flow" and "no flow". Flow was initiated using "urchin stirrers" or paddles that swing at 10 cycles per minute. "No flow" refers to static or zero flow (0 cm s^{-1}). The three irradiance levels were "light", "dark" and "alternation". The dark treatments received <3 μmol photons m^{-2} s^{-1} and the light treatments received approximately 40 μmol photons m^{-2} s^{-1} of light, provided by overheard lights (LED PAR38, 18W). The alternation treatments received 12 hours of dark (<3 μmol photons m^{-2} s^{-1}) and 12 hours of light (40 μmol photons m^{-2} s^{-1}), provided by the same overhead lights. Irradiance was measured using a flat terrestrial LI-250A quantum sensor (LI-COR, Lincoln, USA). All experiments used 5 μm-filtered seawater from the Otago Harbour (salinity ~33ppt and temperature ~11ºC) and took place in a controlled temperature room at approximately 11ºC.

One day prior to beginning the first flow and irradiance post-settlement growth experiment (Experiment #1), ten CCA covered rocks, 4 to 7 cm diameter, were placed on the bottom of 2.5 L glass jars filled with UV sterilized seawater. Temperature was 11ºC and pH_T was 8.09, measured spectrophotometrically (see Chapter 2 for further details). The following day, approximately 60 competent larvae, 62 days old, were pipetted into each glass jar and introduced to the CCA cue. The larvae were given 48 hours to settle before treatments began. During this time, all treatments received minimal light (1-4 μmol photons m^{-2} s^{-1}). After the 48 hours, the light and flow treatments began. After four days in the treatments and six days after being introduced to the CCA cue, five of the ten CCA encrusted rocks were removed from each glass jar. After nine days in the treatment and 11 days after being introduced to the cue, the remaining five encrusted rocks were removed from each glass jar. Though juveniles were not fed, the length of experiments were chosen because *P. huttoni* juveniles require approximately one week in order to develop a functional Aristotle's lantern and digestive system (Fadl et al., 2017), thus growth was examined before and after individuals were capable of ingesting food. However, most—over three quarters—of the larvae settled on the bottom of the glass jar instead of directly upon the CCA covered rocks. Thus, the results from this experiment were analysed and recorded, but are not reported in this thesis due to lack of sample size. Experimental design was adjusted in the following experiments to minimize this possibility of larvae settling on glass instead of coralline algae.

The second (Experiment #2) and third (Experiment #3) experiments examining the effects of irradiance and flow used additional batches of larvae deemed competent to settle. These larvae were 69 and 74 days old in Experiment #2 and #3, respectively. Approximately 4,000 (Experiment #2) or 4,400 (Experiment #3) larvae were placed into 3 L aquaria with approximately 100 (Experiment #2) or 150 (Experiment #3) CCA covered rocks, each 0.5 to 2 cm in diameter. The larvae were given 24 hours to settle on the rocks. After 24 hours, four (Experiment #2) or six (Experiment #3) rocks were placed into each 2.5 L glass jar. Only the larvae that settled on the rocks were used in the experiment. Light and flow treatments started immediately. All rocks were removed from each glass jar after eleven (Experiment #2) or six (Experiment #3) days of treatment. Again, the two experiment durations were chosen in order to examine growth before and after individuals were capable of digesting adult food around seven days old. Despite attempts to increase sample size per replicate, the number of juveniles measured was not as high as anticipated, especially for experiment #3 where the number of juveniles measured per replicate jar ranged from 0 to 3; with four replicate jars per treatment, but some replicate jars had no suitable juveniles to measure (Appendix 11). The number of juveniles measured per replicate in experiment #2 ranged from 0 to 8, with four replicate jars per treatment and only one jar having no suitable juveniles (Appendix 11).

3.2.7 Effects of irradiance and bulk seawater pH

Two experiments were completed examining the effects of irradiance and bulk seawater pH to determine the effects of a DBL on post-settlement growth of *P. huttoni* under OA conditions. There were a total of six treatments (3 bulk pH x 2 irradiance) with three replicate 3 L aquaria. The three pH levels were ambient (pH_T 8.1), predicted near future (pH_T 7.7) and extreme pH (pH_T 7.4). These pH values were used as proxies to represent ppm levels of 400, 800 and 1100 ppm. pH 7.7 or 800 ppm represents predicted near-future levels by 2100 (Gattuso et al., 2015), while pH 7.4 or 1100 ppm represents an extreme pH drop. The two irradiance levels were “light” and “dark”. The dark treatments received <1 μmol photons m^{-2} s^{-1} and the light treatments received 10 μmol photons m^{-2} s^{-1} of light, provided by overheard lights (standard fluorescent tubes, 845). Irradiance was measured using a flat terrestrial LI-250A quantum sensor (LI-COR, Lincoln, USA).

The first growth experiment in OA conditions (Experiment #4) examined the effect of bulk seawater pH and boundary layers on the settlement and post-settlement growth of *P. huttoni*. CCA covered rocks (0.5 to 2 cm diameter) were placed in custom-made inverted settlement chambers, as per methodology from Espinel-Velasco, Agüera and Lamare (*in preparation*).

The chambers were closed by a 100-micron mesh on the top end to allow water circulation while keeping the larvae inside. The chambers were than placed in 3 L sealed aquaria containing water at the desired pH in both light and dark conditions. Next, approximately 30 larvae were added into each chamber, and the chambers were checked for settlement after 6, 18, 30 and 51 hours under a dissecting microscope. Larvae were counted and placed into two categories: (1) not-settled: remaining larvae, indicated by swimming in the water column or crawling on the bottom or (2) settled and metamorphosed: indicated by the presence of juveniles at the bottom of the chambers. After the initial 6 hours, 14.4% to 32.6% of larvae had settled on the CCA in dark conditions. The settlement percentage in light conditions reached 26.1% to 29.7%. Settlement on CCA increased for all treatments during the following hours, reaching settlement of 60.6% to 62.0% in dark conditions and 57.6% to 77.4% in light conditions after 51 hours (Espinel-Velasco Agüera and Lamare, *in preparation*). Simultaneously, at 6, 18, 30 and 51 hours after pipetting, the water in the treatments was changed. New seawater was transferred into the 3 L aquaria from flow-through header tanks maintained at approximate pH_T levels of 8.1 (ambient), 7.7 (medium) and 7.4 (low) controlled by a TUNZE controller and achieved by bubbling 100% CO_2 gas into the system. The pH and temperature of the outgoing and incoming water was measured, with a spectrophotometer and mercury thermometer, respectively. Sample water from each flow-through tank was taken for carbonate chemistry analysis at the beginning of experiment #4.

After counts of settlement stopped at 51 hours, the juveniles and remaining larvae were kept in the same experimental set-up for three additional days to measure growth approximately four days post-settlement. Since larvae settled and metamorphosed at different points throughout this experiment, the age of the juveniles (days post-settlement) was estimated. After 51 hours, pH and temperature were measured and water was changed every 24 hours to keep the pH relatively stable. After three days in the treatment (five days after introduction to the cue), the settlement chambers (falcon tubes) were removed from each tub. This stage was chosen because *P. huttoni* juveniles do not typically start to feed until approximately seven days post-settlement, thus food would not be a confounding factor.

The second growth experiment investigating the effects of irradiance and bulk seawater pH (Experiment #5) used another batch of larvae deemed competent to settle. These larvae were 69 days old. Approximately 4,700 larvae were placed into a 3 L aquaria with approximately 200 CCA covered rocks, each 0.5 to 2 cm in diameter. The larvae were given 24 hours to settle on the rocks. After 24 hours, six rocks were placed into each 3 L aquaria. Rocks were

either visually examined or examined under the dissecting scope to ensure that each rock had at least one juvenile attached. Only the larvae that settled on the rocks were used in the experiment. For the following four days, pH and temperature were measured and water was changed every 24 hours to keep the pH relatively stable. After four days in the treatment (five days after introduction to the cue), the rocks were removed from each tub. This stage was again chosen because *P. huttoni* juveniles do not typically start to feed until approximately seven days post-settlement. The number of juveniles measured per replicate for Experiment #4 ranged from 3 to 11, with three replicates per treatment (Appendix 12). An average of ~ 7 juveniles were measured per replicate. The number of juveniles measured per replicate in Experiment #5 ranged from 15 to 47, with three replicates per treatment and an average of ~28 juveniles measured per replicate (Appendix 12).

3.2.8 Removal and photographing

After removal of the settlement chambers or rocks from the respective treatments, rocks were examined under a dissecting scope. Juveniles were removed from the substrate they settled on by using a Pasteur pipette to flush the juveniles off with a strong water blast. The majority of juveniles were attached to and subsequently removed from CCA substrate. However, because some of the juveniles may have metamorphosed on the bottom of the settlement chamber (falcon tube) or on small sections of the rock without CCA coverage, there is a possibility that some juveniles were not actually living within the DBL above CCA. Despite this, all juveniles collected were photographed for analysis because it was impossible to tell whether juveniles had recently fallen off the substrate during examination or had developed off the substrate.

After removal, juveniles were pipetted into a 1.5 mL Eppendorf tube and fixed with 0.5 mL of paraformaldehyde solution (4% PFA in FSW, buffered). Juveniles were stored in a fridge, then examined and photographed with a camera (Olympus XC50) under a compound microscope (Olympus BX51) within three days of being fixed. No signs of post-fixation change were observed. The same juvenile was photographed multiple times in different focal planes to ensure all spines and the test were in focus in at least one image (Figure 3.4). Most juveniles were imaged on either their aboral or oral surface, although not all could be oriented in this way. Images were sorted and images were discarded if juveniles were (1) not laying flat on their aboral or oral surface, (2) covered by algae, another urchin or other unknown material or (3) if the sea urchin showed signs of disintegration i.e. did not successfully metamorphose and survive.

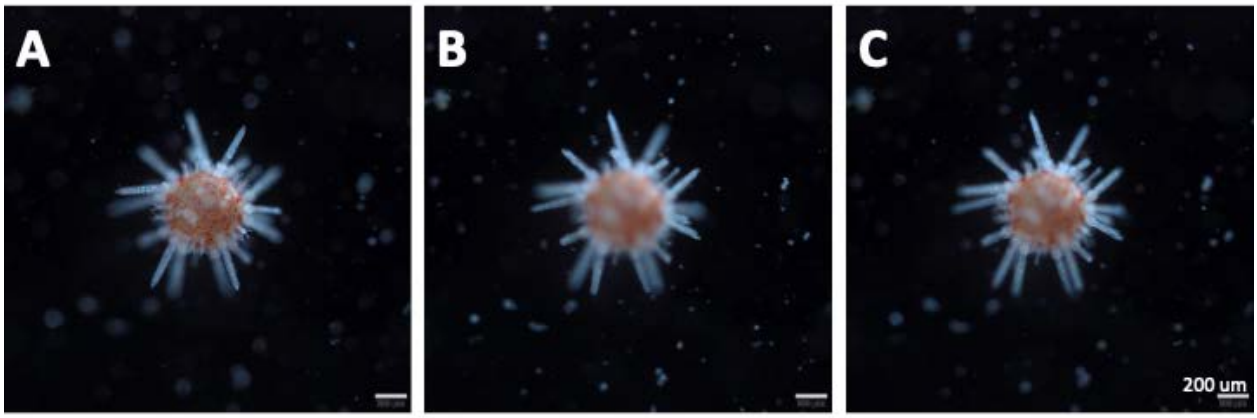

Figure 3.4 Photographs at different focal planes of a juvenile sea urchin, *Pseudechinus huttoni* eleven days post-settlement taken with a compound microscope. Scale bars ~200 μm.

3.2.9 Juvenile morphology

Average spine length and test diameter (Figure 3.5) were measured for each juvenile with Image-J (NIH, Cary, NC, USA). Two test diameters were measured, approximately perpendicular to each other at the longest diameter of the test, and subsequently averaged. The three longest spines were measured from the outer edge of the test to the tip of the spine and subsequently averaged.

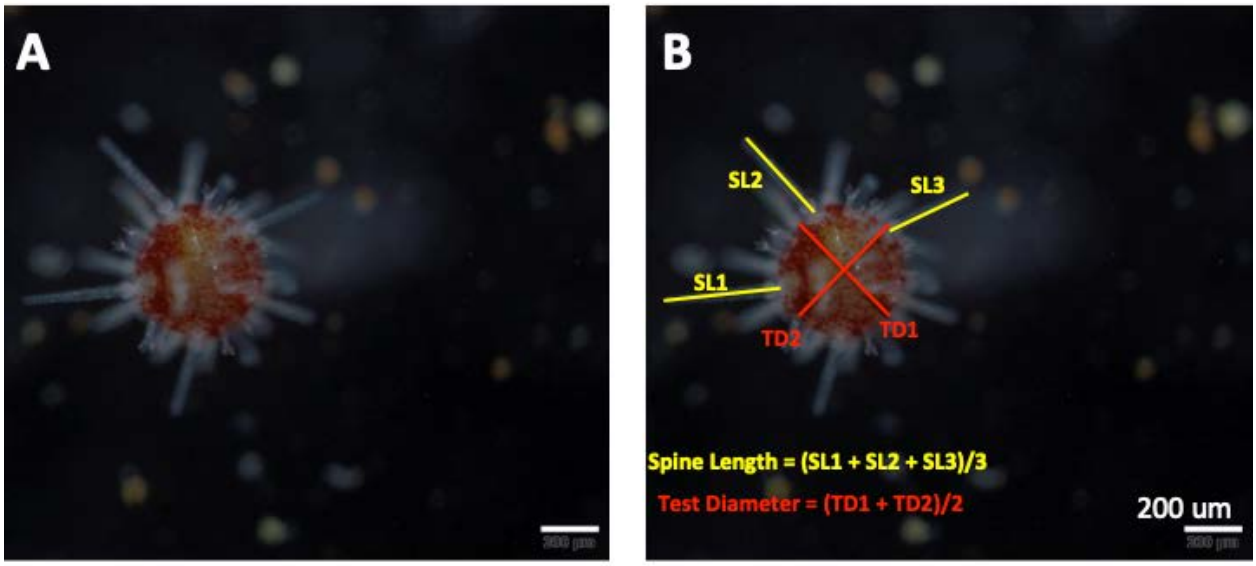

Figure 3.5 (A) Photograph taken with a compound microscope and (B) associated morphometric measurements of a juvenile sea urchin *Pseudechinus huttoni* four days post-settlement. Measurements made are the test diameter (average of two longest diameters) in red and spine length (average of three longest spines) in yellow. Scale bars ~200 μm.

3.2.10 Scanning electron microscopy

Juveniles from the second post-settlement growth experiment (Experiment #5) were prepared for analysis with scanning electron microscopy (SEM) in order to examine the calcification of skeletal elements. Juveniles were prepared in a bleach treatment following the protocol of

Wolfe et al. (2013), where juveniles were placed in a 1% bleach treatment in distilled water for 30 minutes in order to remove the cuticle and provide the best view of the skeleton. The juveniles were then rinsed three times with distilled water and placed in a drying oven at 45°C for 48 hours. The juveniles fell apart after the bleach treatment, leaving pieces of the spine and skeleton to be analysed. These pieces were mounted on stubs with conductive double-sided tape and coated with gold using a Quorum gold coater. Observations and photographs were taken using a Hitachi TM3000 tabletop SEM.

3.2.11 Statistical analysis

For spine length, and test diameter, Levene's tests were used to test for homogeneity of variance (Appendix 2) and QQplots and Shapiro-Wilk Tests were used to test for normality. Only the test diameter of Experiment #2 failed to meet these assumptions. Test diameter in Experiment #2 was log transformed to meet the assumptions of normality and homoscedasticity. A two-way ANOVA was used to test for significant differences in spine length and test diameter among treatments. For morphometrics under present-day conditions (Experiment #2 and 3), fixed factors were irradiance and flow; for morphometrics under OA conditions (Experiment #4 and 5), fixed factors were irradiance and pH, treating pH as a categorical variable rather than continuous. Post-hoc Tukey HSD tests were used to test for pairwise significant differences. I also used a generalised linear model (GLM) to investigate the effects of pH_{DBL} on spine length and test diameter. All statistical analyses were performed using RStudio, version 1.1.453 (RStudio Team, 2016)

3.3 Results

3.3.1 Seawater parameters

Representative carbonate chemistry parameters of the mainstream seawater in the 3 L aquaria and 2.5 L glass jar experiments are given in Table 3.2. Seawater used in 2.5 L glass jars had pH_T level 8.09, while seawater used in 3 L aquaria had sample pH_T levels of 8.09, 7.68 and 7.48, referred to as bulk pH 8.1, 7.7 and 7.4. The pH values before and after water changes in the post-settlement growth experiments manipulating irradiance and bulk seawater pH (Experiments #4 and 5) demonstrate three distinct bulk seawater pH conditions (Figure 3.6 and 3.7; Appendix 9 and 10). pH levels achieved were approximately pH_T 8.1, 7.7 and 7.4, and pH stayed relatively stable (±0.1 units) between water changes.

Table 3.2 Carbonate chemistry parameters (pH_T, total alkalinity, DIC, temperature, salinity, carbonate, saturation state for calcite, saturation state for aragonite and partial pressure of CO_2) in the 3 L aquaria (bulk pH 8.1, bulk pH 7.7 and bulk pH 7.4) and 2.5 L glass jars (bulk pH 8.1). No standard error is reported because only one water sample was taken per treatment.

		3 L aquaria	
	2.5 L jars Bulk pH 8.1	Bulk pH 7.7	Bulk pH 7.4
pH_T	8.09	7.68	7.48
A_T (µEq/kg)	2290	2290	2280
DIC (µmol/kg)	2090	2240	2290
Temperature (°C)	10.5	10.5	10.5
Salinity	34.2	34.2	34.2
$[CO_3^{2-}]$ (µmol/kg)	147	63.1	40.7
Ω_{Ar}	2.23	0.96	0.62
Ω_{ca}	3.51	1.51	0.97
pCO_2 (µatm)	350	999	1620

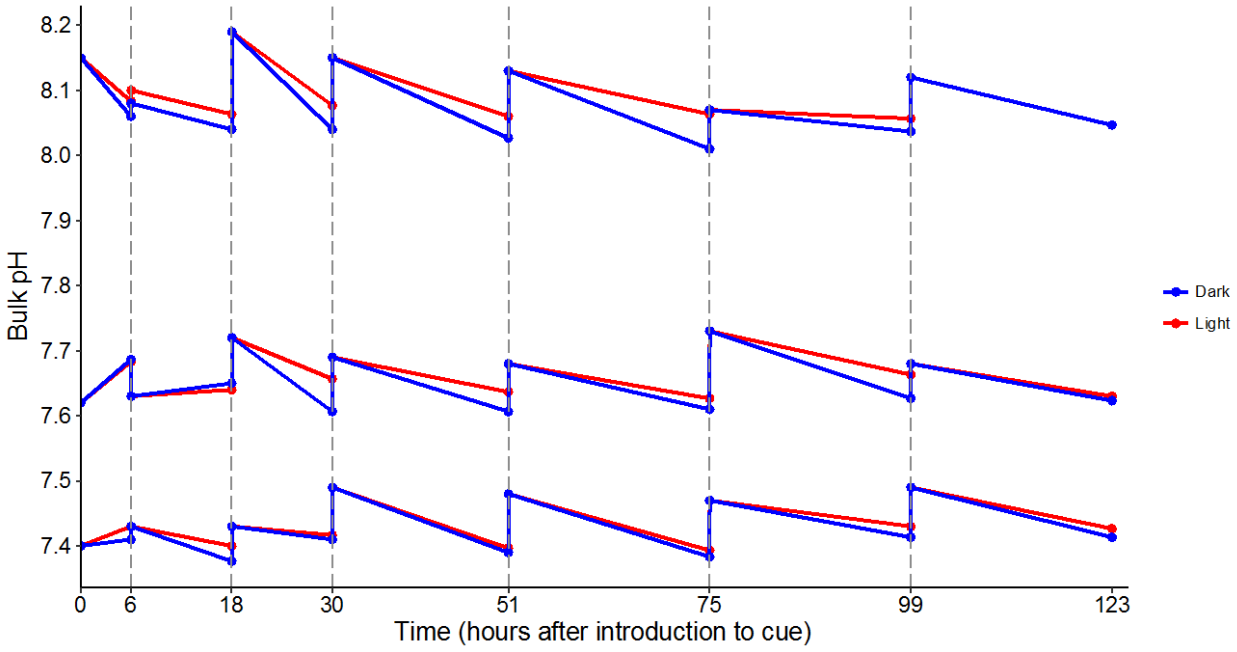

Figure 3.6 Bulk pH values (pH_T) of six treatment conditions in experiment #4 that *Pseudechinus huttoni* larvae settled, metamorphosed and grew. The three bulk seawater pH treatments are referred to as bulk pH 8.1, 7.7 and 7.4. Dark treatments are displayed in blue and light treatments in red. The vertical grey dashed lines represent a water change, where water was replaced from a flow-through header tank to maintain pH levels. pH was measured spectrophotometrically of the new water from the header tank water and of the old water from three replicate aquaria per treatment.

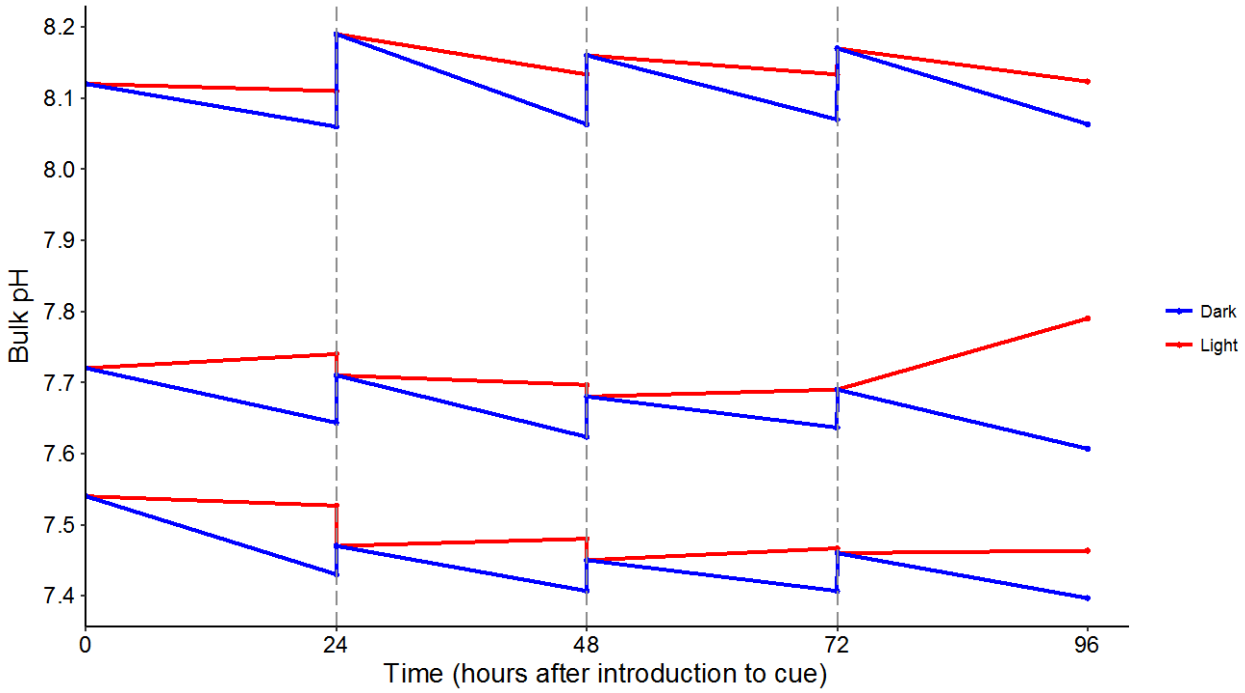

Figure 3.7 Bulk pH values (pH_T) of six treatment conditions in experiment #4 that *Pseudechinus huttoni* larvae grew in. The three bulk seawater pH treatments are referred to as bulk pH 8.1, 7.7 and 7.4. Dark treatments are displayed in blue and light treatments in red. The vertical grey dashed lines represent a water change, where water was replaced from a flow-through header tank to maintain pH levels. pH was measured spectrophotometrically of the new water from the header tank water and of the old water from three replicate aquaria per treatment.

3.3.2 Effects of irradiance and flow on post-settlement growth in the DBL

Six days post-settlement, there were no significant effects of irradiance on test growth or spine development (Table 3.3 and 3.4; Figure 3.8), but eleven days post-settlement, juvenile sea urchins in the dark had longer spines than juveniles in the light or alternation treatments (Figure 3.9). Figures 3.8 and 3.9 display the same data in two different manners, figure 3.8 showing the effects of irradiance and figure 3.9 showing the effects of flow. A two-way ANOVA showed that there was a significant effect of irradiance on spine growth only (Table 3.4). Post-hoc Tukey tests indicated a significant difference between light and dark treatments at no flow ($p = 0.004$) and between dark and alternation treatments at no flow ($p = 0.015$). Post-hoc Tukey tests also revealed a significant difference between the light no flow and dark flow treatments ($p = 0.004$) and between the alternation no flow and dark flow treatments ($p = 0.013$).

Six days post-settlement, juveniles displayed large variability in test diameter and spine length in all treatments. Juveniles in the light treatments had the largest mean test diameter range (mean of 414 to 517 µm). The longest spines (452 µm ± 20; Mean ± SE) were found in the dark and the shortest (275 µm ± 75; Mean ± SE) in the light treatments. Eleven days post-settlement, juvenile spines were significantly different due to irradiance, but test diameter was very similar among treatments. The largest mean test diameter was 515 µm ± 31 (Mean ± SE), found in the dark and the shortest mean test diameter was 470 µm ± 11, found in the light.

Flow did not show any significant effects on test growth and spine development at six or eleven days post-settlement (Table 3.3 and 3.4; Figure 3.9). Six days post-settlement, juveniles in no flow had the largest mean test diameter (517 µm ± 30; Mean ± SE) and juveniles in flow had the shortest mean test diameter (414 µm ± 80; Mean ± SE). In contrast, eleven days post-settlement, juveniles in flow had the largest mean test diameter (515 µm ± 31; Mean ± SE) and juveniles in no flow had the smallest mean test diameter (470 µm ± 11). Spine lengths similarly showed no trends across flow treatments (Figure 3.9).

There were no significant interactive effects of flow and irradiance on test growth or spine length at either six or eleven days post-settlement (Table 3.4). Overall, juvenile sea urchins grew during treatments, with test diameters and spine length were generally higher eleven days post-settlement compared to six days post-settlement (Figure 3.8 and 3.9).

Table 3.3 Test diameter and spine length measurements of *Pseudechinus huttoni* juveniles grown in experimental treatments for 6 and 11 days post-settlement. pH_{DBL} refers to average pH levels from 0 to 0.5 mm above the surface of CCA; for the alternation treatments, it is an average of pH_{DBL} in the dark and light conditions. Values represent mean ± SE.

Experiment #	Age (days post-settlement)	Treatment	pH_{DBL}	Test Diameter (um) Mean ± SE	Spine Length (um) Mean ± SE
3	6	Alt Flow	8.08	452 ± 19	329 ± 46
		Alt No Flow	8.30	436 ± 25	322 ± 56
		Dark Flow	8.08	478 ± 7.7	452 ± 20
		Dark No Flow	8.04	440 ± 28	370 ± 62
		Light Flow	8.08	414 ± 80	275 ± 75
		Light No Flow	8.57	517 ± 30	360 ± 11
2	11	Alt Flow	8.08	474 ± 8.9	421 ± 13
		Alt No Flow	8.30	490 ± 11	386 ± 11
		Dark Flow	8.08	515 ± 31	471 ± 30
		Dark No Flow	8.04	481 ± 18	469 ± 5.3
		Light Flow	8.08	484 ± 12	405 ± 12
		Light No Flow	8.57	470 ± 11	373 ± 8.6

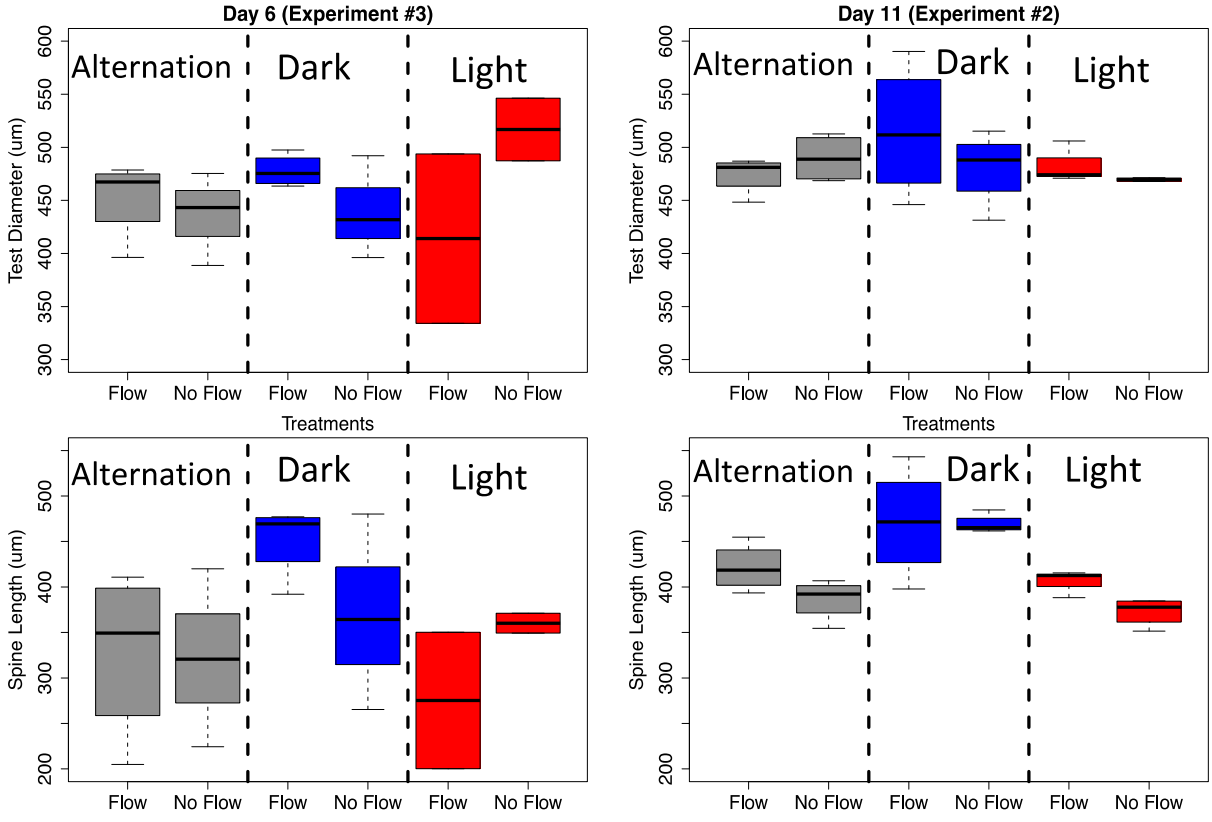

Figure 3.8 Effects of irradiance on test diameter (top row) and spine length (bottom row) in juvenile sea urchins *Pseudechinus huttoni* at six (left column) and eleven (right column) days post-settlement. The colours indicate the irradiance treatment: grey is 12-hour alternation, blue is dark treatment and red is light.

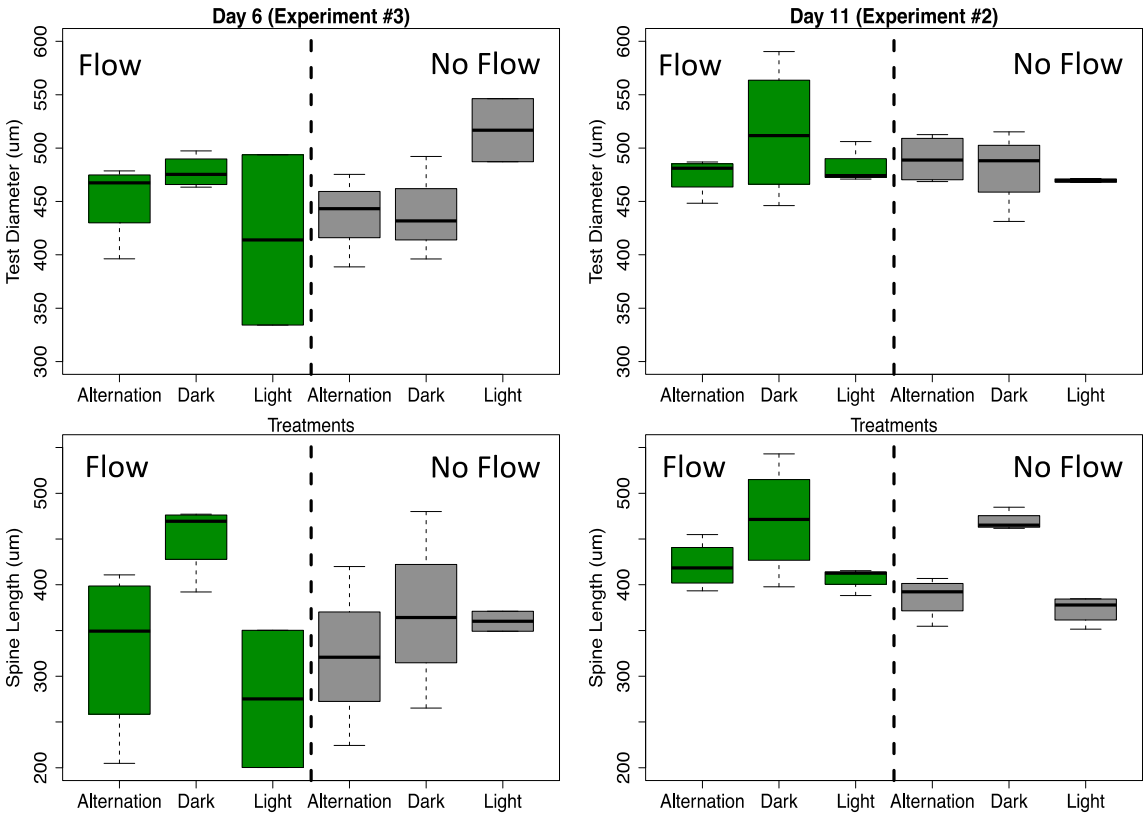

Figure 3.9 Effects of flow on test diameter (top row) and spine length (bottom row) in juvenile sea urchins *Pseudechinus huttoni* at six (left column) and eleven (right column) days post-settlement. The colours indicate the flow treatment: green is flow and grey is no flow.

Table 3.4 Two-way ANOVA examining the effects of irradiance and flow on test diameter and spine length of newly settled *Pseudechinus huttoni* juveniles. Experimental conditions are irradiance (light, dark or 12-hour alternation) and flow (flow or no flow). Significance level is p=0.05, with bold results indicating significant p values.

Experiment #	Age (days post-settlement)	Morphometric	Morphology Factor	Df	SS	MS	*F*	*p*
3	Day 6	Test Diameter	Irradiance	2	1374	687	0.294	0.750
			Flow	1	19.6	19.6	0.008	0.444
			Irradiance:Flow	2	13480	6740	2.89	0.095
			Residuals	12	28022	2335		
	Day 6	Spine Length	Irradiance	2	38005	19002	2.70	0.107
			Flow	1	1036	1036	0.148	0.708
			Irradiance:Flow	2	17825	8913	1.27	0.316
			Residuals	12	84317	7026		
2	Day 11	Test Diameter[a]	Irradiance	2	0.001	<0.001	0.776	0.476
			Flow	1	<0.001	<0.001	0.549	0.469
			Irradiance:Flow	2	0.002	<0.001	1.08	0.361
			Residuals	17	0.014	<0.001		
	Day 11	Spine Length	Irradiance	2	29735	14867	15.7	**<0.001**
			Flow	1	2901	2901	3.06	0.098
			Irradiance:Flow	2	1335	667	0.704	0.508
			Residuals	17	16112	948		

[a]Data log transformed to meet assumptions of parametric two-way ANOVA analysis.

3.3.3 Effects of irradiance and bulk seawater pH on post-settlement growth in the DBL

In the dark, where bulk seawater pH was similar to pH levels within the DBL (see Chapter 2), average spine length was reduced at lower bulk seawater pH levels (Table 3.5; Figure 3.10). For example, in Experiment #5, mean spine length was 380 µm ± 24 at bulk pH 8.1, 369 µm ± 30 at bulk pH 7.7 and 348 µm ± 15 at bulk pH 7.4. Mean test diameter showed contrasting results in the two experiments; mean test diameter was lowest at bulk pH 8.1 in Experiment #4, but highest at bulk pH 8.1 in Experiment #5 (Table 3.5; Figure 3.10). In the dark for Experiment #5, mean (± SE) test diameter decreased sequentially with decreasing bulk pH values. Mean test diameter was 451 µm ± 2.5 at bulk pH 8.1, 448 µm ± 8.1 at bulk pH 7.7 and 439 µm ± 7.9 at bulk pH 7.4.

In contrast, in the light, when bulk seawater pH was lower than that of pH levels within the DBL, average spine length was reduced at higher bulk pH levels (Table 3.5; Figure 3.10). The shortest mean spine lengths were found at bulk pH 8.1 and the longest mean spine lengths were found at bulk pH 7.4 in both experiments. Mean test diameter again showed more variable results; the shortest mean test diameters were found in juveniles grown at bulk pH 7.7 in both experiments.

A two-way ANOVA indicated significant differences among treatments only in spine length for Experiment #4 (Table 3.6). Bulk pH and the interactive effects of irradiance and bulk pH had significant effects on the spine length of *P. huttoni* juveniles approximately four days post-settlement. Post-hoc Tukey tests revealed that the only treatments that differed significantly were light bulk pH 7.4 and light bulk pH 8.1 ($p = 0.028$). In the light treatments, juveniles at bulk pH 8.1 had shorter spines than juveniles at bulk pH 7.4.

At the lowest bulk seawater pH treatment in this study (bulk pH 7.4), mean test diameter and spine length were both higher in the light treatment (where pH within the DBL was likely higher) compared to the dark treatment. In Experiment #5, at bulk pH 7.4, mean test diameter was higher in the light (455 µm ± 5.8; Mean ± SE) and lower in the dark (439 µm ± 7.9; Mean ± SE). In Experiment #4, mean test diameter was also slightly higher in the light (433 µm ± 3.2; Mean ± SE) than in the dark (430 µm ± 4.0; Mean ± SE). However, at bulk seawater pH 7.7, the same trend was not found. In Experiment #5, test diameter was either similar in the light (448 µm ± 8.1) and in the dark (450 µm ± 5.4) or in Experiment #4, test diameter was lower in the light (399 µm ± 6.2) than in the dark (427 µm ± 7.6).

Table 3.5 Test diameter and spine length measurements of newly settled *Pseudechinus huttoni* juveniles in different experimental treatments. pH_{DBL} refers to pH estimated in the DBL at the surface of the organism; it is the average pH from 0 to 0.5 mm above CCA surface. Values represent mean ± SE.

Experiment #	Age (days post-settlement)	Treatment	pH_{DBL}	Test Diameter (um) Mean ± SE	Spine Length (um) Mean ± SE
4	~4	Dark bulk pH 7.4	7.42	430 ± 4.0	165 ± 6.7
		Dark bulk pH 7.7	7.62	427 ± 7.6	169 ± 8.9
		Dark bulk pH 8.1	8.05	424 ± 16	180 ± 18
		Light bulk pH 7.4	8.09	433 ± 3.2	214 ± 2.6
		Light bulk pH 7.7	8.38	399 ± 6.2	165 ± 3.0
		Light bulk pH 8.1	8.64	413 ± 6.5	119 ± 39
5	4	Dark bulk pH 7.4	7.42	439 ± 7.9	348 ± 15
		Dark bulk pH 7.7	7.62	448 ± 8.1	369 ± 30
		Dark bulk pH 8.1	8.05	451 ± 2.5	380 ± 24
		Light bulk pH 7.4	8.09	455 ± 5.8	354 ± 4.9
		Light bulk pH 7.7	8.38	450 ± 5.4	338 ± 7.8
		Light bulk pH 8.1	8.64	462 ± 15	318 ± 25

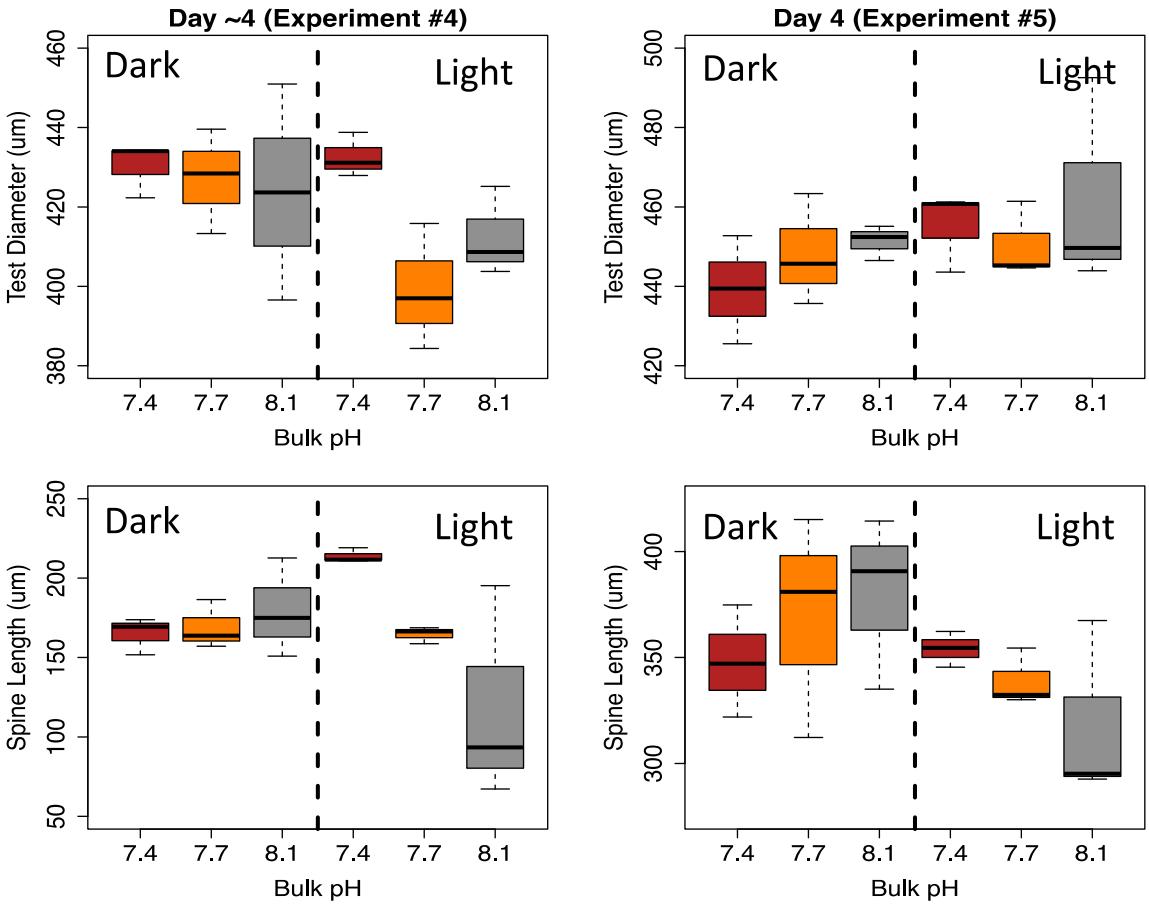

Figure 3.10 Effects of bulk pH on test diameter (top row) and spine length (bottom row) in juvenile sea urchins *Pseudechinus huttoni* four days post-settlement. The colours indicate bulk seawater pH treatments: red is bulk pH 7.4, orange is bulk pH 7.7 and grey is bulk pH 8.1. The black dashed line separates bulk seawater pH treatment conditions in different irradiance conditions, with dark treatments on the left and light treatments on the right.

Table 3.6 Two-way ANOVA examining the effects of irradiance and bulk pH on test diameter and spine length of newly settled *Pseudechinus huttoni* juveniles. Experimental conditions are irradiance (light or dark) and bulk seawater pH (bulk pH 8.1, 7.7 and 7.4). Significance level is p=0.05, with bold results indicating significant p values.

Experiment #	Age (Days post-settlement)	Morphometric	Morphology Factor	Df	SS	MS	*F*	*p*
4	~4	Test Diameter	Irradiance	1	811	811	2.80	0.117
			Bulk pH	1	429	429	1.48	0.244
			Irradiance: Bulk pH	1	90.9	91.0	0.313	0.584
			Residuals	14	4059	290		
	~4	Spine Length	Irradiance	1	137	136	0.157	0.698
			Bulk pH	1	4793	4793	5.55	**0.034**
			Irradiance: Bulk pH	1	9003	9003	10.4	**0.006**
			Residuals	14	12085	863		
5	4	Test Diameter	Irradiance	1	415	415	2.18	0.168
			Bulk pH	1	282	282	1.44	0.250
			Irradiance: Bulk pH	1	13.0	13.0	0.067	0.801
			Residuals	14	2746	196		
	4	Spine Length	Irradiance	1	3706	3706	3.59	0.079
			Bulk pH	1	14.0	14.0	0.014	0.909
			Irradiance: Bulk pH	1	3402	3402	3.29	0.091
			Residuals	14	14460	1033		

3.3.4 pH_{DBL} and post-settlement growth in the DBL

pH levels within the DBL (pH_{DBL}) had no significant effects on test diameter and spine length, except in two cases where a generalised linear model indicated that juveniles at higher pH_{DBL} levels showed reduced growth. In Experiments #2 and 3, where pH levels within the DBL ranged from approximately 8.1 to 8.6, pH_{DBL} showed no significant effects on growth of juvenile sea urchins, except in the single case that of spine length eleven days post-settlement. Spine length in *P. huttoni* juveniles eleven days post-settlement decreased with higher pH_{DBL} values (Figure 3.11; Table 3.7). Otherwise, test diameter and spine length measurements were variable at all pH_{DBL} levels, and especially around 8.1. Morphology measurements were also more variable six days post-settlement than eleven days post-settlement, as indicated by larger 95% confidence intervals (Figure 3.11). In Experiments #4 and 5, pH_{DBL} ranged from approximately 7.4 to 8.6. Across this range of pH levels, a generalised linear model showed only one significant difference of pH_{DBL} on juvenile morphology; test diameter significantly decreased as pH_{DBL} increased in Experiment #4 (Figure 3.12; Table 3.7). 95% confidence intervals indicate variability of morphological measurements across pH_{DBL}.

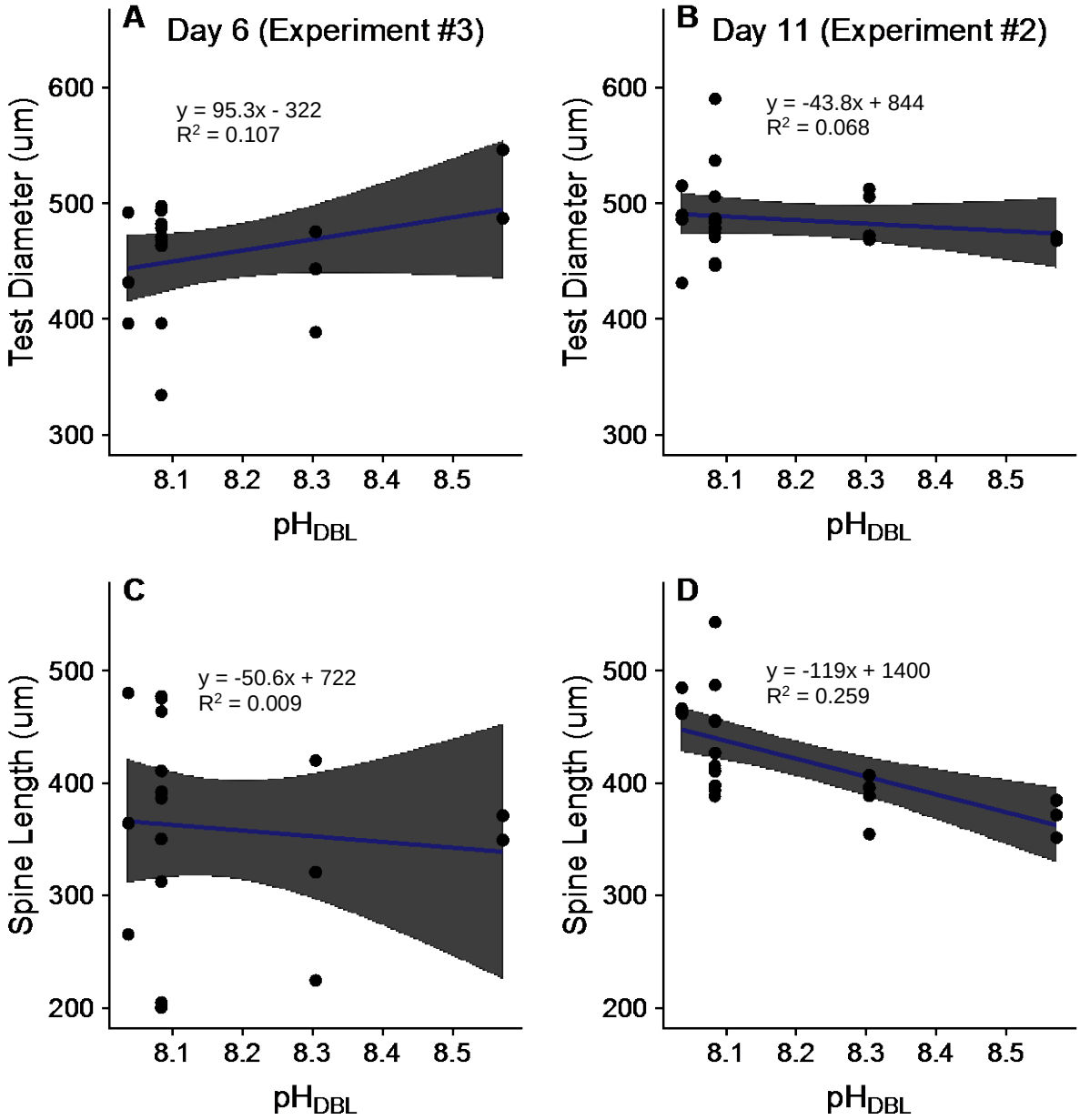

Figure 3.11 Effects of pH_{DBL} (average pH levels in the first 0 to 0.5 mm above the surface of CCA) on test diameter (top row) and spine length (bottom row) in juvenile sea urchins *Pseudechinus huttoni* six (left column) and eleven (right column) days post-settlement. Dots represent the mean morphological measurements from a replicate. The solid blue line is a generalised linear model and the shaded area is a 95% confidence interval.

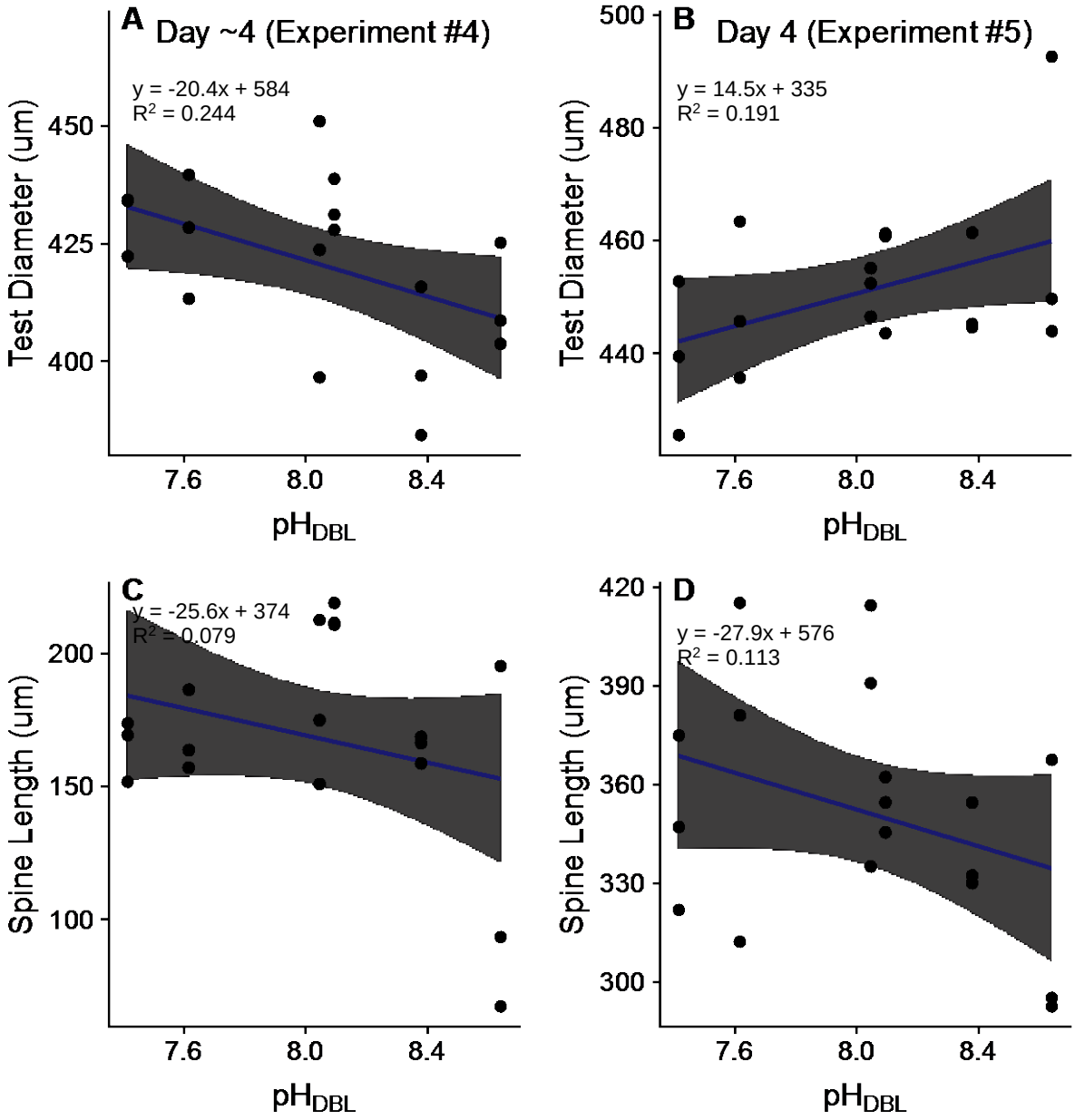

Figure 3.12 Effects of pH_{DBL} (average pH levels in the first 0 to 0.5 mm above the surface of CCA) on test diameter (top row) and spine length (bottom row) in juvenile sea urchins *Pseudechinus huttoni* six (left column) and eleven (right column) days post-settlement. Dots represent the mean morphological measurements from a replicate. The solid blue line is a generalised linear model and the shaded area is a 95% confidence interval.

Table 3.7 Generalised linear model (GLM) of the effect of pH_{DBL} on morphometric measurements of newly settled *Pseudechinus huttoni*. pH_{DBL} is an estimate of the average pH levels from 0 to 0.5 mm above the surface of CCA. pH_{DBL} levels were generated by manipulating flow and irradiance in experiments #2 and 3 and by manipulating bulk seawater pH and irradiance in experiments #4 and 5. *p* values < 0.05 are in bold.

		GLM				
Parameter	**Factor**	**Estimate**	**Std. Error**	**t value**	**Pr(>|t|)**	**AIC**
Test Diameter						
Experiment 2[a]	pH_{DBL}	-0.026	0.031	-0.836	0.413	-94.3
Experiment 3	pH_{DBL}	95.3	68.9	1.38	0.186	195
Experiment 4	pH_{DBL}	-20.4	9.00	-2.27	**0.037**	155
Experiment 5	pH_{DBL}	14.5	7.46	1.94	0.070	183
Spine Length						
Experiment 2	pH_{DBL}	-159	40.0	-3.97	**<0.001**	235
Experiment 3	pH_{DBL}	-50.6	132	-0.384	0.706	218
Experiment 4	pH_{DBL}	-25.6	21.8	-1.17	0.259	187
Experiment 5	pH_{DBL}	-27.9	19.5	-1.43	0.172	148

[a] Data log transformed to meet assumptions of parametric analysis.

3.3.5 Scanning electron microscopy

Scanning electron microscopy indicated that there were no observable differences in structural integrity or morphology of the sea urchin spine across the pH_{DBL} conditions, generated by various levels of bulk seawater pH and irradiance treatments (Figure 3.13). Calcification did not appear to be impaired, nor was there any indication of degradation of calcified surfaces in any of the treatments. Juvenile calcification appeared similar in all treatments, showing no loss of structural integrity, indicated by smooth surfaces on all skeletons and no evidence of pitting or erosion on the primary and secondary spines. Evidence of fine calcification (i.e. secondary spination) was present along the edges of the juvenile spine. Additionally, stereom lattice structure was normal in the spines and test.

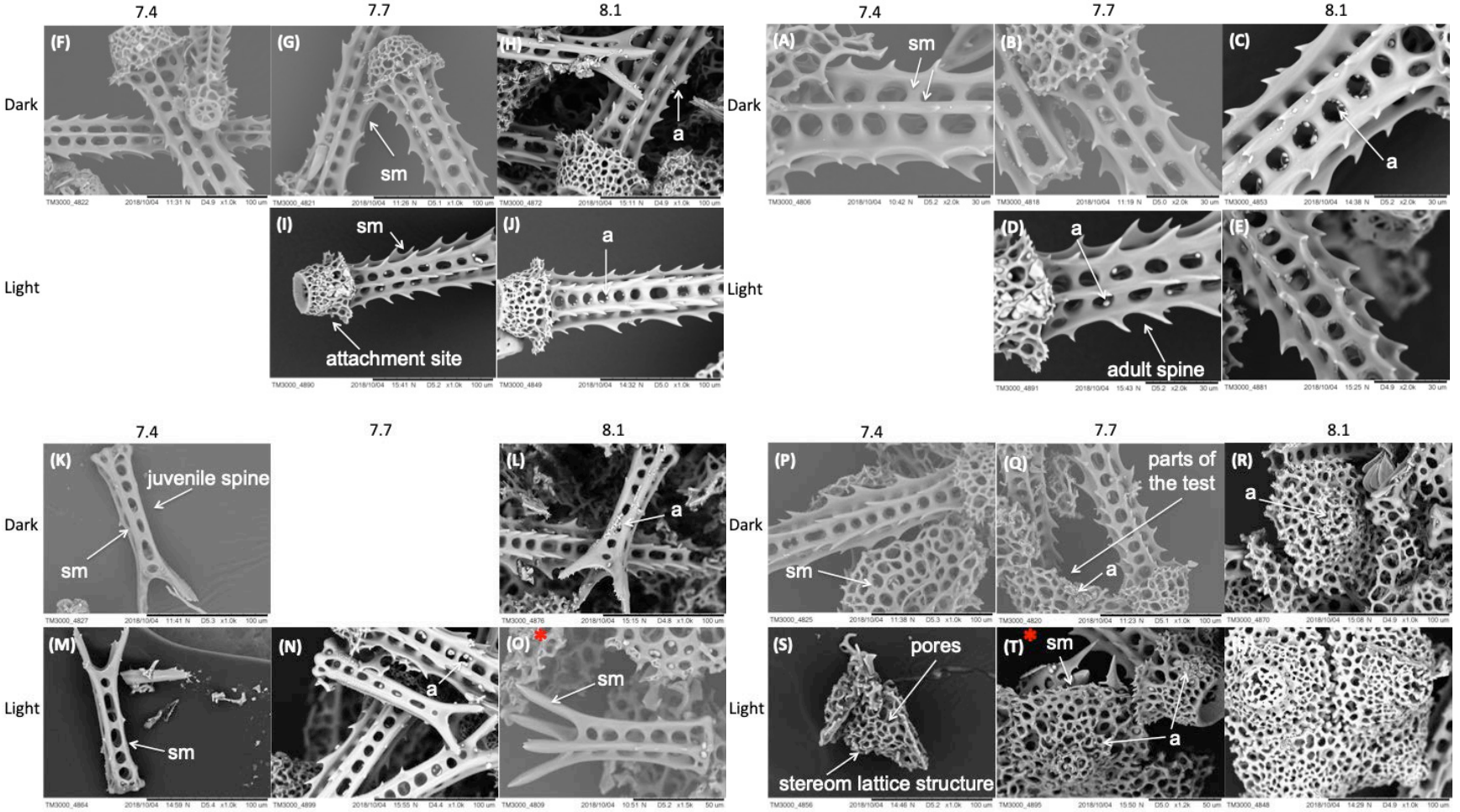

Figure 3.13 Scanning electron micrographs of (A-E) attachment sites of adult spines, (F-J) middle of adult spines, (K-O) juvenile spines, and (P-U) parts of the test, of *Pseudechinus huttoni* juveniles 4 days post-settlement grown in six treatment conditions (bulk pH 7.4, 7.7 and 8.1 in irradiance levels of light and dark. Scale bars in SEM micrographs are 30 µm for images A-E, 100 µm for images F-U. The red asterisk (image O and T) denotes a scale bar of 50 µm. Due to breakage of the spines during the preparation process, no full pieces of the

skeleton were photographed for juveniles in the light bulk pH 7.4 or dark bulk pH 7.7 treatment. *sm* smooth surface. *a* artefact (a product of sample preparation for the SEM).

3.4 Discussion

Newly settled sea urchins *Pseudechinus huttoni* grew in experimental conditions, but growth showed no strong response to pH in the CCA boundary layer, whether induced by flow, irradiance or bulk seawater pH. pH levels in the DBL (pH_{DBL}) varied with irradiance, flow and bulk seawater pH, but pH_{DBL} levels had few significant effects on growth in terms of test diameter and spine length. In the few cases with a significant effect, increased pH levels within the DBL generally reduced growth. Overall, post-settlement growth of *P. huttoni* in the DBL showed large variability. The effects of the DBL on post-settlement growth were difficult to discern based on the lack of observable trends in different boundary layer conditions, but the overall trends observed from all experiments suggest that *P. huttoni* juveniles may be relatively robust to OA. These are the first measurements of juvenile sea urchins under different DBL conditions, and support the hypothesis that juvenile echinoderms are potentially pre-adapted or tolerant to the effects of OA, with effects of low pH potentially only seen at extreme levels in the bulk seawater (pH_T 7.4 and below) (Byrne et al., 2009; Wolfe et al., 2013b; Dupont and Thorndyke, 2013; Chan et al., 2015; Dupont et al., 2010b; Espinel-Velasco et al., 2018; Byrne et al., 2010b; Byrne et al., 2017; Byrne, 2011).

Flow and irradiance determine DBL thickness and oxygen/pH concentrations in the DBL, but flow and irradiance did not significantly impact test growth or spine development, except in one case. Analyses indicated only one significant effect due to irradiance; juvenile sea urchins eleven days post-settlement had longer spines in the dark than in the light or alternation treatments. This was surprising because lower pH levels are generally expected to reduce growth and dark conditions are associated with decreased pH. However, in this experiment, pH levels in the DBL stayed within ~0.1 units of mainstream values, between approximately estimated pH_T 8.0 and 8.1. Other studies have found that nighttime pH decreases are usually less than the pH increase during the day (Cornwall et al., 2013b; Larkum et al., 2003). In this experiment, the ratio of algal biomass to water volume, which determines the magnitude of pH change within the DBL (Cornwall et al., 2013b; Wahl et al., 2018), may have been too low to adequately assess the effect of nighttime pH decreases on post-settlement growth since pH_{DBL} didn't decrease significantly below ambient seawater pH levels. Although nighttime pH decreases are usually less than those during the day, pH has still been found to decrease nearly 0.35 units below ambient mainstream seawater above coralline algae at night (Hurd et al., 2011; Wootton et al., 2008) and decrease nearly 0.5 units below mainstream seawater in intertidal environments at night (Wolfe et al., 2013b). The similarity in growth across flow and irradiance treatments in ambient bulk pH and the longer

tests and spines from six to eleven days post-settlement, where pH_{DBL} ranged from approximately 8.0 to 8.6, demonstrates that juvenile sea urchins *P. huttoni* can grow adequately in a range of pH fluctuations.

It was originally hypothesized that reduced bulk seawater pH would impair growth of juvenile sea urchins, except under a thick DBL in the daytime where pH was raised, which would act as an environmental buffer. The observed growth of newly settled sea urchins in different bulk pH levels did not fully support this hypothesis. In the light, juvenile sea urchins at higher bulk pH levels displayed reduced growth in terms of test diameter and spine length. In the dark, reduced bulk seawater pH did not significantly affect test diameter or spine length of *P. huttoni*. While there was some indication of an environmental buffer in the light treatments at bulk pH 7.4, demonstrated by increased spine length and test diameter in the light compared to the dark, this finding was not statistically significant and there wasn't a strong indication of this trend at bulk pH 7.7. Moreover, the generalised linear models suggested that *P. huttoni* growth was not significantly reduced at lower pH levels.

Scanning electron microscopy (SEM) supported the finding that *P. huttoni* calcification and growth was not reduced at lower pH_{DBL} or bulk seawater pH levels. SEM micrographs revealed no apparent differences in structural details of the juvenile skeletons in any of the treatments. Other experiments using scanning electron microscopy to examine spine morphology and skeleton structure found that SEM results highlighted some of the biggest differences in calcification and supported other growth measurements, such as quantitative reductions in weight (Albright et al., 2012). SEM of the spines of *H. erythrogramma* juveniles showed that at increased temperature and decreased pH, there was no terminal thorn, a characteristic of growing spines (Wolfe et al., 2013b). Additionally, at pH 7.4, there was noticeable dissolution of the spine tips (Wolfe et al., 2013b). SEM images also revealed the degradation of sea urchin pluteus larval skeletons under reduced pH in species including *P. huttoni* (Clark et al., 2009). None of these signs were evident in this study, thus supporting the finding that *P. huttoni* may be relatively tolerant of reduced seawater pH.

The finding that *P. huttoni* juveniles can grow in varying pH levels supports the theory that calcifiers who already live in naturally fluctuating environments are more tolerant to reduced pH levels (Wahl et al., 2018; Wahl et al., 2015b; Noisette and Hurd, 2018; Melzner et al., 2009; Hurd et al., 2011; Boyd et al., 2016). Previous studies have examined the effects of the DBL under OA conditions for marine organisms such as macroalgae (Hurd et al., 2011;

Cornwall et al., 2013a; Cornwall et al., 2014; Cornwall et al., 2017; Cornwall et al., 2013b; Hendriks et al., 2017; Noisette and Hurd, 2018) and corals (Chan et al., 2016; Larkum et al., 2003), but this study is the first to examine the effects on juvenile sea urchins. Three central hypotheses have developed predicting the effects of diffusion boundary layers on marine organisms in ocean acidification conditions. (1) In fluctuating environments, calcifiers are exposed to (detrimental) low pH/carbonate chemistry for shorter periods of time; DBL microhabitats will provide a refuge from OA (Wahl et al., 2018; Wahl et al., 2015b; Cornwall et al., 2014; Noisette and Hurd, 2018; Melzner et al., 2009). (2) Calcifiers who already live in these fluctuating environments are pre-adapted and thus more tolerant to extreme pH levels; environments with strong temporal and spatial variability have pre-selected for organisms with a higher phenotypic plasticity or more robust genotypes (Wahl et al., 2018; Wahl et al., 2015b; Noisette and Hurd, 2018; Melzner et al., 2009; Hurd et al., 2011; Boyd et al., 2016). (3) Calcifiers who live in these fluctuating environments already experience a great degree of stress and the combined effects of environmental fluctuations and climate change (e.g. reduced seawater pH due to ocean acidification) will push organisms beyond their thresholds of tolerance (Boyd et al., 2016; Hofmann et al., 2011).

Early post-settlement growth of *P. huttoni* did not appear to be impaired by reduced seawater pH, thus supporting the second hypothesis. *Pseudechinus huttoni* juveniles grew in experimental conditions, as indicated by larger test diameter and spines at eleven days compared to six days post settlement in all pH_{DBL} levels (8.0 to 8.6), irrespective of treatment. However, growth showed no strong or consistent effect of pH in the CCA boundary layer, whether induced by flow, irradiance or bulk seawater pH. In coastal environments, such as fjords, where *P. huttoni* are found, pH variability is large, ranging up to 0.8 units within macrophyte diffusive boundary layers (Krause-Jensen et al., 2015). *P. huttoni* may thus have increased tolerance to reduced pH levels. While the findings of this experiment support the second hypothesis, it is also possible that DBLs will still act as a refuge for other marine organisms by reducing duration of exposure to low pH. These hypotheses are not necessarily mutually exclusive. Additionally, further research could explore the stress thresholds of juvenile sea urchins to understand tipping points associated with the third hypothesis.
The negative effects of reduced seawater pH previously seen in larval *P. huttoni* (Clark et al., 2009) were not reflected in the responses of juvenile *P. huttoni*. However, the responses seen in juvenile *P. huttoni* support observations seen in other juvenile sea urchins (Wolfe et al., 2013b). In this respect, the effects of OA on sea urchins are life history specific, with effects on juveniles being variable and in some cases non-detected (Byrne et al., 2009; Wolfe et al.,

2013b; Dupont and Thorndyke, 2013; Chan et al., 2015; Dupont et al., 2010b; Espinel-Velasco et al., 2018; Byrne et al., 2010b; Byrne et al., 2017; Byrne, 2011). For example, juveniles of *Heliocidaris erythrogramma* were robust to increased temperature and ocean acidification conditions; two-weeks post-settlement, juvenile survival and test growth were resilient to both higher temperature (+2-4°C) and reduced pH (pH_{NBS} 7.4), spine development was robust to low pH above 7.4 (Wolfe et al., 2013b). My results support the hypothesis that due to the large natural pH fluctuations they experience during life in slow-flow coastal environments, juvenile sea urchins may be more resilient to ocean acidification conditions.

Marine life from more variable environments possess higher phenotypic plasticity and are thus thought to be able to tolerate more environmental heterogeneity (Boyd et al., 2016). Phenotypic plasticity is defined as "the ability of individual genotypes to produce different phenotypes when exposed to different environmental conditions" (Pigliucci et al., 2006). Carbonate system fluctuations may pre-acclimatize or pre-adapt organisms to survive at these extreme pH levels (Eriander et al., 2015; Wolfe et al., 2013b). By modifying their morphology and physiology, sea urchins can acclimate or adapt (Dupont et al., 2010b; Dupont and Thorndyke, 2013). Phenotypic plasticity was originally viewed as a short-term response, on the scale of hours to days, to environmental heterogeneity (Stearns, 1989; Stearns, 1992). However, phenotypic plasticity is now also being considered as a response to stressful environmental conditions (Brakefield, 1997). While phenotypic plasticity will likely play a role in both short-term acclimatization and longer-term adaptation, the exact manner needs to be further studied (Boyd et al., 2016).

Phenotypic plasticity defines to what extent organisms can tolerate altered conditions until it reaches its physiological limit (Litchman et al., 2012). While juvenile sea urchins appeared robust to reduced pH in this experiment, it is possible that this physiological limit may be surpassed when natural fluctuations are superimposed onto mean climate change (Boyd et al., 2016). This may be another explanation for the lack of detectable results on effects of pH on juvenile growth. Effects of reduced pH may only become discernable at very extreme pH values below those used in this experiment, bulk pH 7.4 and pH_{DBL} 7.4. Indeed, negative effects on skeleton growth (test diameter, spine number, and stereom pore size) of juvenile *Heliocidaris erythrogramma* were largely restricted to the lowest pH treatments used (pH 7.2-6.9) (Wolfe et al., 2013a), and decreased spine growth was seen only at pH 7.4 (Wolfe et al., 2013b). We may only be seeing the very beginning of that threshold in this experiment. Future experiments could incorporate a range of pH levels in order to accurately assess

tipping points. While pH levels 7.4 and below are extreme and not predicted to be reached in the bulk seawater in the near future (Gattuso et al., 2015), extreme levels are useful for examining tolerance levels of juvenile growth (Wolfe et al., 2013a).

Other possible areas of future work include: (1) incorporate fluctuating acidified conditions at reduced bulk seawater pH, (2) increase the duration of experiments, and (3) examine a wider variety of growth parameters. Previous research has found that fluctuating pH treatments can elicit different effects on organisms than stable acidified conditions. For example, diurnal pH fluctuations increased the variance, but not mean growth of the barnacle *Balanus improvises* (Eriander et al., 2015). In different pH variability regimes (pH_T 7.4 to 8.1), larval development of the mussel *Mytilus galloprovincialis* was impacted by the timing of exposure to different pH levels, whereas larval shell growth was correlated with mean exposure regardless of variability (Kapsenberg et al., 2018). Some organisms may possibly utilize these fluctuations to their benefit. For example, in acidified conditions, adult mussels are able to shift most of their calcification activity into the daytime when the local pH is higher due to macrophyte activity (Wahl et al., 2018).

Additionally, extending the durations of experiments may enable other trends to become apparent. Many previous experiments are relatively short-term (day, weeks or months), and longer exposure has since revealed otherwise hidden negative impacts (Dupont et al., 2010b). Effects of reduced seawater pH may not be present until after juveniles start to feed, later as adults, or even in future generations (Wolfe et al., 2013b; García et al., 2015). The larvae in this experiment grew in ambient pH conditions with ample food. As extremely plastic organisms, it is possible that they were able to rely on their larval resources to maintain growth, before starting to digest adult food (Wolfe et al., 2013b). Negative impacts of reduced seawater pH may have thus been hidden. For example, reduced growth due to low pH in adult sea urchins *Echinometra mathaei* and *Hemicentrotus pulcherrimus* did not show up until 12 and 14 weeks respectively (Shirayama and Thornton, 2005). Certain life-cycle bottlenecks or developmental processes may impact future life-history stages or generations, thus controlling future population responses (Dupont et al., 2010b).

It is also possible that the growth responses measured in this experiment come at the cost of other processes, or are representative of many indirect effects of reduced seawater pH. Fitness can be investigated using non-lethal measures (Dupont et al., 2010b). For example, the test diameter of the juvenile sea urchin, *Paracentrotus lividus*, was larger when larvae and

juveniles were reared at pH_{NBS} 7.7 compared to pH_{NBS} 8.1, likely due to the consequence of an increased metabolism under non-limiting energy conditions (García et al., 2015). It is also possible that longer spines are not necessarily indicative of good growing conditions. Longer spines are typically thought of as a helpful defensive structure, but could also be seen as a disadvantage, requiring more energy once the adult digestive system is fully developed (García et al., 2015). Other growth parameters are necessary to corroborate morphometric measurements. Some seemingly small-scale sub-lethal effects may actually have larger more negative effects on long-term fitness (Dupont et al., 2010b). Further research is necessary to confirm the hypothesis that a thick daytime DBL is able to increase pH enough to act as an environmental buffer for some organisms at potentially corrosive low pH levels.

Overall, newly settled organisms likely experience different pH levels than those in the overlying bulk seawater as a result of the diffusion boundary layer—an important consideration when investigating the effects of ocean acidification on marine organisms. Under present-day conditions, organisms that live on the benthos in slow flow environments, already experience large fluctuations in pH due to biological activity within the DBL. The DBL will thus play a critical role in modulating the effects of future OA conditions for species living on the seafloor with the potential to both confer resilience and decrease exposure to low pH. This finding, supported by observations in other juvenile sea urchins (Wolfe et al., 2013b), indicates that the previously studied negative effects of OA on larval *P. huttoni* (Clark et al., 2009) are not reflected in the response of juvenile *P. huttoni*. The larval stages of organisms, living in the water column, may be more susceptible to OA and thus a more critical bottleneck than the post-settlement juvenile stages living on the benthos.

Chapter 4: General discussion

4.1 Main findings and ecological implications

The aim of this research was to understand the variability in pH and oxygen that small calcifying marine organisms experience when they have settled on coralline algal covered substrates and are living in the diffusion boundary layer. Due to the presence of a DBL, the chemical conditions that newly settled organisms experience is different than that of mainstream seawater. The constant exposure to variable pH fluctuations within the DBL may have allowed juvenile organisms to adapt to living and calcifying in a range of pH levels, thus conferring potential resilience to OA conditions at this life-history stage. This finding supports observations of resilience seen in other juvenile sea urchins (Wolfe et al., 2013b), and demonstrates that the early post-settlement stage may not be as sensitive to the negative effects of OA as larval *P. huttoni* (Clark et al., 2009). The main findings and ecological implications of this work are listed in Table 4.1 and demonstrated in Figure 4.1.

Oxygen measurements demonstrated that crustose coralline algae can modify water column properties at the mm-scale within its local environment. Under light conditions, CCA was found to increase oxygen concentrations (and calculated pH concentrations) at its surface up to approximately 0.8 units above the bulk seawater pH under static flow. Under dark conditions, CCA decreased surface oxygen (and calculated pH concentrations), but only up to nearly 0.09 units below the bulk seawater pH in static flow. CCA photosynthesis and respiration are the likely drivers of these observed oxygen (and pH) changes. This study also demonstrated that seawater velocity determines DBL thickness. The DBL was thicker, reaching above 2 mm, in zero or slow flow (1 cm s^{-1}) in comparison to fast flow (5 cm s^{-1}) where it was less than 0.2 mm thick. Bulk seawater pH had no significant effects on the development or gradient of a DBL in this study, but does change the estimated range of pH values reached by changing the mainstream pH levels.

The effects of irradiance, flow and bulk seawater pH, on post-settlement growth of *P. huttoni* were varied. While flow had no significant effects on growth, juveniles in dark conditions had longer spines than juveniles in the light or alternation treatments, but only at eleven days post-settlement. The only significant effect of bulk seawater pH on growth was surprising, indicating that in the light, juveniles at bulk seawater pH 8.1 had shorter spines than juveniles at bulk pH 7.4. The pH levels within the DBL (pH_{DBL}) supported this finding, finding no

significant effects on test diameter and spine length, except in two cases where juveniles at higher pH_{DBL} levels showed reduced growth. In this study, we did not observe or could not detect reduced growth of *P. huttoni* juveniles at reduced bulk seawater pH. There was no strong effect of varying levels of pH within the DBL on the post-settlement growth of *P. huttoni* juveniles.

These observations carry important ecological implications for marine invertebrates living in slow-flow coastal environments under predicted future ocean acidification conditions. Previously, it was thought that calcifying organisms such as sea urchins would be particularly susceptible to OA (McClintock et al., 2011). Much of the subsequent research has focused on the larval stages of these organisms, documenting many negative effects (see reviews by Dupont et al. 2010; Byrne 2011; Kroeker et al. 2013; Przeslawski et al. 2015; Byrne et al. 2017 and Espinel-Velasco et al. 2018), including negative effects on the larval stage of this study organism *P. huttoni* (Clark et al., 2009). However, in contrast to their larval counterparts, juvenile sea urchins have been found to be relatively robust to the effects of OA (Albright et al., 2012; Wolfe et al., 2013b). This study proposes the idea that this resilience is likely due in part, due to the diffusion boundary layer. The development of a DBL around aquatic organisms due to biological activity leads to steep concentration gradients and a pronounced difference between bulk seawater pH and the pH that organisms actually experience (Chan et al., 2016; Larkum et al., 2003; Jørgensen and Des Marais, 1990; Cornwall et al., 2014; Boudreau and Jorgensen, 2001). Juvenile sea urchins living on algal surfaces experience temporal and spatial pH fluctuations, whereas planktotrophic larvae live in the water column at more constant pH levels. Consequently, juvenile sea urchins may be acclimated or adapted to growing and calcifying in a range of pH levels. This finding reveals that post-metamorphic juvenile stages may not be a critical life-history bottleneck under ocean acidification conditions, as the juvenile stage appears less sensitive to reduced pH than the previously studied larval stage.

Table 4.1 A summary of the main findings and ecological implications of this study. Chapter two focused on the oxygen and pH variability in the diffusion boundary layer (DBL) above crustose coralline algae (CCA). Chapter three focused on the effects of coralline algal diffusion boundary layers on the early post-settlement growth of juvenile sea urchins *Pseudechinus huttoni*.

DBL Findings	Juvenile Sea Urchin Growth Findings	Ecological Implications
CCA can modify local water column properties	Flow, irradiance and bulk seawater pH have variable and conflicting effects on post-settlement growth of juvenile *P. huttoni*	Organisms above algal surfaces experience different pH levels than the bulk seawater pH
In the light, CCA increase oxygen/pH above bulk seawater pH. In the dark, CCA decrease oxygen/pH below bulk seawater pH	Reduced pH levels in the DBL do not consistently correspond to reduced growth	Organisms living in environments with naturally fluctuating pH may be more tolerant to extreme pH situations
Seawater velocity determines DBL thickness. The DBL is thicker in slow flow	SEM images revealed no observable differences in calcification at different bulk seawater pH levels	Juvenile sea urchins do not appear to be as sensitive to OA as larvae. Thus, the larval rather than the juvenile stage may be a potential life-history bottleneck under OA conditions

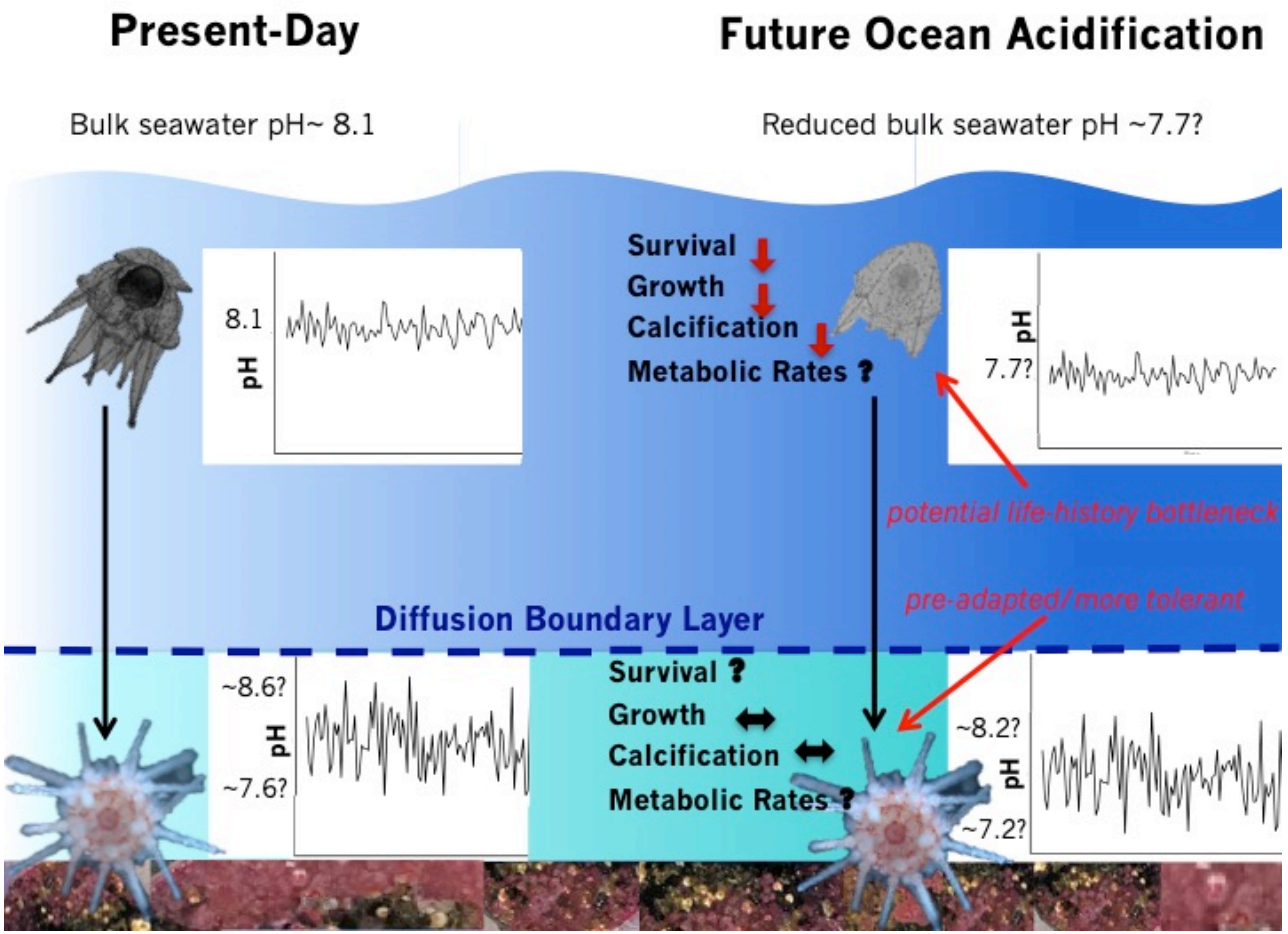

Figure 4.1 The transition of sea urchins from the planktotrophic larval stage to juvenile life on the benthos in present-day conditions (ambient bulk seawater pH ~ 8.1) and in future ocean acidification conditions (reduced bulk seawater pH). Juvenile life-history stages living on algal surfaces on the seafloor experience large fluctuations in pH within the diffusion boundary layer (up to +/- 0.5 pH units (Hurd, 2015; Hofmann et al., 2011; Cornwall et al., 2013a)). Juveniles may thus be pre-adapted to living and growing at a range of pH levels, and therefore more resilient to reduced bulk seawater pH

due to ocean acidification. Planktotrophic larvae living in the water column experience more constant pH levels, and thus may be more susceptible to ocean acidification. Consequently, the larval rather than the juvenile stage may be a potential life-history bottleneck in ocean acidification conditions.

4.2 Future Research

This research examines the effects of local pH conditions in the DBL amongst large-scale pH changes associated with ocean acidification. This study highlights the need to measure oxygen and pH levels within the DBL, when examining growth of organisms in the context of OA. While this experiment was unable to measure pH directly due to experimental constraints, this would be measured in order to further understand the processes at work within the DBL, including dissolution and calcification in addition to photosynthesis and respiration. Future work could also clearly distinguish between pH of the mainstream seawater and pH within the microenvironment of the study organism (bulk pH and pH_{DBL} in this experiment). The recent work that has investigated how the DBL modifies the effects of OA has largely been limited to coral reefs and macroalgae (Short et al., 2015; Chan et al., 2016; Cornwall et al., 2013b; Noisette and Hurd, 2018). However, consideration of the DBL is crucial to understanding the widespread impacts of OA because a wide range of marine life, such as bacteria, diatoms, many settling larvae, bryozoans and juvenile barnacles, all live within the DBL and will be subsequently impacted (Wahl et al., 2015b).

Further research could also be conducted to understand how natural pH fluctuations will interact with bulk seawater pH decreases. This study examined the effects of alternating light treatments in ambient seawater pH, but not in reduced seawater pH. Fluctuating pH_{DBL} levels will likely elicit different effects than static pH_{DBL} conditions under OA. The limited number of previous studies that have examined organism responses to fluctuating pH under OA have found varying effects, but suggest that constant low pH elicits different responses from fluctuating low pH (Eriander et al., 2015; Cornwall et al., 2013a; Wahl et al., 2018; Shaw et al., 2012; Dufault et al., 2012; Alenius and Munguia, 2012; Wahl et al., 2015b; Kapsenberg et al., 2018). Since the duration of exposure to stress is linked to response magnitude (Boyd et al., 2016; Helmuth, 2009), environmental fluctuations may offer respite from the predicted corrosive reduced seawater by providing a microhabitat with alternating periods of stress (i.e. nighttime local pH decreases) and release from stress (i.e. daytime local pH increases) (Wahl et al., 2015b).

While this study focused on one species of sea urchins, the potential of acclimation or adaptation in other species could be examined. Environmental heterogeneity can significantly influence the sensitivity of organisms to ocean acidification (Boyd et al., 2016). The growth of other species of marine life in fluctuating OA conditions, from similarly heterogeneous environments that potentially possess higher phenotypic plasticity could be studied. Further

research is necessary to confirm the hypothesis of resilience due to life in the diffusion boundary layer (Boyd et al., 2016).

There is also a need for OA research to examine extreme bulk seawater pH levels, lower than bulk seawater pH 7.4, to assess tipping points. This study found few effects of reduced bulk seawater pH at either pH 7.7 or 7.4, and points to potential acclimation of *P. huttoni* to reduced pH, but the threshold of acclimation or adaptation may be surpassed when natural fluctuations are superimposed onto mean climate change (Boyd et al., 2016). The combined effects of environmental fluctuations and climate change (e.g. reduced seawater pH due to ocean acidification) could push organisms outside their tolerance threshold window (Boyd et al., 2016).

Additionally, while this study focused mainly on the effects of pH, future oceans will have many global-change related stressors, not limited to reduced seawater pH. Future oceans also face increased ocean temperatures, hypoxia, changes in nutrient concentrations or stratification, and changes in salinity concentrations from freshwater runoff (Espinel-Velasco et al., 2018; Przeslawski et al., 2015). All of these stressors likely also have interactive effects. One notable and relevant example in the context of diffusion boundary layers is the interactive effect of temperature. Higher temperatures decrease seawater viscosity while increasing diffusion and metabolic rates. Thus, higher temperatures ultimately lead to a steeper pH gradient and decreased DBL thickness (Wahl et al., 2015b). While still untested, this might suggest that under a combined impact of increased temperature and low pH, boundary layers have less potential as an environmental buffer. Future research could attempt to incorporate additional stressors.

4.3 Concluding remarks

Ocean acidification research has expanded rapidly in the past few decades, becoming a key area of study (Kroeker et al., 2013). Much of this research has, however, investigated the effects of constant levels of low bulk seawater pH, rather than the effects of diurnally fluctuating pH or small-scale variability such as the effects of pH within the DBL (Eriander et al., 2015; Chan et al., 2016; Wahl et al., 2018). Failure to incorporate and account for microhabitats such as the DBL may cause a discrepancy between early models predicting OA to be a major threat to marine biodiversity (Kleypas et al., 1999) and more recent experimental evidence suggesting a more complex, variation in sensitivity and tolerance to OA (Hendriks I.E., 2010; Ries et al., 2009; Chan et al., 2016). Due to the presence of a

diffusion boundary layer, the chemical conditions that newly settled organisms experience is different than that of mainstream seawater.

In order to adequately understand, examine and predict organismal responses to OA, the effects of the DBL should be considered. Otherwise, it is possible to underestimate current and future acclimation abilities and/or stress by not accounting for boundary layers. In the context of OA, the DBL has the potential to confer resilience, decrease exposure to low pH and determine stress tolerance thresholds. The effects of varying pH levels within the diffusion boundary layer will be especially apparent for calcifying marine organisms (particularly immediately post-metamorphosis) that live above photosynthesizing organisms in slow flow environments. While most OA studies on sea urchins have examined pre-settlement stages, newly settled organisms were thought to be especially vulnerable to the effects of OA (Albright et al., 2012; see review by Espinel-Velasco et al. 2018). Following this important life-history transition to the benthos, juveniles will need to calcify and grow rapidly and are often small enough to live fully within the DBL (less than ~2 mm). However, this study suggests that marine organisms with limited mobility that live in fluctuating pH environments, such as the juvenile sea urchin *P. huttoni*, are acclimated or adapted to living in a range of pH conditions. This indicates that the early post-settlement stage may not be as sensitive to OA as the larval stage, where negative effects have been previously documented. The larval stage may indeed be the crucial life-history bottleneck in OA conditions, rather than the newly settled juvenile stages. Life in the diffusion boundary layers may have increased tolerance of juvenile *P. huttoni* to reduced bulk seawater pH, thereby conferring greater resilience to future ocean acidification conditions.

References

Albright, R., Bland, C., Gillette, P., Serafy, J. E., Langdon, C. & Capo, T. R. 2012. Juvenile growth of the tropical sea urchin *Lytechinus variegatus* exposed to near-future ocean acidification scenarios. *Journal of experimental marine biology and ecology,* 426-427**,** 12-17.

Albright, R. & Langdon, C. 2011. Ocean acidification impacts multiple early life history processes of the Caribbean coral *Porites astreoides*. *Global Change Biology,* 17**,** 2478-2487.

Albright, R., Mason, B., Miller, M. & Langdon, C. 2010. Ocean acidification compromises recruitment success of the threatened Caribbean coral *Acropora palmata*. *Proceedings of the National Academy of Sciences,* 107**,** 20400-20404.

Alenius, B. & Munguia, P. 2012. Effects of pH variability on the intertidal isopod, *Paradella dianae*. *Marine and Freshwater Behaviour and Physiology,* 45**,** 245-259.

Andersson, A., Mackenzie, F. & Bates, N. 2008. Life on the margin: Implications of ocean acidification on Mg-calcite, high latitude and cold-water marine calcifiers. *Marine Ecology Progress Series,* 373**,** 265-273.

Anthony, K. R., Kleypas, J. A. & Gattuso, J. P. 2011. Coral reefs modify their seawater carbon chemistry—implications for impacts of ocean acidification. *Global Change Biology,* 17**,** 3655-3666.

Björk, M., Axelssson, L. & Beer, S. 2004. Why is *Ulva intestinalis* the only macroalga inhabiting isolated rockpools along the Swedish Atlantic Coast? *Marine Ecology Progress Series***,** 109-116.

Boudreau, B. P. & Jorgensen, B. B. 2001. *The benthic boundary layer: Transport processes and biogeochemistry,* Oxford University Press.

Boyd, P. W., Cornwall, C. E., Davison, A., Doney, S. C., Fourquez, M., Hurd, C. L., Lima, I. D. & McMinn, A. 2016. Biological responses to environmental heterogeneity under future ocean conditions. *Global Change Biology,* 22**,** 2633-2650.

Brakefield, P. M. 1997. Phenotypic plasticity and fluctuating asymmetry as responses to environmental stress in the butterfly *Bicyclus anynana*. *Environmental stress, adaptation and evolution.* Springer.

Burdett, H. L., Aloisio, E., Calosi, P., Findlay, H. S., Widdicombe, S., Hatton, A. D. & Kamenos, N. A. 2012. The effect of chronic and acute low pH on the intracellular DMSP production and epithelial cell morphology of red coralline algae. *Marine Biology Research,* 8**,** 756-763.

Byrne, M. 2011. Impact of ocean warming and ocean acidification on marine invertebrate life history stages: Vulnerabilities and potential for persistence in a changing ocean. *In:* Gibson, R. N., Atkinson, R., Gordon, J., Smith, I. & Hughes, D. (eds.) *Oceanography and Marine Biology: An Annual Review*. Boca Raton, FL: CRC Press.

Byrne, M., Ho, M., Selvakumaraswamy, P., Nguyen, H. D., Dworjanyn, S. A. & Davis, A. R. 2009. Temperature, but not pH, compromises sea urchin fertilization and early development under near-future climate change scenarios. *Proceedings of the Royal Society B: Biological Sciences,* 276**,** 1883-1888.

Byrne, M., Ho, M., Wong, E., Soars, N. A., Selvakumaraswamy, P., Shepard-Brennand, H., Dworjanyn, S. A. & Davis, A. R. 2010a. Unshelled abalone and corrupted urchins: development of marine calcifiers in a changing ocean. *Proceedings of the Royal Society B: Biological Sciences,* 278**,** 2376-2383.

Byrne, M., Ross, P. M., Dworjanyn, S. A. & Parker, L. 2017. Larval Ecology in the face of changing climate--impacts of ocean warming and ocean acidification *In:* Carrier, T., Reitzel, A. & Heyland, A. (eds.) *Ecolutionary Ecology of marine invertebrate larvae* Oxford University Press.

Byrne, M., Soars, N., Selvakumaraswamy, P., Dworjanyn, S. A. & Davis, A. R. 2010b. Sea urchin fertilization in a warm, acidified and high pCO_2 ocean across a range of sperm densities. *Marine Environmental Research,* 69**,** 234-239.

Byrne, M., Soars, N. A., Ho, M. A., Wong, E., McElroy, D., Selvakumaraswamy, P., Dworjanyn, S. A. & Davis, A. R. 2010c. Fertilization in a suite of coastal marine invertebrates from SE Australia is robust to near-future ocean warming and acidification. *Marine Biology,* 157**,** 2061-2069.

Caldeira, K. & Wickett, M. E. 2003. Anthropogenic carbon and ocean pH. *Nature,* 425**,** 365.

Chan, K. Y. K., García, E. & Dupont, S. 2015. Acidification reduced growth rate but not swimming speed of larval sea urchins. *Scientific Reports,* 5**,** 9764.

Chan, N. C. S., Wangpraseurt, D., Kühl, M. & Connolly, S. R. 2016. Flow and Coral Morphology Control Coral Surface pH: Implications for the Effects of Ocean Acidification. *Frontiers in Marine Science,* 3.

Chino, Y., Saito, M., Yamasu, K., Suyemitsu, T. & Ishihara, K. 1994. Formation of the Adult Rudiment of Sea Urchins is Influenced by Thyroid Hormones. *Developmental Biology,* 161**,** 1-11.

Clark, D., Lamare, M. & Barker, M. 2009. Response of sea urchin pluteus larvae (Echinodermata: Echinoidea) to reduced seawater pH: a comparison among a tropical, temperate, and a polar species. *Marine Biology,* 156**,** 1125-1137.

Cornwall, C. E. 2013. *Macroalgae as ecosystem engineers and the implications for ocean acidification.* PhD, Univeristy of Otago.

Cornwall, C. E., Boyd, P. W., McGraw, C. M., Hepburn, C. D., Pilditch, C. A., Morris, J. N., Smith, A. M. & Hurd, C. L. 2014. Diffusion Boundary Layers Ameliorate the Negative Effects of Ocean Acidification on the Temperate Coralline Macroalga *Arthrocardia corymbosa*. *PLoS ONE,* 9**,** e97235.

Cornwall, C. E., Comeau, S. & McCulloch, M. T. 2017. Coralline algae elevate pH at the site of calcification under ocean acidification. *Global Change Biology,* 23**,** 4245-4256.

Cornwall, C. E., Hepburn, C. D., McGraw, C. M., Currie, K. I., Pilditch, C. A., Hunter, K. A., Boyd, P. W. & Hurd, C. L. 2013a. Diurnal fluctuations in seawater pH influence the response of a calcifying macroalga to ocean acidification. *Proceedings of the Royal Society B: Biological Sciences,* 280.

Cornwall, C. E., Hepburn, C. D., Pilditch, C. A. & Hurd, C. L. 2013b. Concentration boundary layers around complex assemblages of macroalgae: Implications for the effects of ocean acidification on understory coralline algae. *Limnology and Oceanography,* 58**,** 121-130.

Cornwall, C. E., Pilditch, C. A., Hepburn, C. D. & Hurd, C. L. 2015. Canopy macroalgae influence understorey corallines' metabolic control of near-surface pH and oxygen concentration. *Marine Ecology Progress Series,* 525**,** 81-95.

De Beer, D. & Larkum, A. 2001. Photosynthesis and calcification in the calcifying algae Halimeda discoidea studied with microsensors. *Plant, Cell & Environment,* 24**,** 1209-1217.

Delille, B., Borges, A. & Delille, D. 2009. Influence of giant kelp beds (*Macrocystis pyrifera*) on diel cycles of pCO_2 and DIC in the Sub-Antarctic coastal area. *Estuarine, Coastal and Shelf Science,* 81**,** 114-122.

Denny, M. W., and D. S. Wethey 2000. Physical processes that generate patterns in marine communities. *Marine Community Ecology***,** 3-37.

Dickson, A. G., Sabine, C. L. & Christian, J. R. 2007. Guide to best practices for Ocean CO_2 measurements. *North Pacific Marine Science Organization.*

Doney, S. C., Fabry, V. J., Feely, R. A. & Kleypas, J. A. 2009. Ocean Acidification: The Other CO_2 Problem. *Annual Review of Marine Science,* 1**,** 169-192.

Dufault, A. M., Cumbo, V. R., Fan, T.-Y. & Edmunds, P. J. 2012. Effects of diurnally oscillating pCO_2 on the calcification and survival of coral recruits. *Proceedings of the Royal Society of London B: Biological Sciences,* 279.

Dupont, S., Dorey, N. & Thorndyke, M. 2010a. What meta-analysis can tell us about vulnerability of marine biodiversity to ocean acidification? *Estuarine, Coastal and Shelf Science,* 89**,** 182-185.

Dupont, S., Ortega-Martínez, O. & Thorndyke, M. 2010b. Impact of near-future ocean acidification on echinoderms. *Ecotoxicology,* 19**,** 449-462.

Dupont, S. & Pörtner, H. 2013. Marine science: get ready for ocean acidification. *Nature,* 498**,** 429.

Dupont, S. & Thorndyke, M. 2013. Direct impacts of near-future ocean acidification on sea urchins. *Climate Change Perspective from the Atlantic: Past, Present and Future***,** 461-485.

Dworjanyn, S. A. & Byrne, M. 2018. Impacts of ocean acidification on sea urchin growth across the juvenile to mature adult life-stage transition is mitigated by warming. *Proc. R. Soc. B,* 285**,** 20172684.

Eriander, L., Wrange, A.-L. & Havenhand, J. 2015. Simulated diurnal pH fluctuations radically increase variance in—but not the mean of—growth in the barnacle Balanus improvisus. *ICES Journal of Marine Science,* 73**,** 596-603.

Espinel-Velasco, N., Hoffman, L., Aguera, A., Byrne, M., Dupont, S., Uthicke, S., Webster, N. S. & Lamare, M. 2018. Effects of ocean acidification on the settlement and metamorphosis of marine invertebrate and fish larvae: a review. *Marine Ecology Progress Series (in press)*

Fabry, V. J., Seibel, B. A., Feely, R. A. & Orr, J. C. 2008. Impacts of ocean acidification on marine fauna and ecosystem processes. *ICES Journal of Marine Science,* 65**,** 414-432.

Fadl, A. E. A., Mahfouz, M. E., El-Gamal, M. M. T. & Heyland, A. 2017. New biomarkers of post-settlement growth in the sea urchin *Strongylocentrotus purpuratus*. *Heliyon,* 3**,** e00412.

Farr, T., Broom, J., Hart, D., Neill, K. & Nelson, W. 2009. Common coralline algae of northern New Zealand: An identification guide *NIWA Information Series No. 70.*

Feely, R. A., Doney, S. C. & Cooley, S. R. 2009. Ocean Acidification: Present Conditions and Future Changes in a High-CO_2 World. *Oceanography,* 22**,** 36-47.

Foster, T., Gilmour, J., Chua, C., Falter, J. & McCulloch, M. 2015. Effect of ocean warming and acidification on the early life stages of subtropical *Acropora spicifera*. *Coral Reefs,* 34**,** 1217-1226.

Frankignoulle, M. & Distèche, A. 1984. CO_2 chemistry in the water column above a Posidonia seagrass bed and related air-sea exchanges. *Oceanologica acta,* 7**,** 209-219.

Friedlingstein, P., Cox, P., Betts, R., Bopp, L., Bloh, W. v., Brovkin, V., Cadule, P., Doney, S., Eby, M., Fung, I., Bala, G., John, J., Jones, C., Joos, F., Kato, T., Kawamiya, M., Knorr, W., Lindsay, K., Matthews, H. D., Raddatz, T., Rayner, P., Reick, C., Roeckner, E., Schnitzler, K.-G., Schnur, R., Strassmann, K., Weaver, A. J., Yoshikawa, C. & Zeng, N. 2006. Climate–Carbon Cycle Feedback Analysis: Results from the C4MIP Model Intercomparison. *Journal of Climate,* 19**,** 3337-3353.

Gao, K. & Zheng, Y. 2010. Combined effects of ocean acidification and solar UV radiation on photosynthesis, growth, pigmentation and calcification of the coralline alga *Corallina sessilis* (Rhodophyta). *Global Change Biology,* 16**,** 2388-2398.

García, E., Hernández, J. C., Clemente, S., Cohen-Rengifo, M., Hernández, C. A. & Dupont, S. 2015. Robustness of *Paracentrotus lividus* larval and post-larval development to pH levels projected for the turn of the century. *Marine Biology,* 162**,** 2047-2055.

Gattuso, J.-P., Magnan, A., Billé, R., Cheung, W. W. L., Howes, E. L., Joos, F., Allemand, D., Bopp, L., Cooley, S. R., Eakin, C. M., Hoegh-Guldberg, O., Kelly, R. P., Pörtner, H.-O., Rogers, A. D., Baxter, J. M., Laffoley, D., Osborn, D., Rankovic, A., Rochette, J., Sumaila, U. R., Treyer, S. & Turley, C. 2015. Contrasting futures for ocean and society from different anthropogenic CO_2 emissions scenarios. *Science,* 349**,** aac4722.

Hadfield, M. G. & Paul, V. J. 2001. Natural Chemical Cues for Settlement and Metamorphosis of Marine-Invertebrate Larvae *In:* McClintock, J. B. & Baker, B. J. (eds.) *Marine Chemical Ecology* CRC Press 2001.

Hall-Spencer, J. M., Rodolfo-Metalpa, R., Martin, S., Ransome, E., Fine, M., Turner, S. M., Rowley, S. J., Tedesco, D. & Buia, M.-C. 2008. Volcanic carbon dioxide vents show ecosystem effects of ocean acidification. *Nature,* 454**,** 96.

Hansen, A., Hondzo, M. & Hurd, C. 2011. Photosynthetic oxygen flux by *Macrocystis pyrifera:* A mass transfer model with experimental validation. *Marine Ecology Progress Series,* 434**,** 45-55.

Harvey, B. P., Gwynn‐Jones, D. & Moore, P. J. 2013. Meta‐analysis reveals complex marine biological responses to the interactive effects of ocean acidification and warming. *Ecology and Evolution,* 3**,** 1016-1030.

Havenhand, J., Buttler, F. R., Thorndyke, M. & Williamson, J. 2008. Near-future levels of ocean acidification reduce fertilization success in a sea urchin. *Current Biology,* 18**,** R651-R652.

Helmuth, B. 2009. From cells to coastlines: how can we use physiology to forecast the impacts of climate change? *Journal of Experimental Biology,* 212**,** 753-760.

Hendriks I.E., D. C. M., Álvarez, M. 2010. Vulnerability of marine biodiversity to ocean acidification: A meta-analysis. *Estuarine, Coastal and Shelf Science,* 86**,** 157-164.

Hendriks, I. E., Duarte, C. M. & Álvarez, M. 2010. Vulnerability of marine biodiversity to ocean acidification: A meta-analysis. *Estuarine, Coastal and Shelf Science,* 86**,** 157-164.

Hendriks, I. E., Duarte, C. M., Marbà, N. & Krause-Jensen, D. 2017. pH gradients in the diffusive boundary layer of subarctic macrophytes. *Polar Biology,* 40**,** 2343-2348.

Hofmann, G. E., Barry, J. P., Edmunds, P. J., Gates, R. D., Hutchins, D. A., Klinger, T. & Sewell, M. A. 2010. The Effect of Ocean Acidification on Calcifying Organisms in Marine Ecosystems: An Organism-to-Ecosystem Perspective. *Annual Review of Ecology, Evolution, and Systematics,* 41**,** 127-147.

Hofmann, G. E., Smith, J. E., Johnson, K. S., Send, U., Levin, L. A., Micheli, F., Paytan, A., Price, N. N., Peterson, B., Takeshita, Y., Matson, P. G., Crook, E. D., Kroeker, K. J., Gambi, M. C., Rivest, E. B., Frieder, C. A., Yu, P. C. & Martz, T. R. 2011. High-Frequency Dynamics of Ocean pH: A Multi-Ecosystem Comparison. *PLoS ONE,* 6**,** e28983.

Hofmann, L. C., Yildiz, G., Hanelt, D. & Bischof, K. 2012. Physiological responses of the calcifying rhodophyte, *Corallina officinalis* (L.), to future CO_2 levels. *Marine Biology,* 159**,** 783-792.

Huggett, M. J., McMahon, K. & Bernasconi, R. 2018. Future warming and acidification result in multiple ecological impacts to a temperate coralline alga. *Environmental Microbiology*.

Hurd, C. L. 2000. Water motion, marine macroalgal physiology, and production. *Journal of Phycology,* 36**,** 453-472.

Hurd, C. L. 2015. Slow-flow habitats as refugia for coastal calcifiers from ocean acidification. *Journal of Phycology,* 51**,** 599-605.

Hurd, C. L., Cornwall, C. E., Currie, K., Hepburn, C. D., McGraw, C. M., Hunter, K. A. & Boyd, P. W. 2011. Metabolically induced pH fluctuations by some coastal calcifiers exceed projected 22nd century ocean acidification: a mechanism for differential susceptibility? *Global Change Biology,* 17**,** 3254-3262.

Hurd, C. L., Hepburn, C. D., Currie, K. I., Raven, J. A. & Hunter, K. A. 2009. Testing the effects of ocean acidification on algal metabolism: Considerations for experimental designs. *Journal of Phycology,* 45**,** 1236-1251.

Hurd, C. L. & Pilditch, C. A. 2011. Flow-induced morphological variations affect diffusion boundary‐layer thickness of *macrocystis pyrifera* (heterokontophyta, laminariales) *Journal of Phycology,* 47**,** 341-351.

IPCC 2007. Climate Change 2007: The Physial Science Basis. Contribution of Working Group I to the Fourth Assessment Report of the Intergovernmental Panel on Climate Change. *In:* Solomon, S. (ed.).

Irwin, S. & Davenport, J. 2002. Hyperoxic boundary layers inhabited by the epiphytic meiofauna of Fucus serratus. *Marine Ecology Progress Series,* 244**,** 73-79.

Jones, H. F. E., Pilditch, C. A., Bryan, K. R. & Hamilton, D. P. 2011. Effects of infaunal bivalve density and flow speed on clearance rates and near-bed hydrodynamics. *Journal of experimental marine biology and ecology,* 401**,** 20-28.

Jørgensen, B. B. & Des Marais, D. J. 1990. The diffusive boundary layer of sediments: oxygen microgradients over a microbial mat. *Limnology and Oceanography,* 35**,** 1343-1355.

Kamenos, N. A., Burdett, H. L., Aloisio, E., Findlay, H. S., Martin, S., Longbone, C., Dunn, J., Widdicombe, S. & Calosi, P. 2013. Coralline algal structure is more sensitive to rate, rather than the magnitude, of ocean acidification. *Global Change Biology,* 19**,** 3621-3628.

Kamenos, N. A., Perna, G., Gambi, M. C., Micheli, F. & Kroeker, K. J. 2016. Coralline algae in a naturally acidified ecosystem persist by maintaining control of skeletal mineralogy and size. *Proceedings of the Royal Society B: Biological Sciences,* 283**,** 20161159.

Kapsenberg, L., Miglioli, A., Bitter, M. C., Tambutté, E., Dumollard, R. & Gattuso, J.-P. 2018. Ocean pH fluctuations affect mussel larvae at key developmental transitions. *Proceedings of the Royal Society B: Biological Sciences,* 285**,** 20182381.

Kaspar, H. F. 1992. Oxygen conditions on surfaces of coralline red algae. *Marine Ecology Progress Series,* 81**,** 97-100.

Kirby, S., Lamare, M. D. & Barker, M. F. 2006. Growth and morphometrics in the New Zealand sea urchin *Pseudechinus huttoni* (Echinoidea: Temnopleuridae). *New Zealand Journal of Marine and Freshwater Research,* 40**,** 413-428.

Kleypas, J. A., Buddemeier, R. W., Archer, D., Gattuso, J.-P., Langdon, C. & Opdyke, B. N. 1999. Geochemical consequences of increased atmospheric carbon dioxide on coral reefs. *Science,* 284**,** 118-120.

Koehl, M. A. R. 2007. Mini review: Hydrodynamics of larval settlement into fouling communities. *Biofouling,* 23**,** 357-368.

Koehl, M. A. R. & Hadfield, M. G. 2010. Hydrodynamics of Larval Settlement from a Larva's Point of View. *Integr Comp Biol,* 50**,** 539-551.

Krause-Jensen, D., Duarte, C. M., Hendriks, I. E., Meire, L., Blicher, M. E., Marbà, N. & Sejr, M. K. 2015. Macroalgae contribute to nested mosaics of pH variability in a subarctic fjord. *Biogeosciences,* 12**,** 4895-4911.

Kroeker, K. J., Kordas, R. L., Crim, R., Hendriks, I. E., Ramajo, L., Singh, G. S., Duarte, C. M. & Gattuso, J. P. 2013. Impacts of ocean acidification on marine organisms: quantifying sensitivities and interaction with warming. *Global Change Biology,* 19**,** 1884-1896.

Kroeker, K. J., Kordas, R.L., Crim, R.N., and Singh, G.G. 2010. Meta-analysis reveals negative yet variable effects of ocean acidification on marine organisms. *Ecology Letters,* 13**,** 1419-1434.

Kroeker, K. J., Micheli, F. & Gambi, M. C. 2012. Ocean acidification causes ecosystem shifts via altered competitive interactions. *Nature Climate Change,* 3**,** 156.

Kuffner, I. B., Andersson, A. J., Jokiel, P. L., Ku'ulei, S. R. & Mackenzie, F. T. 2008. Decreased abundance of crustose coralline algae due to ocean acidification. *Nature Geoscience,* 1**,** 114.

Kurihara, H. 2008. Effects of CO_2-driven ocean acidification on the early developmental stages of invertebrates. *Marine Ecology Progress Series,* 373**,** 275-284.

Lamare, M. & Barker, M. 2001. Settlement and recruitment of the New Zealand sea urchin *Evechinus chloroticus*. *Marine Ecology Progress Series,* 218**,** 153-166.

Langdon, C., Takahashi, T., Sweeney, C., Chipman, D., Goddard, J., Marubini, F., Aceves, H., Barnett, H. & Atkinson, M. J. 2000. Effect of calcium carbonate saturation state on the calcification rate of an experimental coral reef. *Global Biogeochemical Cycles,* 14**,** 639-654.

Larkum, A. W., Koch, E.-M. & Kühl, M. 2003. Diffusive boundary layers and photosynthesis of the epilithic algal community of coral reefs. *Marine Biology,* 142**,** 1073-1082.

Lichtenberg, M., Nørregaard, R. D. & Kühl, M. 2017. Diffusion or advection? Mass transfer and complex boundary layer landscapes of the brown alga *Fucus vesiculosus*. *Journal of the Royal Society Interface,* 14**,** 20161015.

Litchman, E., Edwards, K. F., Klausmeier, C. A. & Thomas, M. K. 2012. Phytoplankton niches, traits and eco-evolutionary responses to global environmental change. *Marine Ecology Progress Series,* 470**,** 235-248.

Manríquez, P. H., Torres, R., Matson, P. G., Lee, M. R., Jara, M. E., Seguel, M. E., Sepúlveda, F. & Pereira, L. 2017. Effects of ocean warming and acidification on the

early benthic ontogeny of an ecologically and economically important echinoderm. *Marine Ecology Progress Series,* 563**,** 169-184.

Manzello, D. P. 2010. Ocean acidification hotspots: Spatiotemporal dynamics of the seawater CO_2 system of eastern Pacific coral reefs. *Limnology and Oceanography,* 55**,** 239-248.

Martin, S., Cohu, S., Vignot, C., Zimmerman, G. & Gattuso, J. P. 2013. One‐year experiment on the physiological response of the Mediterranean crustose coralline alga, *Lithophyllum cabiochae,* to elevated pCO_2 and temperature. *Ecology and Evolution,* 3**,** 676-693.

Marubini, F., Ferrier-Pages, C. & Cuif, J.-P. 2003. Suppression of skeletal growth in scleractinian corals by decreasing ambient carbonate-ion concentration: a cross-family comparison. *Proceedings of the Royal Society B: Biological Sciences,* 270**,** 179-184.

McClary, D. J. & Sewell, M. A. 2003. Hybridization in the sea: gametic and developmental constraints on fertilization in sympatric species of *Pseudechinus* (Echinodermata: Echinoidea). *Journal of experimental marine biology and ecology,* 284**,** 51-70.

McClintock, J. B., Amsler, M. O., Angus, R. A., Challener, R. C., Schram, J. B., Amsler, C. D., Mah, C. L., Cuce, J. & Baker, B. J. 2011. The Mg-Calcite Composition of Antarctic Echinoderms: Important Implications for Predicting the Impacts of Ocean Acidification. *The Journal of Geology,* 119**,** 457-466.

McCoy, S. J. & Kamenos, N. A. 2015. Coralline algae (*Rhodophyta*) in a changing world: integrating ecological, physiological, and geochemical responses to global change. *Journal of Phycology,* 51**,** 6-24.

McCoy, S. J. & Pfister, C. A. 2014. Historical comparisons reveal altered competitive interactions in a guild of crustose coralline algae. *Ecology Letters,* 17**,** 475-483.

McKnight, D. G. 1969. *An outline distribution of the New Zealand shelf fauna: Benthos survey, station list, and distribution of the echinoidea,* Dept. of Scientific and Industrial Research.

McNeil, B. I. & Matear, R. J. 2008. Southern Ocean acidification: A tipping point at 450-ppm atmospheric CO_2. *Proceedings of the National Academy of Sciences,* 105**,** 18860-18864.

Melzner, F., Gutowska, M., Langenbuch, M., Dupont, S., Lucassen, M., Thorndyke, M., Bleich, M. & Pörtner, H.-O. 2009. Physiological basis for high CO_2 tolerance in marine ectothermic animals: pre-adaptation through lifestyle and ontogeny? *Biogeosciences,* 6**,** 2313-2331.

Morris, S. & Taylor, A. C. 1983. Diurnal and seasonal variation in physico-chemical conditions within intertidal rock pools. *Estuarine, Coastal and Shelf Science,* 17**,** 339-355.

Morse, A. N., Iwao, K., Baba, M., Shimoike, K., Hayashibara, T. & Omori, M. 1996. An ancient chemosensory mechanism brings new life to coral reefs. *The Biological Bulletin,* 191**,** 149-154.

Nelson, K. S. 2016. *Biofilm response to Ocean Acidification and the effects on Serpulid Polychaete Settlement.* Masters of Science, University of Otago

Nelson, W. 2009. Calcified macroalgae–critical to coastal ecosystems and vulnerable to change: a review. *Marine and Freshwater Research,* 60**,** 787-801.

Nguyen, H. D. & Byrne, M. 2014. Early benthic juvenile P*arvulastra exigua* (Asteroidea) are tolerant to extreme acidification and warming in its intertidal habitat. *Journal of experimental marine biology and ecology,* 453**,** 36-42.

Ni, S., Taubner, I., Böhm, F., Winde, V. & Böttcher, M. E. 2018. Effect of temperature rise and ocean acidification on growth of calcifying tubeworm shells (*Spirorbis spirorbis*): an in situ benthocosm approach. *Biogeosciences,* 15**,** 1425-1445.

Nishihara, G. N. & Ackerman, J. D. 2007. On the determination of mass transfer in a concentration boundary layer. *Limnology and Oceanography: Methods,* 5**,** 88-96.

NOAA. 2018. *Trends in Atmospheric Carbon Dioxide* [Online]. https://www.esrl.noaa.gov/gmd/ccgg/trends/global.html. [Accessed 2018 2018].

Noisette, F. & Hurd, C. 2018. Abiotic and biotic interactions in the diffusive boundary layer of kelp blades create a potential refuge from ocean acidification. *Funct Ecol,* 32**,** 1329–1342.

O'Leary, J. K., Barry, J. P., Gabrielson, P. W., Rogers-Bennett, L., Potts, D. C., Palumbi, S. R. & Micheli, F. 2017. Calcifying algae maintain settlement cues to larval abalone following algal exposure to extreme ocean acidification. *Scientific Reports,* 7**,** 5774.

Orr, J. C., Fabry, V. J., Aumont, O., Bopp, L., Doney, S. C., Feely, R. A., Gnanadesikan, A., Gruber, N., Ishida, A., Joos, F., Key, R. M., Lindsay, K., Maier-Reimer, E., Matear, R., Monfray, P., Mouchet, A., Najjar, R. G., Plattner, G.-K., Rodgers, K. B., Sabine, C. L., Sarmiento, J. L., Schlitzer, R., Slater, R. D., Totterdell, I. J., Weirig, M.-F., Yamanaka, Y. & Yool, A. 2005. Anthropogenic ocean acidification over the twenty-first century and its impact on calcifying organisms. *Nature,* 437**,** 681.

Pigliucci, M., Murren, C. J. & Schlichting, C. D. 2006. Phenotypic plasticity and evolution by genetic assimilation. *Journal of Experimental Biology,* 209**,** 2362-2367.

Pöhn, M., Vopel, K., Grünberger, E. & Ott, J. 2001. Microclimate of the brown alga *Feldmannia caespitula* interstitium under zero-flow conditions. *Marine Ecology Progress Series,* 210**,** 285-290.

Porzio, L., Buia, M. C. & Hall-Spencer, J. M. 2011. Effects of ocean acidification on macroalgal communities. *Journal of experimental marine biology and ecology,* 400**,** 278-287.

Przeslawski, R., Byrne, M. & Mellin, C. 2015. A review and meta‐analysis of the effects of multiple abiotic stressors on marine embryos and larvae. *Global Change Biology,* 21**,** 2122-2140.

Ragazzola, F., Foster, L. C., Form, A., Anderson, P. S., Hansteen, T. H. & Fietzke, J. 2012. Ocean acidification weakens the structural integrity of coralline algae. *Global Change Biology,* 18**,** 2804-2812.

Raven, J. A. & Hurd, C. L. 2012. Ecophysiology of photosynthesis in macroalgae. *Photosynthesis Research,* 113**,** 105-125.

Ries, J. B. 2006. Mg fractionation in crustose coralline algae: Geochemical, biological, and sedimentological implications of secular variation in the Mg/Ca ratio of seawater. *Geochimica et Cosmochimica Acta,* 70**,** 891-900.

Ries, J. B. 2011. Skeletal mineralogy in a high-CO_2 world. *Journal of experimental marine biology and ecology,* 403**,** 54-64.

Ries, J. B., Cohen, A. L. & McCorkle, D. C. 2009. Marine calcifiers exhibit mixed responses to CO_2-induced ocean acidification. *Geology,* 37**,** 1131-1134.

Roberts, R. 2001. A review of settlement cues for larval abalone (*Haliotis* spp.). *Journal of Shellfish Research,* 20**,** 571-586.

Rodríguez, A., Hernández, J., Brito, A. & Clemente, S. 2017. Effects of ocean acidification on juvenile sea urchins: Predator-prey interactions. *Journal of experimental marine biology and ecology,* 493**,** 31-40.

Roleda, M. Y., Cornwall, C. E., Feng, Y., McGraw, C. M., Smith, A. M. & Hurd, C. L. 2015. Effect of Ocean Acidification and pH Fluctuations on the Growth and Development of Coralline Algal Recruits, and an Associated Benthic Algal Assemblage. *PLoS ONE,* 10**,** e0140394.

Sabine, C. L., Feely, R. A., Gruber, N., Key, R. M., Lee, K., Bullister, J. L., Wanninkhof, R., Wong, C. S., Wallace, D. W. R., Tilbrook, B., Millero, F. J., Peng, T.-H., Kozyr, A., Ono, T. & Rios, A. F. 2004. The Oceanic Sink for Anthropogenic CO_2. *Science,* 305**,** 367-371.

Saderne, V., Fietzek, P. & Herman, P. M. J. 2013. Extreme variations of pCO_2 and pH in a macrophyte meadow of the Baltic Sea in summer: evidence of the effect of photosynthesis and local upwelling. *PLoS ONE,* 8**,** e62689.

Schoepf, V., Cornwall, C. E., Pfeifer, S. M., Carrion, S. A., Alessi, C., Comeau, S. & McCulloch, M. T. 2018. Impacts of coral bleaching on pH and oxygen gradients across the coral concentration boundary layer: a microsensor study. *Coral Reefs,* 37**,** 1169-1180.

Semesi, I. S., Beer, S. & Björk, M. 2009. Seagrass photosynthesis controls rates of calcification and photosynthesis of calcareous macroalgae in a tropical seagrass meadow. *Marine Ecology Progress Series,* 382**,** 41-47.

Shaw, E. C., McNeil, B. I. & Tilbrook, B. 2012. Impacts of ocean acidification in naturally variable coral reef flat ecosystems. *Journal of Geophysical Research: Oceans,* 117.

Shears, N. & Babcock, R. 2004a. *Quantitative Classification Of New Zealand's Shallow Subtidal Reef Communities*.

Shears, N. T., and R. C. Babock 2007. Quantitative description of mainland New Zealand's shallow subtidal reef communities. *Science for Conservation*.

Shears, N. T. & Babcock, R. C. 2004b. *Community composition and structure of shallow subtidal reefs in northeastern New Zealand*, Wellington, N.Z, Dept. of Conservation.

Shirayama, Y. & Thornton, H. 2005. Effect of increased atmospheric CO_2 on shallow water marine benthos. *Journal of Geophysical Research: Oceans,* 110.

Short, J. A., Pedersen, O. & Kendrick, G. A. 2015. Turf algal epiphytes metabolically induce local pH increase, with implications for underlying coralline algae under ocean acidification. *Estuarine, Coastal and Shelf Science,* 164**,** 463-470.

Siikavuopio, S., Mortensen, A., Dale, T. & Foss, A. 2007. Effects of carbon dioxide exposure on feed intake and gonad growth in green sea urchin, *Strongylocentrotus droebachiensis*. *Aquaculture,* 266**,** 97-101.

Spilling, K., Titelman, J., Greve, T. M. & Kühl, M. 2010. Microsensor Measurements of the External and Internal Microenvironment of *Fucus Vesiculosus* (Phaeophyceae). *Journal of Phycology,* 46**,** 1350-1355.

Stearns, S. 1989. Trade-offs in life-history evolution. *Functional Ecology,* 3**,** 259-268.

Stearns, S. 1992. *The Evolution of Life Histories,* Oxford, UK, Oxford University Press.

Steneck, R. S. 1986. The Ecology of Coralline Algal Crusts: Convergent Patterns and Adaptative Strategies. *Annual Review of Ecology and Systematics,* 17**,** 273-303.

Stumpp, M., Trübenbach, K., Brennecke, D., Hu, M. Y. & Melzner, F. 2012. Resource allocation and extracellular acid–base status in the sea urchin *Strongylocentrotus*

droebachiensis in response to CO_2 induced seawater acidification. *Aquatic Toxicology,* 110-111**,** 194-207.

Truchot, J.-P. & Duhamel-Jouve, A. 1980. Oxygen and carbon dioxide in the marine intertidal environment: diurnal and tidal changes in rockpools. *Respiration physiology,* 39**,** 241-254.

Uthicke, S., Pecorino, D., Albright, R., Negri, A. P., Cantin, N., Liddy, M., Dworjanyn, S., Kamya, P., Byrne, M. & Lamare, M. 2013. Impacts of ocean acidification on early life-history stages and settlement of the coral-eating sea star *Acanthaster planci*. *PLoS ONE,* 8**,** e82938.

Vogel, S. 1994. Life in Moving Fluids. *Princeton University Press.*

Wahl, M., Buchholz, B., Winde, V., Golomb, D., Guy‐Haim, T., Müller, J., Rilov, G., Scotti, M. & Böttcher, M. E. 2015a. A mesocosm concept for the simulation of near‐natural shallow underwater climates: The Kiel Outdoor Benthocosms (KOB). *Limnology and Oceanography: Methods,* 13**,** 651-663.

Wahl, M., Covachã, S. S., Saderne, V., Hiebenthal, C., Müller, J. D., Pansch, C. & Sawall, Y. 2018. Macroalgae may mitigate ocean acidification effects on mussel calcification by increasing pH and its fluctuations. *Limnology and Oceanography,* 63**,** 3-21.

Wahl, M., Saderne, V. & Sawall, Y. 2015b. How good are we at assessing the impact of ocean acidification in coastal systems? Limitations, omissions and strengths of commonly used experimental approaches with special emphasis on the neglected role of fluctuations. *Marine and Freshwater Research,* 67**,** 25-36.

Waldbusser, G. G., Hales, B., Langdon, C. J., Haley, B. A., Schrader, P., Brunner, E. L., Gray, M. W., Miller, C. A. & Gimenez, I. 2015. Saturation-state sensitivity of marine bivalve larvae to ocean acidification. *Nature Clim. Change,* 5**,** 273-280.

Wallace, R. B., Baumann, H., Grear, J. S., Aller, R. C. & Gobler, C. J. 2014. Coastal ocean acidification: The other eutrophication problem. *Estuarine, Coastal and Shelf Science,* 148**,** 1-13.

Wangensteen, O. S., Dupont, S., Casties, I., Turon, X. & Palacín, C. 2013. Some like it hot: temperature and pH modulate larval development and settlement of the sea urchin *Arbacia lixula*. *Journal of experimental marine biology and ecology,* 449**,** 304-311.

Wangpraseurt, D., Weber, M., Røy, H., Polerecky, L., de Beer, D., Suharsono & Nugues, M. M. 2012. In Situ Oxygen Dynamics in Coral-Algal Interactions. *PLoS ONE,* 7**,** e31192.

Webster, N. S., Uthicke, S., Botté, E. S., Flores, F. & Negri, A. P. 2013. Ocean acidification reduces induction of coral settlement by crustose coralline algae. *Global Change Biology,* 19**,** 303-315.

Weiner, S. & Dove, P. M. 2003. An overview of biomineralization processes and the problem of the vital effect. *Reviews in mineralogy and geochemistry,* 54**,** 1-29.

Widdows, J., D. Brinsley, M., Bowley, N. & Barrett, C. 1998. A Benthic Annular Flume for In Situ Measurement of Suspension Feeding/Biodeposition Rates and Erosion Potential of Intertidal Cohesive Sediments. *Estuarine, Coastal and Shelf Science,* 46**,** 27-38.

Wolfe, K., A Dworjanyn, S. & Byrne, M. 2013a. Thermal and pH/pCO_2 fluctuations in the intertidal habitat of *Heliocidaris erythrogramma*: effects on post-metamorphic juveniles. *Cah. Biol. Mar.,* 54**,** 657-666.

Wolfe, K., Dworjanyn, S. A. & Byrne, M. 2013b. Effects of ocean warming and acidification on survival, growth and skeletal development in the early benthic juvenile sea urchin (*Heliocidaris erythrogramma*). *Global Change Biology,* 19**,** 2698-2707.

Wootton, J. T., Pfister, C. A. & Forester, J. D. 2008. Dynamic patterns and ecological impacts of declining ocean pH in a high-resolution multi-year dataset. *Proceedings of the National Academy of Sciences,* 105**,** 18848-18853.

Appendices

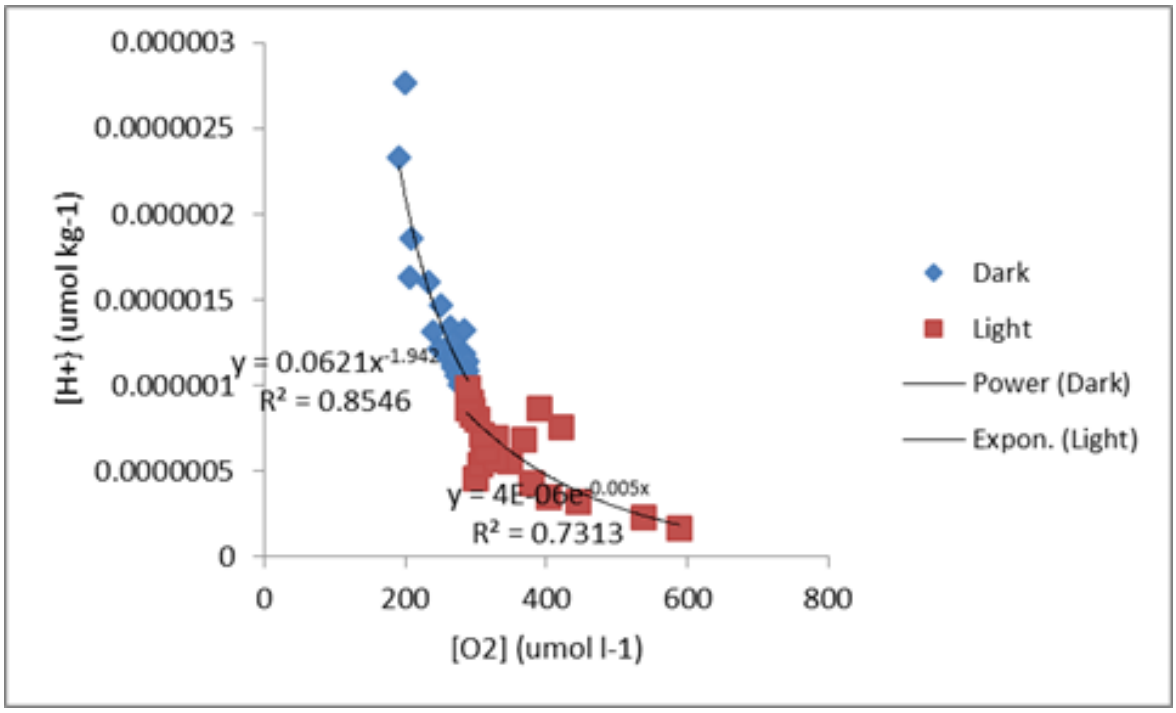

Appendix 1. The relationships between pH and oxygen in the DBL in the dark (blue) and light (red) above coralline algae as defined by Cornwall (2013). In this experiment, oxygen was used as a proxy for pH.

Appendix 2. Levene's test to determine homogeneity of variances for standardised surface oxygen concentration, DBL thickness, test diameter and spine length. *p* values less than 0.05 are in bold.

	Levene Test		
	Df	**F value**	**Pr(>F)**
Surface O_2 Concentration			
Annular Flume	7	4.76	**0.002**
2.5 L Glass Jars	3	9.72	**0.001**
3 L Aquaria	5	21.6	**<0.001**
DBL Thickness			
Annular Flume[a]	7	1.90	0.115
2.5 L Glass Jars[a]	3	2.64	0.094
3 L Aquaria[a]	5	0.355	0.873
Test Diameter			
Experiment 2 [b]	5	2.81	0.050
Experiment 3	5	2.33	0.107
Experiment 4	5	1.05	0.435
Experiment 5	5	0.440	0.812
Spine Length			
Experiment 2	5	2.32	0.089
Experiment 3	5	0.976	0.471
Experiment 4	5	1.23	0.354
Experiment 5	5	0.553	0.734

[a] Data were square root transformed

[b] Data were log transformed

Appendix 3. Post-Hoc Dunn test investigating pairwise comparisons on DBL thickness in the annular flume of eight independent treatments (2 irradiance levels x 2 bulk seawater pH levels x 2 flow levels). *p* values less than 0.05 are in bold.

	DBL Thickness						
	Dark pH 8.1 Fast	Dark pH 8.1 Slow	Dark pH 7.4 Fast	Dark pH 7.4 Slow	Light pH 8.1 Fast	Light pH 8.1 Slow	Light pH 7.4 Fast
Dark pH 8.1 Slow	0.323	-	-	-	-	-	-
Dark pH 7.4 Fast	0.625	0.625	-	-	-	-	-
Dark pH 7.4 Slow	0.625	0.625	1.00	-	-	-	-
Light pH 8.1 Fast	1.00	0.328	0.625	0.625	-	-	-
Light pH 8.1 Slow	**<0.001**	**0.012**	**0.003**	**0.003**	**<0.001**	-	-
Light pH 7.4 Fast	0.051	0.051	0.051	0.051	0.051	0.051	-
Light pH 7.4 Slow	**0.003**	**0.042**	**0.012**	**0.012**	**0.003**	0.625	0.290

Appendix 4. Post-Hoc Dunn test investigating pairwise comparisons on DBL thickness in 2.5 L glass jars of four independent treatments (2 irradiance levels x 2 flow levels). *p* values less than 0.05 are in bold.

	DBL Thickness		
	Dark Flow	Dark No Flow	Light Flow
Dark No Flow	0.324	-	-
Light Flow	0.228	0.827	-
Light No Flow	**<0.001**	**0.019**	**0.034**

Appendix 5. Post-Hoc Dunn test investigating pairwise treatment comparisons on DBL thickness in 3 L aquaria of six independent treatments (2 irradiance levels x 3 bulk seawater pH levels). *p* values less than 0.05 are in bold.

DBL Thickness					
	Dark pH 8.1	Dark pH 7.4	Dark pH 7.7	Light pH 8.1	Light pH 7.4
Dark pH 7.4	**0.019**	-	-	-	-
Dark pH 7.7	0.146	0.367	-	-	-
Light pH 8.1	**0.012**	0.881	0.293	-	-
Light pH 7.4	**0.020**	0.980	0.381	0.861	-
Light pH 7.7	**0.013**	0.900	0.304	0.980	0.881

Appendix 6. Post-Hoc Games-Howell test investigating effects of treatment, irradiance, bulk seawater pH and flow on standardised surface oxygen concentration in the annular flume. There were eight treatments (2 irradiance levels x 2 bulk seawater pH levels x 2 flow levels). *p* values less than 0.05 are in bold.

Surface O_2 Concentration			
	n	**means**	**variances**
Dark pH 8.1 Fast	4	0.99	**<0.001**
Dark pH 8.1 Slow	4	0.94	**0.002**
Dark pH 7.4 Fast	4	0.94	**0.001**
Dark pH 7.4 Slow	4	0.94	**0.001**
Dark pH 8.1 Fast	4	1.12	0.062
Dark pH 8.1 Slow	4	2.05	0.368
Dark pH 7.4 Fast	4	1.26	**0.044**
Dark pH 7.4 Slow	4	1.93	0.639
Dark	16	0.95	**0.001**
Light	16	1.59	0.399
pH 8.1	16	1.3	0.31
pH 7.4	16	1.3	0.31
Fast	16	1.1	**0.039**
Slow	16	1.5	0.498

Appendix 7. Post-Hoc Games-Howell test investigating effects of treatment, irradiance and flow on standardised surface oxygen concentration in 2.5 L glass jars. There were four independent treatments (2 irradiance levels x 2 flow levels). *p* values less than 0.05 are in bold.

Surface O_2 Concentration			
	n	**means**	**variances**
Dark Flow	4	0.99	**<0.001**
Dark No Flow	4	0.91	**0.005**
Light Flow	4	1.01	**0.001**
Light No Flow	5	2.21	0.215
Dark	8	0.95	**0.004**
Light	9	1.68	0.511
Flow	8	1.01	**<0.001**
No Flow	9	2.21	0.585

Appendix 8. Post-Hoc Games-Howell test investigating effects of treatment, irradiance, and bulk seawater pH on standardised surface oxygen concentration in 3 L aquaria. There were six independent treatments (2 irradiance levels x 3 bulk seawater pH levels). *p* values less than 0.05 are in bold.

Surface O_2 Concentration			
	n	**means**	**variances**
Dark pH 7.4	4	0.90	**0.003**
Dark pH 7.7	4	0.92	**<0.001**
Light pH 8.1	4	0.95	**<0.001**
Light pH 7.4	4	2.22	1.06
Light pH 7.7	4	2.29	0.428
Light pH 8.1	4	2.06	0.694
Dark	12	0.92	**0.001**
Light	12	2.19	0.604
pH 7.4	8	1.5	0.650
pH 7.7	8	1.6	0.950
pH 8.1	8	1.6	0.720

Appendix 9. Average pH_T in six experimental treatments that newly settled sea urchins, *Pseudechinus huttoni* grew in during Experiment #4. pH was measured of incoming water from header flow-through tanks ("in") and of water in the three replicate tubs for each treatment immediately prior to water changes ("out"). Values represent the single measurement for "in" (n=1) and mean ± SE for "out" (n=3).

Time (hours after introduction to cue)		**pH_{Bulk} 8.1**		**pH_{Bulk} 7.7**		**pH_{Bulk} 7.4**	
		Light	Dark	Light	Dark	Light	Dark
0	in	8.15	8.15	7.62	7.62	7.4	7.4
6	out	8.08±0.009	8.06±0.006	7.68±0.003	7.69±0.003	7.43±0	7.41±0.01
	in	8.10	8.10	7.63	7.63	7.43	7.43
18	out	8.06±0.003	8.04±0.006	7.64±0.006	7.65±0.01	7.4±0.015	7.38±0.003
	in	8.19	8.19	7.72	7.72	7.43	7.43
30	out	8.08±0.003	8.04±0.006	7.66±0.003	7.61±0.009	7.42±0.003	7.41±0.01
	in	8.15	8.15	7.69	7.69	7.49	7.49
51	out	8.06±0	8.03±0.009	7.64±0.009	7.61±0.003	7.40±0.009	7.39±0.006
	in	8.13	8.13	7.68	7.68	7.48	7.48
75	out	8.06±0.07	8.01±0.008	7.63±0.012	7.61±0	7.39±0.003	7.38±0.007
	in	8.07	8.07	7.73	7.73	7.47	7.47
99	out	8.06±0.003	8.04±0.003	7.66±0.003	7.63±0.007	7.43±0.006	7.41±0.009
	in	8.12	8.12	7.68	7.68	7.49	7.49
123	out	8.05±0.009	8.05±0.007	7.63±0.006	7.62±0.009	7.42±0.009	7.41±0.012

Appendix 10. Average pH_T in six experimental treatments that newly settled sea urchins, *Pseudechinus huttoni* grew in during Experiment #5. pH was measured of incoming water from header flow-through tanks ("in") and of water in the three replicate tubs for each treatment immediately prior to water changes ("out"). Values represent the single measurement for "in" (n=1) and mean ± SE for "out" (n=3).

Time (hours after introduction to cue)		pH_T 8.1		pH_T 7.7		pH_T 7.4	
		Light	**Dark**	**Light**	**Dark**	**Light**	**Dark**
0	in	8.12	8.12	7.72	7.72	7.54	7.54
24	out	8.11±0.006	8.06±0.006	7.74±0.006	7.64±0.003	7.53±0.009	7.43±0.015
	in	8.19	8.19	7.71		7.47	7.47
48	out	8.13±0.017	8.06±0.003	7.70±0.009	7.62±0.009	7.48±0.015	7.41±0.003
	in	8.16	8.16	7.68	7.68	7.45	7.45
72	out	8.13±0.009	8.07±0.006	7.69±0.012	7.64±0.007	7.47±0.009	7.41±0.009
	in	8.17	8.17	7.69	7.69	7.46	7.46
96	out	8.12±0.003	8.06±0.003	7.79±0.009	7.61±0.003	7.46±0.003	7.40±0.003

Appendix 11. Sample size of juvenile sea urchins *Pseudechinus huttoni* measured per replicate and per treatment in Experiment #2 and #3.

Treatment	Experiment #2		Experiment #3	
	Number of juveniles measured		Number of juveniles measured	
	per replicate	per treatment	per replicate	per treatment
Alternation Flow				
Rep 1	6		1	
Rep 2	3	14	1	4
Rep 3	4		1	
Rep 4	1		1	
Alternation No Flow				
Rep 1	4		1	
Rep 2	3	16	1	4
Rep 3	8		2	
Rep 4	1		0	
Light Flow				
Rep 1	4		0	
Rep 2	4	14	1	2
Rep 3	6		0	
Rep 4	0		1	
Light No Flow				
Rep 1	2		0	
Rep 2	5	16	2	5
Rep 3	3		3	
Rep 4	6		0	
Dark Flow				
Rep 1	1		2	
Rep 2	1	9	2	6
Rep 3	6		1	
Rep 4	1		1	
Dark No Flow				
Rep 1	2		1	
Rep 2	2	16	1	3
Rep 3	4		1	
Rep 4	8		0	

Appendix 12. Sample size of juvenile sea urchins *Pseudechinus huttoni* measured per replicate and per treatment in Experiment #4 and #5.

Treatment	Experiment #4		Experiment #5	
	Number of juveniles measured		Number of juveniles measured	
	per replicate	per treatment	per replicate	per treatment
Dark 7.4				
Rep 1	47	118	7	23
Rep 2	31		9	
Rep 3	40		7	
Dark 7.7				
Rep 1	39	109	7	22
Rep 2	35		8	
Rep 3	35		7	
Dark 8.1			16	
Rep 1	22	65	6	16
Rep 2	15		7	
Rep 3	28		3	
Light 7.4				
Rep 1	19	58	11	28
Rep 2	17		7	
Rep 3	22		10	
Light 7.7				
Rep 1	34	89	8	23
Rep 2	32		9	
Rep 3	23		6	
Light 8.1				
Rep 1	28	70	7	18
Rep 2	21		6	
Rep 3	21		5	